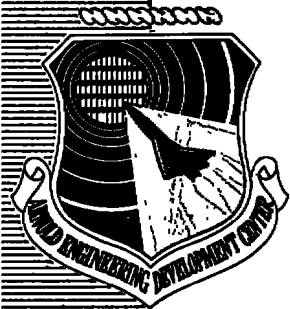AEDC-TR-76-45

AFATL-TR-76-36

ey. 2

AERODYNAMIC LOAD CHARACTERISTICS OF SIX 0.05-SCALE STORES IN THE FLOW FIELD OF AN F-4C AIRCRAFT AT MACH NUMBERS FROM 0.5 TO 1.1

PROPULSION WIND TUNNEL FACILITY
ARNOLD ENGINEERING DEVELOPMENT CENTER
AIR FORCE SYSTEMS COMMAND
ARNOLD AIR FORCE STATION, TENNESSEE 37389

August 1976

Final Report for Period November 19 — 20, 1975

Approved for public release; distribution unlimited.

Prepared for

AIR FORCE ARMAMENT LABORATORY (DLJC)
EGLIN AFB, FLORIDA 32542

NOTICES

When U. S. Government drawings specifications, or other data are used for any purpose other than a definitely related Government procurement operation, the Government thereby incurs no responsibility nor any obligation whatsoever, and the fact that the Government may have formulated, furnished, or in any way supplied the said drawings, specifications, or other data, is not to be regarded by implication or otherwise, or in any manner licensing the holder or any other person or corporation, or conveying any rights or permission to manufacture, use, or sell any patented invention that may in any way be related thereto.

Qualified users may obtain copies of this report from the Defense Documentation Center.
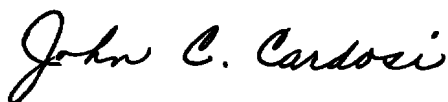
References to named commercial products in this report are not to be considered in any sense as an endorsement of the product by the United States Air Force or the Government.

This report has been reviewed by the Information Office (OI) and is releasable to the National Technical Information Service (NTIS). At NTIS, it will be available to the general public, including foreign nations.

APPROVAL STATEMENT

This technical report has been reviewed and is approved for publication.

FOR THE COMMANDER

JOHN C. CARDOSI
Lt Colonel, USAF
Chief Air Force Test Director, PWT
Directorate of Test

ALAN L. DEVEREAUX
Colonel, USAF
Director of Test

REPORT DOCUMENTATION PAGE		READ INSTRUCTIONS BEFORE COMPLETING FORM
1 REPORT NUMBER AEDC-TR-76-45 AFATL-TR-76-36	2 GOVT ACCESSION NO.	3 RECIPIENT'S CATALOG NUMBER
4 TITLE (and Subtitle) AERODYNAMIC LOAD CHARACTERISTICS OF SIX 0.05-SCALE STORES IN THE FLOW FIELD OF AN F-4C AIRCRAFT AT MACH NUMBERS FROM 0.5 TO 1.1		5 TYPE OF REPORT & PERIOD COVERED Final Report - November 19 - 20, 1975
		6. PERFORMING ORG. REPORT NUMBER
7 AUTHOR(s) G. R. Gomillion, ARO, Inc.		8. CONTRACT OR GRANT NUMBER(s)
9 PERFORMING ORGANIZATION NAME AND ADDRESS Arnold Engineering Development Center (XO) Air Force Systems Command Arnold Air Force Station, Tennessee 37389		10 PROGRAM ELEMENT, PROJECT, TASK AREA & WORK UNIT NUMBERS Program Element 62602F Project 2567, Task 02
11 CONTROLLING OFFICE NAME AND ADDRESS Air Force Armament Laboratory (DLJC) Eglin AFB, Florida 32542		12. REPORT DATE August 1976
		13 NUMBER OF PAGES 75
14 MONITORING AGENCY NAME & ADDRESS(if different from Controlling Office)		15. SECURITY CLASS. (of this report) UNCLASSIFIED
		15a. DECLASSIFICATION/DOWNGRADING SCHEDULE N/A

16 DISTRIBUTION STATEMENT (of this Report)

Approved for public release; distribution unlimited.

17 DISTRIBUTION STATEMENT (of the abstract entered in Block 20, if different from Report)

18 SUPPLEMENTARY NOTES

Available in DDC

19. KEY WORDS (Continue on reverse side if necessary and identify by block number)

aerodynamic	stores
loads	flow field
characteristics	F-4C aircraft
scale model	Mach numbers

20 ABSTRACT (Continue on reverse side if necessary and identify by block number)

Wind-tunnel tests were conducted using six 0.05-scale stores with various afterbody shapes to investigate the store aerodynamic load characteristics in the flow field of the F-4C aircraft. The store models had a hemispherical nose and a cylindrical midsection with various afterbody shapes. Three store models had cruciform pattern fins on a blunted cone-shaped afterbody. The other three store models had blunted cone, blunted ogive, and cylindrical-

DD FORM 1JAN 73 1473 EDITION OF 1 NOV 65 IS OBSOLETE

20. ABSTRACT (Continued)

shaped afterbodies, respectively. All finned store models were tested in both "X" and "+" fin orientations. Free-stream store loads data were also obtained at yaw angles between -6 and 30 deg. All store loads data are presented for Mach numbers from 0.5 to 1.1.

AFSC -
Arnold AFS Tenn

PREFACE

CONTENTS

ILLUSTRATIONS

TABLE

1.0 INTRODUCTION

A store loads test was conducted in the Aerodynamic Wind Tunnel (4T) of the Propulsion Wind Tunnel (PWT) facility, using the captive trajectory system (CTS), to determine the aerodynamic characteristics of six stores with different afterbody shapes in the flow field of an F-4C aircraft. Three of the six store models had finned afterbodies and were tested in both the "X" (ϕ_M = 45 deg) and "+" (ϕ_M = 0) fin orientations. For the store load characteristics near the F-4C aircraft, all the stores were oriented relative to the store carriage position on the bottom station (station 1) of a triple ejection rack (TER) located on the left inboard pylon, and the position of the stores was varied in the vertical plane of the carriage position. Also, store load characteristics were obtained at yaw angles between -6 to 30 deg with the store positioned as far as possible from the F-4C model. The data thus obtained are termed "free-stream" data. All store loads data were obtained at Mach numbers from 0.5 to 1.1 except for one finned configuration in the X fin orientation which was, in addition, tested at M_∞ = 1.2.

2.0 APPARATUS

2.1 TEST FACILITY

The Aerodynamic Wind Tunnel (4T) is a closed-loop, continuous flow, variable density tunnel in which the Mach number can be varied from 0.1 to 1.3. Also; nozzle blocks can be installed to give nominal Mach numbers of 1.6 and 2.0. At all Mach numbers, the stagnation pressure can be varied from 300 to 3,700 psfa. The test section is 4 ft square and 12.5 ft long with perforated, variable porosity (0.5- to 10-percent open) walls. It is completely enclosed in a plenum chamber from which the air can be evacuated, allowing part of the tunnel airflow to be removed through the perforated walls of the test section. A more thorough description of the tunnel may be found in the Test Facilities Handbook.[1]

When using the CTS, two separate and independent support systems are used to support the models. The parent-aircraft model is inverted in the test section and supported by an offset sting attached to the main pitch sector. The store model is supported by the CTS, which extends down from the tunnel top wall and provides store movement (six degrees of freedom) independent of the parent-aircraft model. An isometric drawing of a typical CTS store installation is shown in Fig. 1. Also shown in Fig. 1 is a block diagram of the computer loop used during store load testing. The analog system and the

---

[1]Test Facilities Handbook (Tenth Edition). "Propulsion Wind Tunnel Facility, Vol. 4." Arnold Engineering Development Center, May 1974.

digital computer work as an integrated unit and, utilizing required input information, control the store movement during a store loads test. Store positioning is accomplished by use of six individual d-c electric motors. Maximum translational travel of the CTS is ±15 in. from the tunnel centerline in the lateral and vertical directions and 36 in. in the axial direction. Maximum angular displacements are ±45 deg in pitch and yaw and ±360 deg in roll. A schematic showing the test section details and the location of the models in the tunnel is shown in Fig. 2.

2.2 TEST ARTICLES

The basic dimensions of the 0.05-scale F-4C parent model are presented in Fig. 3. The parent model is geometrically similar to the full-scale airplane except that the tail section is removed to minimize interference with CTS support movement. Details of the pylon, TER, and 370-gal fuel tank are shown in Figs. 4, 5, and 6, respectively. The TER was mounted on the left inboard pylon and was aligned with the 30-in. suspension lug position. The 370-gal fuel tank was mounted to the outboard pylon on the left wing (all other pylon stations were empty).

Details of the six 0.05-scale store models with various afterbody shapes are presented in Fig. 7. The numbering sequence and roll orientations of the stores for the TER stations are shown in Fig. 8. A typical tunnel installation photograph showing parent aircraft, store model, and CTS is presented in Fig. 9. Throughout the test and for all configurations, all store loads data near the F-4C aircraft were obtained with the store initially positioned on the TER at station 1, while dummy models of the same configuration were positioned on the TER at stations 2 and 3.

2.3 INSTRUMENTATION

A 0.30-in.-diam, moment-type, six-component internal strain-gage balance was used to obtain store aerodynamic force and moment data. Translation and angular positions of the store were obtained from CTS analog inputs, and parent-model angle of attack was determined using a strain-gaged pendulum located in the model. Balance, sting, and support deflections caused by the aerodynamic loads on the store models were accounted for in the data reduction program to calculate the true model angles. Also, corrections were made for model weight to calculate the net aerodynamic forces on the stores. The TER contained a touch wire system which enabled the store to be accurately positioned relative to the parent aircraft. The system was also wired to automatically stop the CTS motion and give visual indication should the store or sting support make contact with any surface other than the touch wire.

3.0 TEST PROCEDURE AND PRECISION OF MEASUREMENTS

3.1 TEST DESCRIPTION

Store aerodynamic force and moment data were obtained in the flow field of the F-4C aircraft at Mach numbers from 0.5 to 1.2 and for aircraft angles of attack of 0, 1, 2, and 4 deg. Store free-stream data were obtained at Mach numbers from 0.5 to 1.2 and for a yaw angle range from -6 to 30 deg. The total pressure was held constant at approximately 1,200 psfa, and the variation of Reynolds number and dynamic pressure with Mach number is shown in Fig. 10. For each survey, tunnel conditions were held constant at the desired Mach number, while the store position was varied and data were recorded at each selected store position.

3.2 DATA ACQUISITION

To obtain store loads data in the vicinity of the F-4C aircraft, test conditions were established in the tunnel and the parent model was positioned at the desired angle of attack. The store model was then oriented to a reference position corresponding to the store carriage location. After the store was set at the desired position, operational control of the CTS was switched to the digital computer which controlled the store movement during each survey through commands to the CTS analog system. Aerodynamic store loads were then measured at a series of preprogrammed positions near the F-4C aircraft. Store free-stream data were obtained by moving the store model as far forward as possible to minimize the influence of the parent aircraft on the free-stream data. In each case, the store model nose was approximately 4 in. aft of the parent-aircraft nose and the store centerline was more than 7 in. below the aircraft WL 0. At this point, test conditions were established and the store was yawed through the desired angle range to obtain data at each selected yaw angle.

3.3 PRECISION OF MEASUREMENTS

The aerodynamic coefficient and store position data are subject to errors resulting from uncertainties in tunnel conditions, balance measurements, and CTS positioning accuracy. The maximum errors in positioning a store at a specified point are ±0.08 ft (full scale) in X_T, Y_T, and Z_T, ±0.15 deg in pitch and yaw, and ±1.0 deg in roll.

The estimated maximum uncertainties associated with measured tunnel conditions and aerodynamic coefficients are given in Table 1. The uncertainty quoted for Mach number relates to the variation of Mach number in the vicinity of the test article. The uncertainty for setting and maintaining Mach number during a store load survey is approximately

±0.005. The uncertainty in parent angle-of-attack measurements is estimated to be 0.1 deg. The estimated uncertainties in force and moment coefficients are based on 95-percent probability and include possible errors in balance calibration curve fits, instrumentation errors, Mach number uncertainties, and in the case of moment coefficients, transfer of forces from the balance force system center to the moment reference point of the store.

4.0 RESULTS AND DISCUSSION

4.1 FREE-STREAM DATA

The variation of the free-stream aerodynamic coefficients with yaw angle for all store configurations and roll angles tested are presented in Figs. 11 through 14. To obtain the free-stream data, a store configuration was positioned in the tunnel such that the store nose was approximately 4 in. (model scale) aft of the F-4C aircraft nose and the store centerline was more than 7 in. (model scale) below the WL 0 of the aircraft and centered about the aircraft BL 0. Since all store configurations are symmetrical about the vertical and horizontal axes, the following analysis for the yaw plane can be applied to the pitch plane as well.

The variations of the free-stream aerodynamic coefficients with yaw angle for store configurations 1, 2, and 3 (finned stores) comparing roll angles of 0 ("+" fin orientation) and 45 deg ("X" fin orientation) are shown in Figs. 11 through 13, respectively. The + fin orientation of the finned stores produced the largest side force for all Mach numbers and, with increasing Mach number, the magnitude of C_Y increased. As expected, the magnitude of C_Y increased slightly as fin size increased. The variations of yawing-moment coefficient with yaw angle were quite nonlinear with a noticeable change in slope in the neighborhood of ψ = 8 deg. For the moment reference point indicated in Fig. 7, and for small angles of attack, the finned stores were approximately neutrally stable at Mach numbers from 0.5 to 0.9 and unstable at M_∞ = 1.1. At yaw angles greater than about 8 deg, the fins became more effective and the + orientation produced considerably greater yawing moments than the X orientations. The fin effectiveness increased with fin size but was not affected much by changes in Mach number, except at M_∞ = 1.1 where the effectiveness was appreciably less than at the subsonic Mach numbers.

The variations of the free-stream aerodynamic coefficients with yaw angle comparing store configurations 4, 5, and 6 (unfinned stores) are shown in Fig. 14. The side-force coefficients of configuration 6 were significantly larger than those of configurations 4 and 5 which were nearly equal. The side-force coefficients for the unfinned stores increased as Mach number increased. As expected, the unfinned stores were statically unstable with

configurations 4 and 5 having similar characteristics and both being more unstable than configuration 6. Configurations 4 and 5 had smaller C_A values than configuration 6, except at $M_\infty = 1.1$ where there were but little differences in C_A for all the unfinned stores.

4.2 FLOW-FIELD DATA

Selected data showing the variation of the aerodynamic coefficients versus Z at the $X = 0$ position in the F-4C aircraft flow field are presented in Figs. 15 through 23. It would normally be expected that a store near the aircraft wing leading edge would experience an upwash. This, in fact, is indicated by the normal force of all the store configurations shown in Figs. 15 through 23. Briefly ignoring the $Z = 0$ case, for all store configurations at Mach numbers 0.5, 0.7, and 0.9, the normal force rapidly decreased in value as Z increased until at approximately $5 < Z < 9$ ft the normal force reached the free-stream value as indicated in Figs. 11 through 14 (see Section 4.1). For $Z > 5$ ft and for $M_\infty = 1.1$, the normal force tended to fluctuate about the free-stream value. Inspection of Figs. 15 through 23 shows, in most cases, the normal-force coefficients at $Z = 0$ are much less than those for small values of Z. This is particularly evident for Mach numbers 0.9 and 1.1 and was apparently a real aerodynamic effect. The rapid change in C_N values with changes in Z near $Z = 0$, and the uncertainty in Z characteristic of the CTS resulted in considerable scatter in the C_N values at $Z = 0$; however, certain trends are evident. The normal-force coefficient at the carriage position ($Z = 0$) was generally near its maximum value at $M_\infty = 0.5$ and decreased sharply in value at $M_\infty = 0.9$ where the normal-force coefficient was generally negative. At $M_\infty = 1.1$, the normal-force coefficient at the carriage position was generally larger than at $M_\infty = 0.9$. Comparing data for store configurations 1, 2, and 3 for $\phi_M = 0$ and 45 deg (Figs. 15 through 20) at the carriage position, the normal force was smaller for $\phi_M = 0$ which can possibly be explained by the fact that it was necessary to have a larger distance between the store and the TER/dummy models for $\phi_M = 0$ in order to prevent store contact.

For store configurations 1, 2, and 3 at $\phi_M = 0$ and 45 deg and Mach numbers 0.5, 0.7, and 0.9, the data in Figs. 15 through 20 show that the pitching-moment coefficients decreased in magnitude from a maximum nose down value at the carriage position to near free-stream values at large Z as indicated in Figs. 11 through 13 (see Section 4.1). Generally, the influence of the parent-aircraft flow field on the pitching moment is seen to extend beyond $Z = 10$ ft, which is farther than is evident from the normal-force coefficients. For $M_\infty = 1.1$, the pitching moments fluctuate widely at large values of Z. For configurations 1 through 3, the carriage position nose down pitching-moment coefficients increased in magnitude as Mach number was increased from 0.5 to 1.1. The store configurations 4, 5, and 6, as shown in Figs. 21 through 23, displayed similar

pitching-moment characteristics as configurations 1, 2, and 3 (Figs. 15 through 20), except that at $M_\infty = 0.5$ and 0.7 the pitching moments near the carriage position were significantly less negative.

It would be expected that the stores positioned on the wing would experience some outboard crossflow. The significant negative side force shown in Figs. 15 through 23 generally confirm this side flow. The effect is more pronounced for $a > 1$ deg and $Z < 5$ ft.
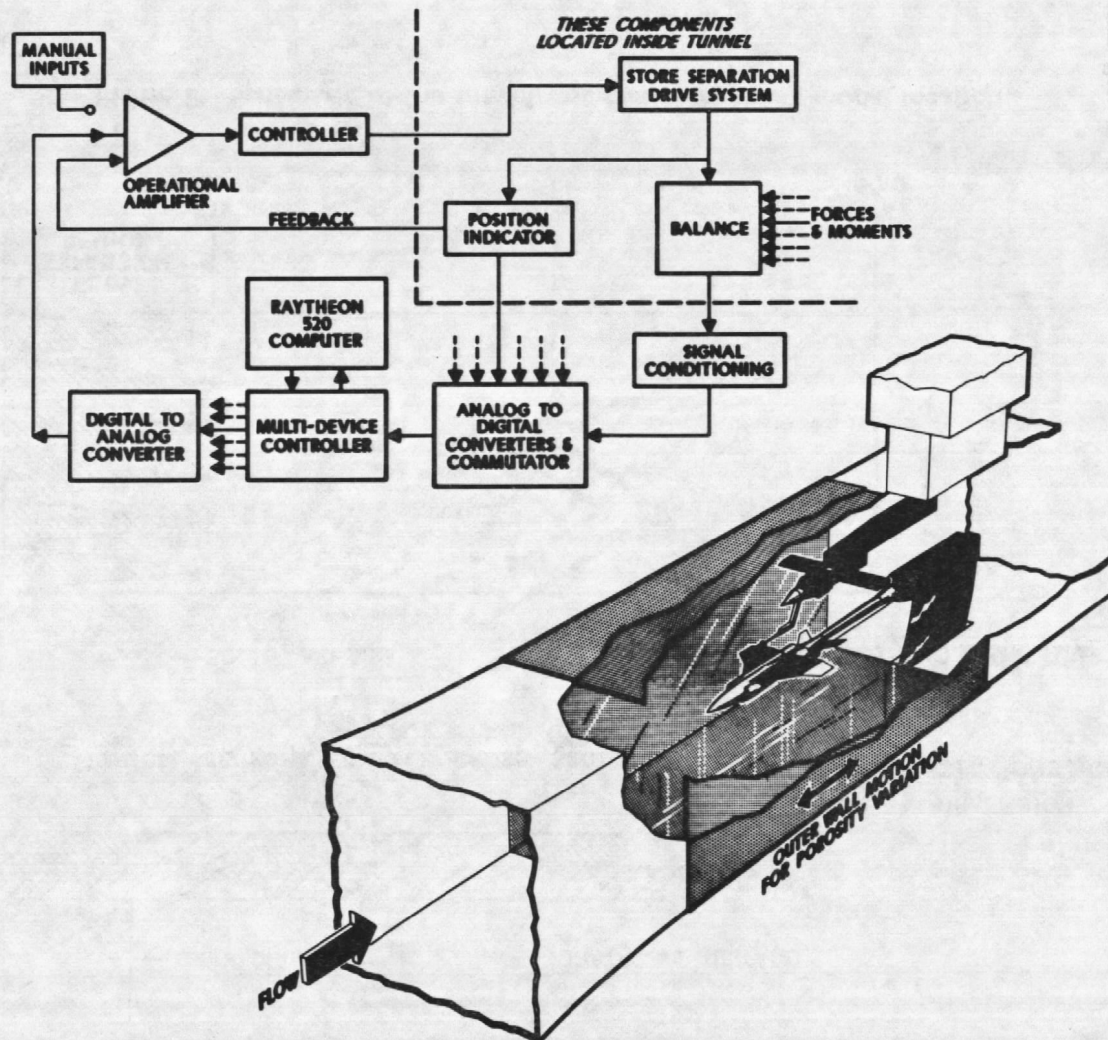
Figure 1. Isometric drawing of a typical store separation installation and a
block diagram of the computer control loop.

60°
0.500 DIAM
AIRSTREAM SURFACE
0.375
0.375

TYPICAL PERFORATED WALL CROSS SECTION

DIMENSIONS AND TUNNEL
STATIONS IN INCHES

SOLID AREAS
PERFORATED WALLS (10 % MAXIMUM OPEN AREA)

CTS STING SUPPORT
F-4 MODEL
STORE

FLOW
EXPANSION
REGION

STA. 0.0
STA. 36.0
STA. 90.1
STA. 150.0
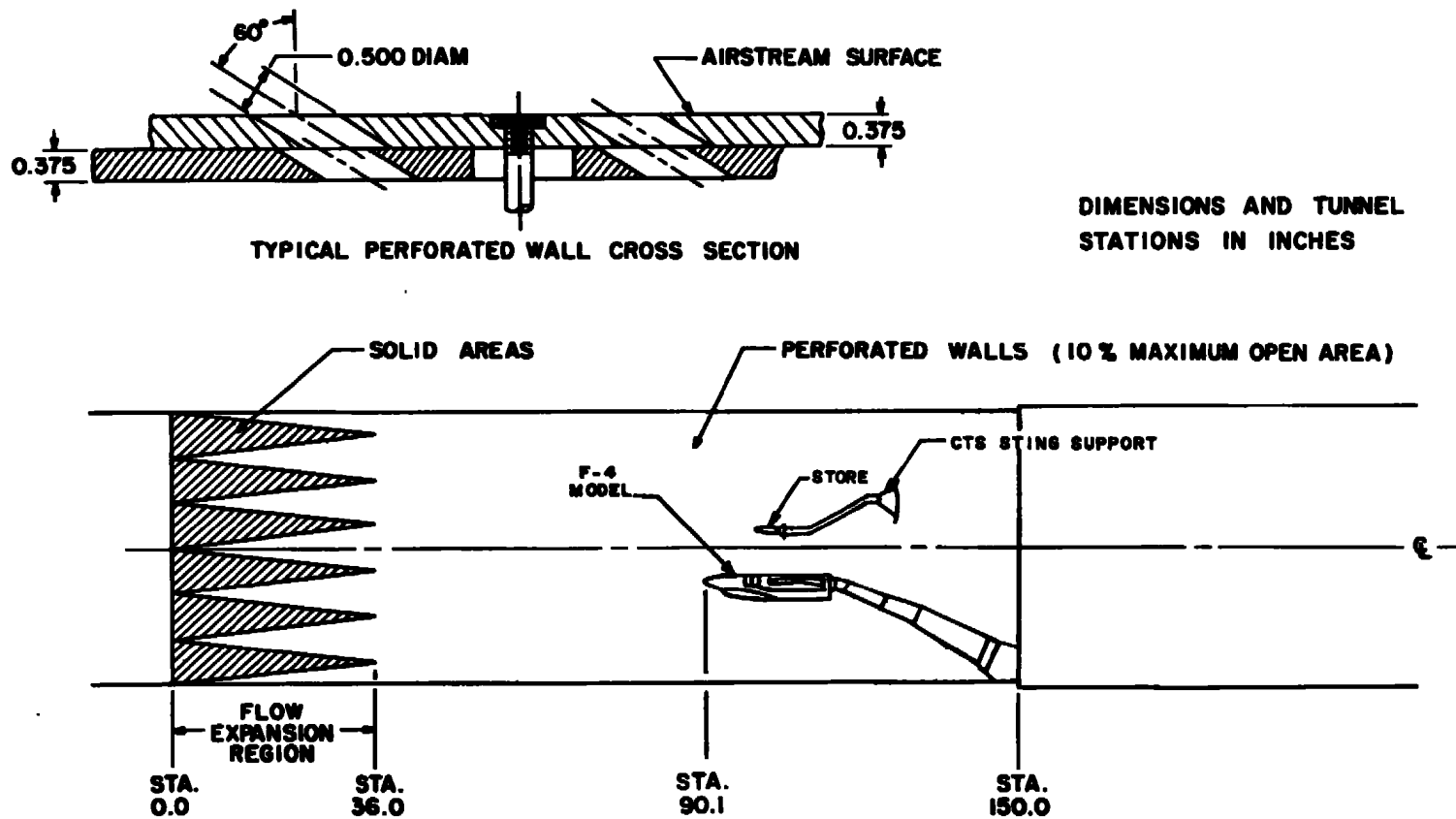
Figure 2. Schematic of the tunnel test section showing model location.

12

WL 0.00

BL 11.560

BL 6.625

BL 4.075

BL 4.075
¢ INBOARD
PYLON

BL 6.625
¢ OUTBOARD
PYLON

FS -1.355 FS 0.000

FS 25.942

BL 11.560
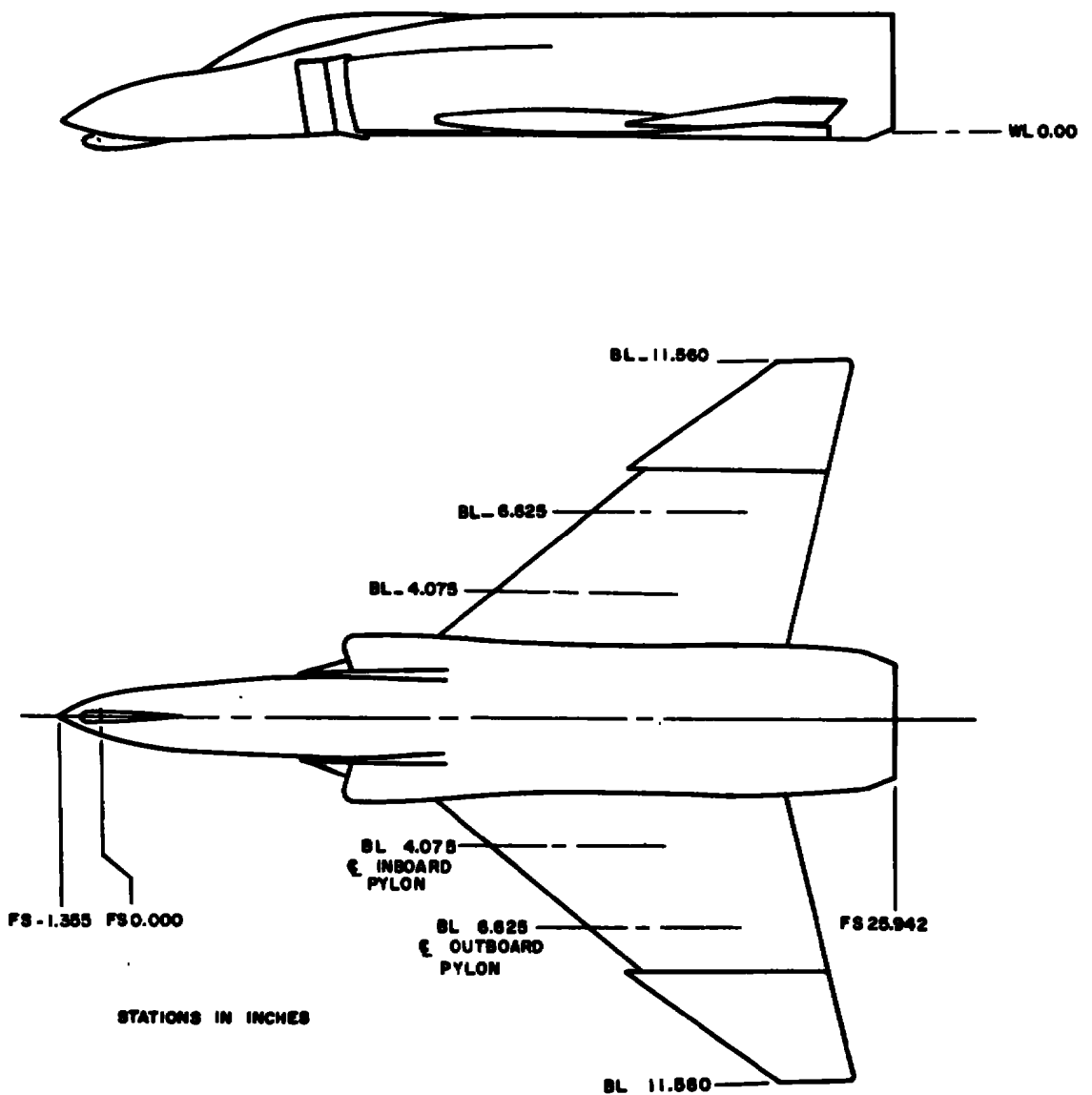
STATIONS IN INCHES

Figure 3. Dimensional sketch of the F-4C parent-aircraft model.

13
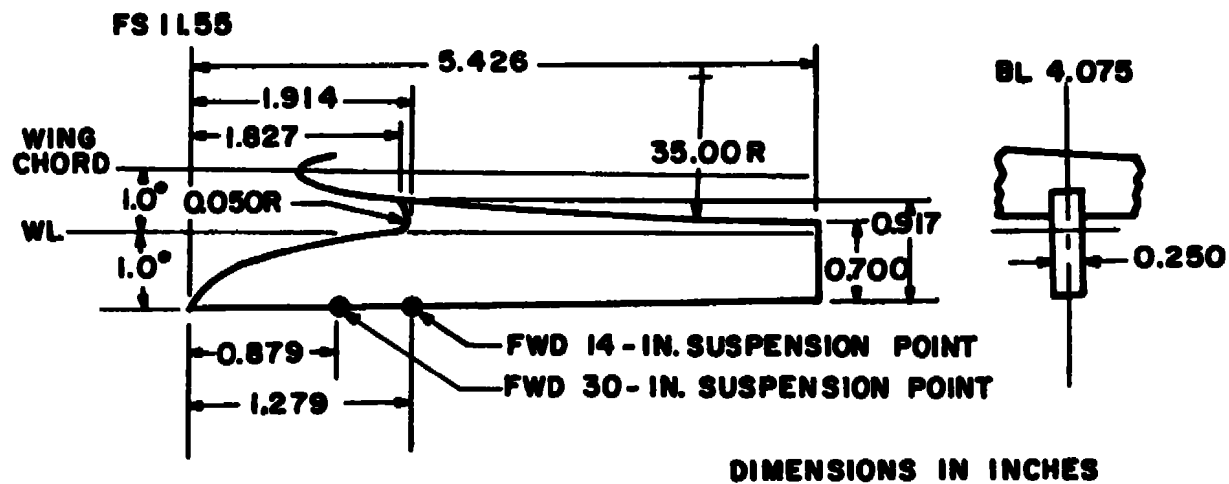
Figure 4. Dimensional sketch of the inboard pylon model.
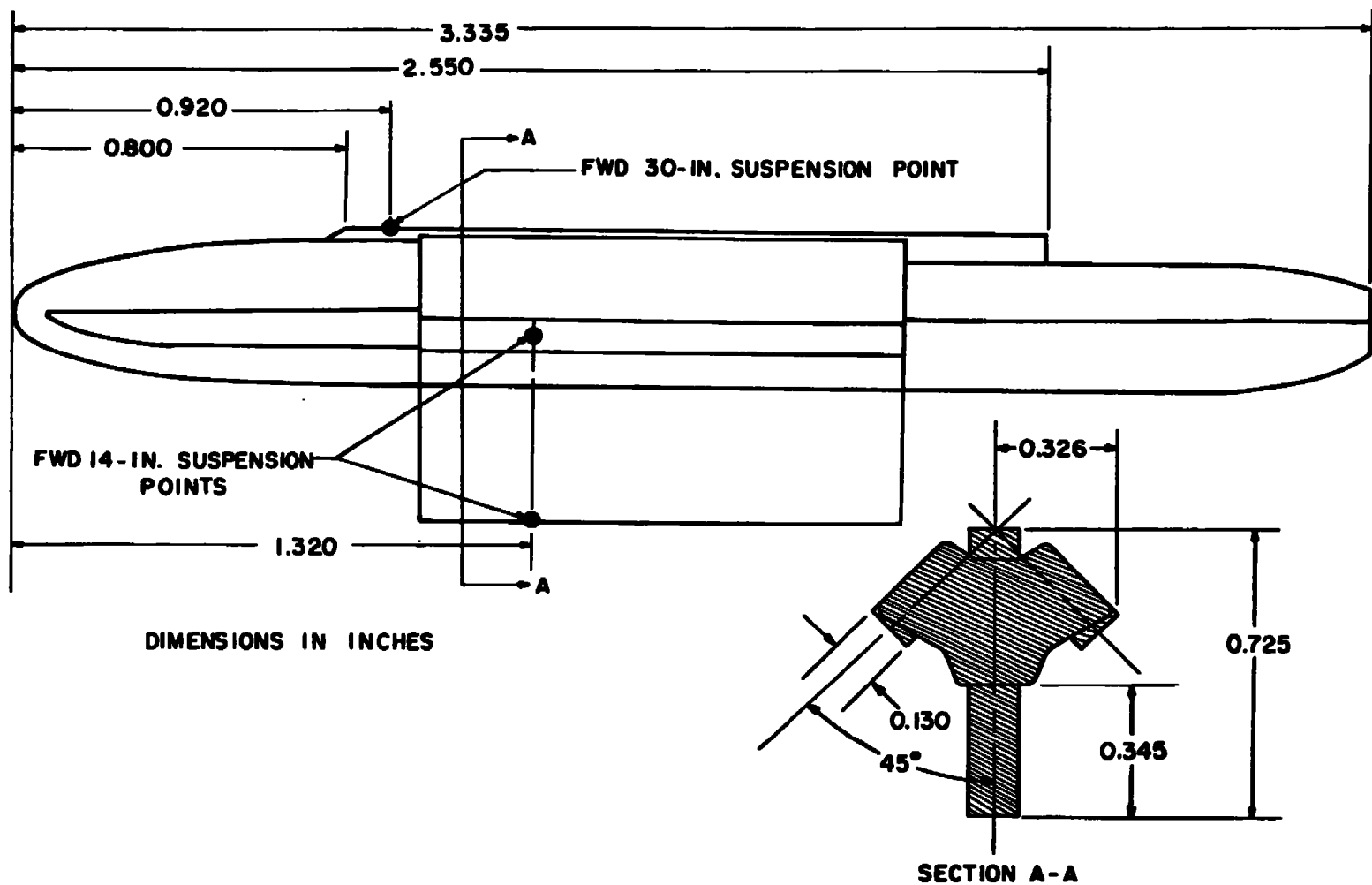
Figure 5. Dimensional sketch of the TER model.

3.335

2.550

0.920

0.800

A

FWD 30-IN. SUSPENSION POINT

FWD 14-IN. SUSPENSION POINTS

1.320

A

DIMENSIONS IN INCHES

0.326

0.725

0.130

0.345

45°

SECTION A-A

FS
10.652

FS
16.050

BL
6.625

0.500

0.480

W. L. 0.0

1.5°

€

1.300

12.000

STA
0.0
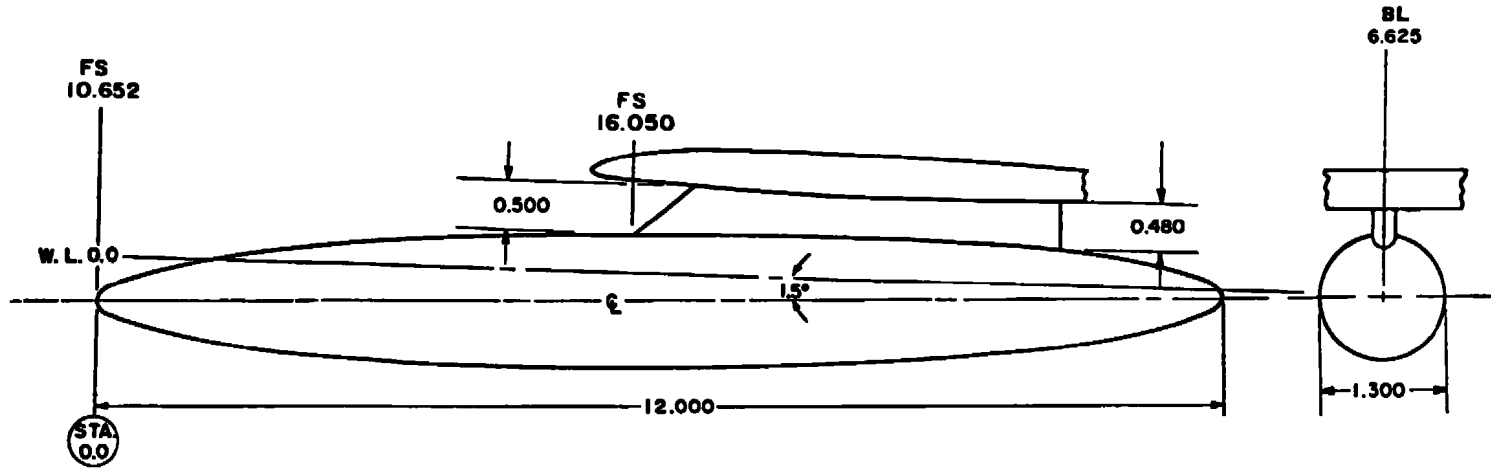
NOTE: MODEL STATIONS AND
DIMENSIONS IN INCHES

BODY CONTOUR, TYPICAL BOTH ENDS

STATION	BODY DIAM	STATION	BODY DIAM
0.000	0 000	2 500	1.116
0.025	0 100	2.750	1.156
0.050	0 144	3 000	1 190
0.150	0.258	3 250	1.218
0 250	0.340	3.500	1.242
0 500	0 498	3 750	1.260
0 750	0.622	4 000	1 274
1 000	0 724	4 250	1.286
1 250	0 812	4.500	1 294
1.500	0 890	4 750	1 298
1.750	0.958	5 000	1 300
2 000	1 016	6 000	1.300
2 250	1 070		

Figure 6. Dimensional sketch of the 370-gal fuel tank model.
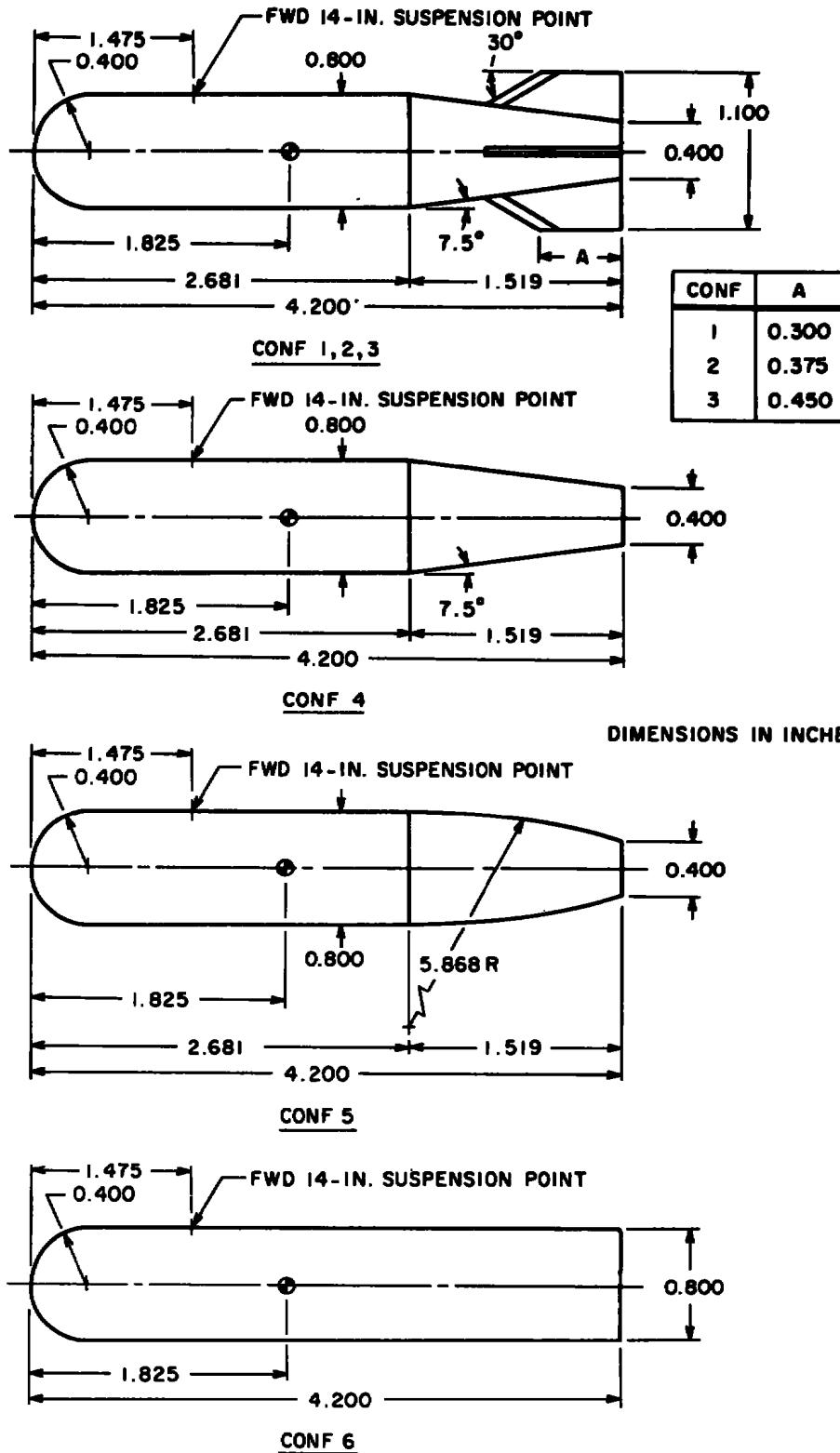
Figure 7. Dimensional sketch of store models.

17
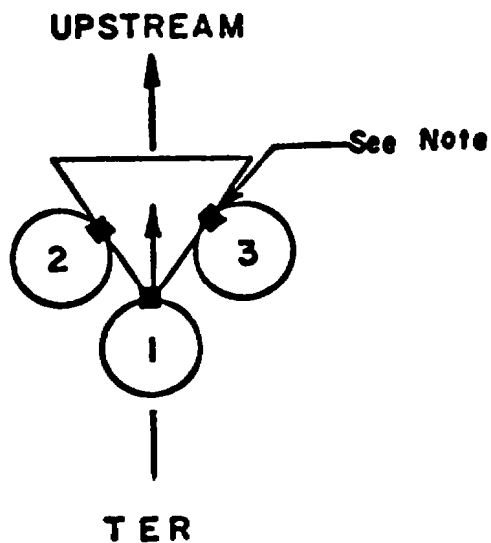
NOTE: The square indicates the orientation of the suspension lugs.

STATION	ROLL ORIENTATION, deg
1	0
2	45
3	-45

Figure 8. Schematic of the TER store stations and orientations.

Figure 9. Tunnel installation photograph showing parent-aircraft model, a store model, and CTS.
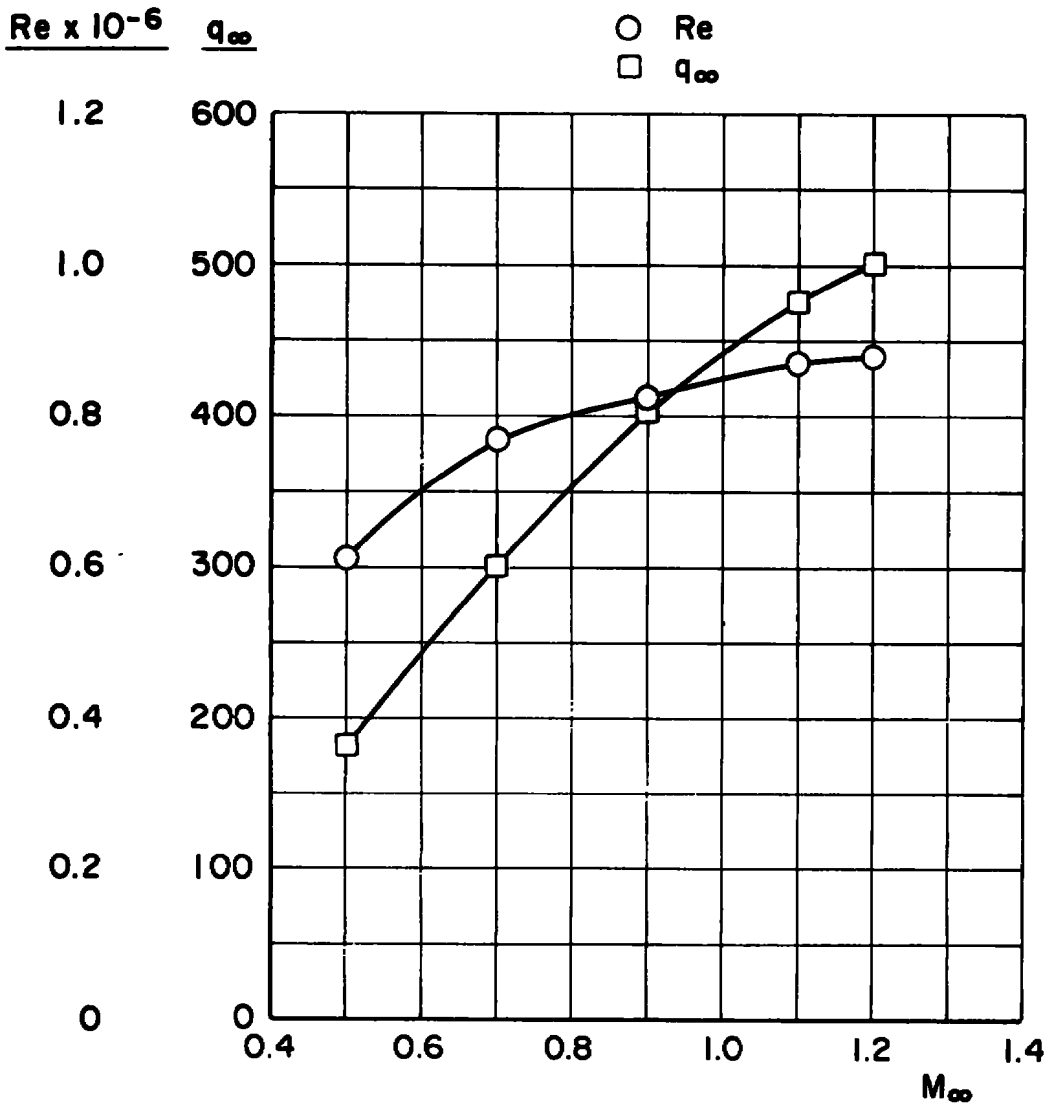
Figure 10. Variation of Reynolds number and dynamic pressure with Mach number.

a. $M_\infty = 0.5$
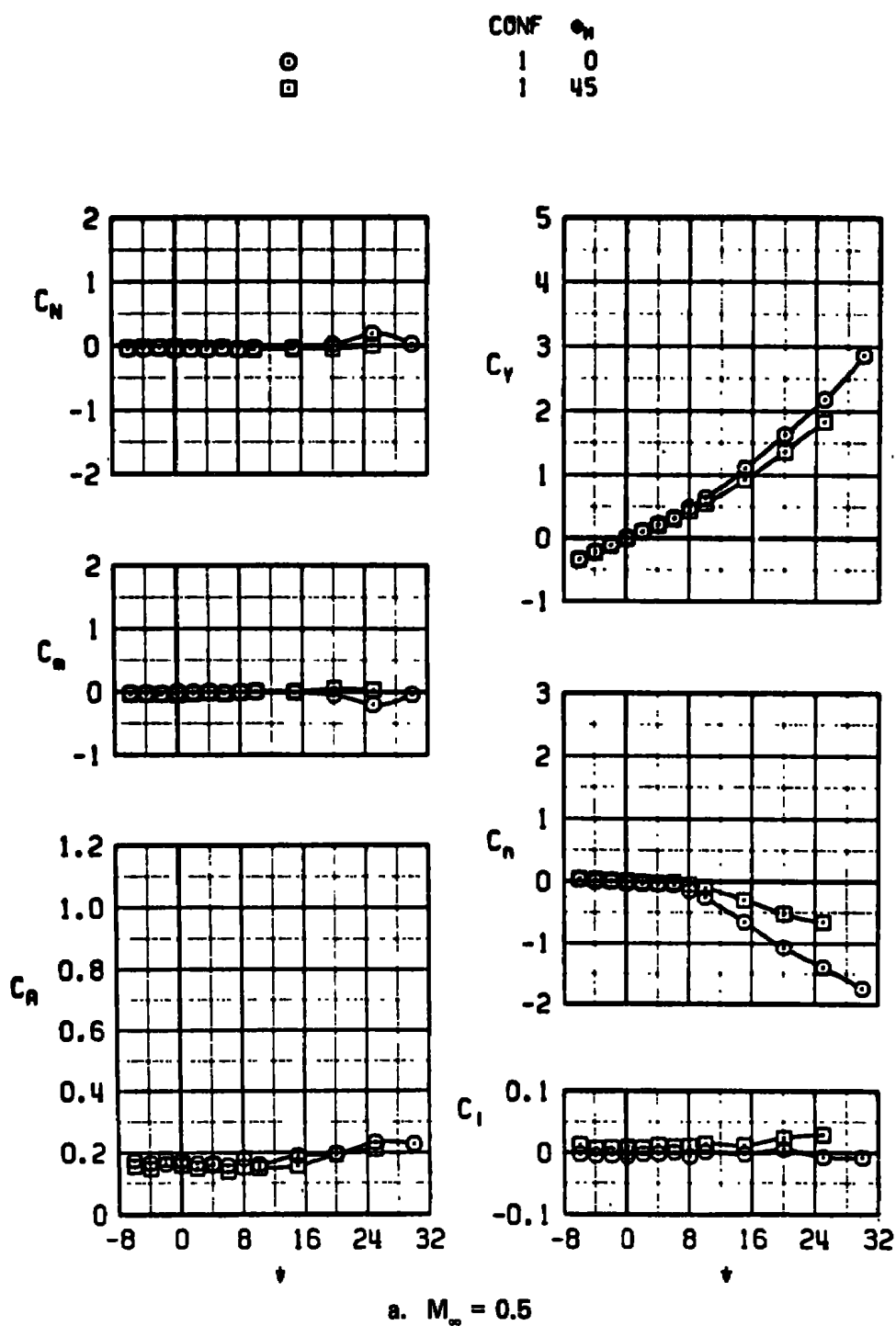
Figure 11. Comparison of free-stream aerodynamic coefficients versus yaw angle
for configuration 1 at $\phi_M = 0$ and 45 deg.

21
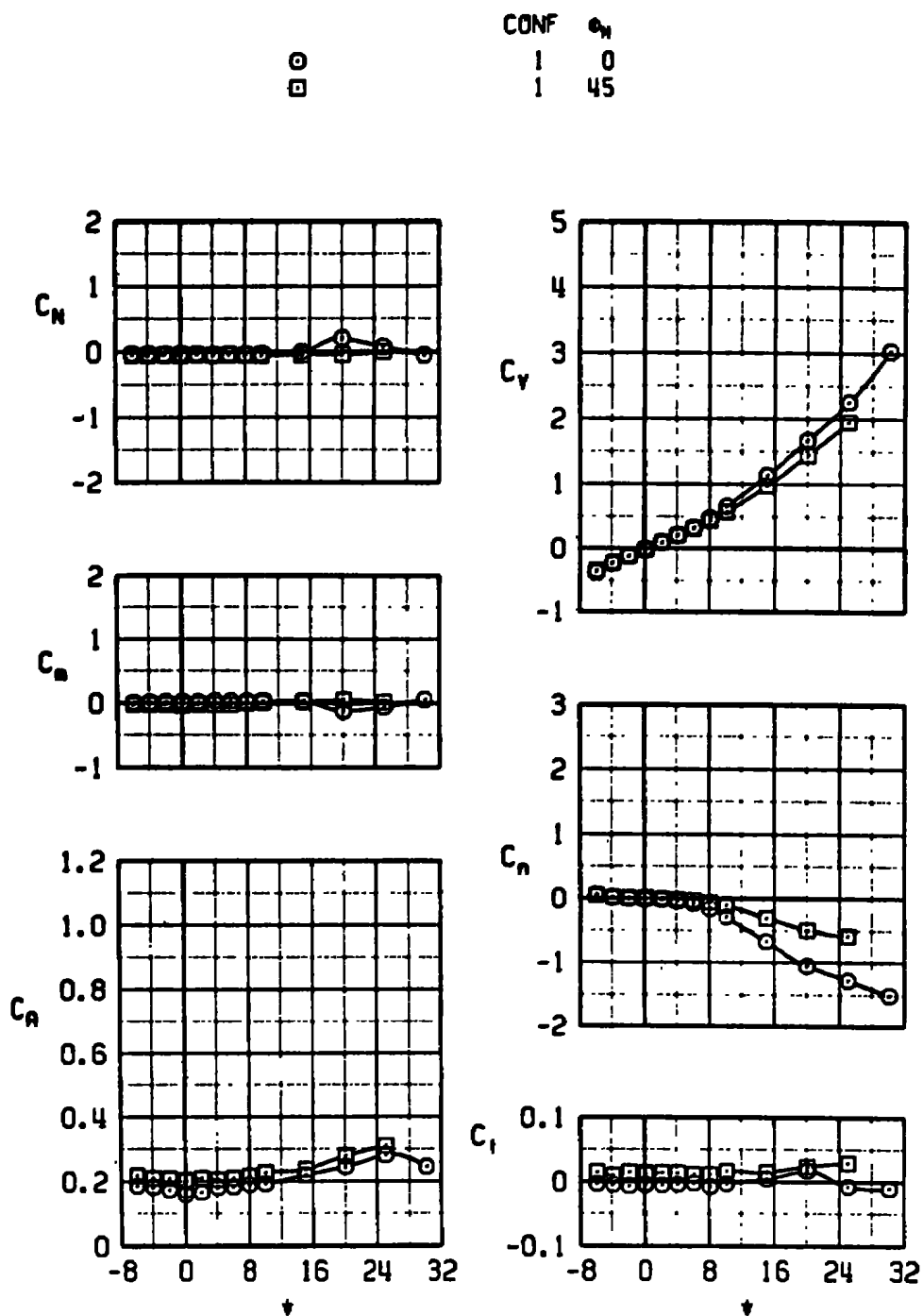
b. $M_\infty = 0.7$
Figure 11. Continued.
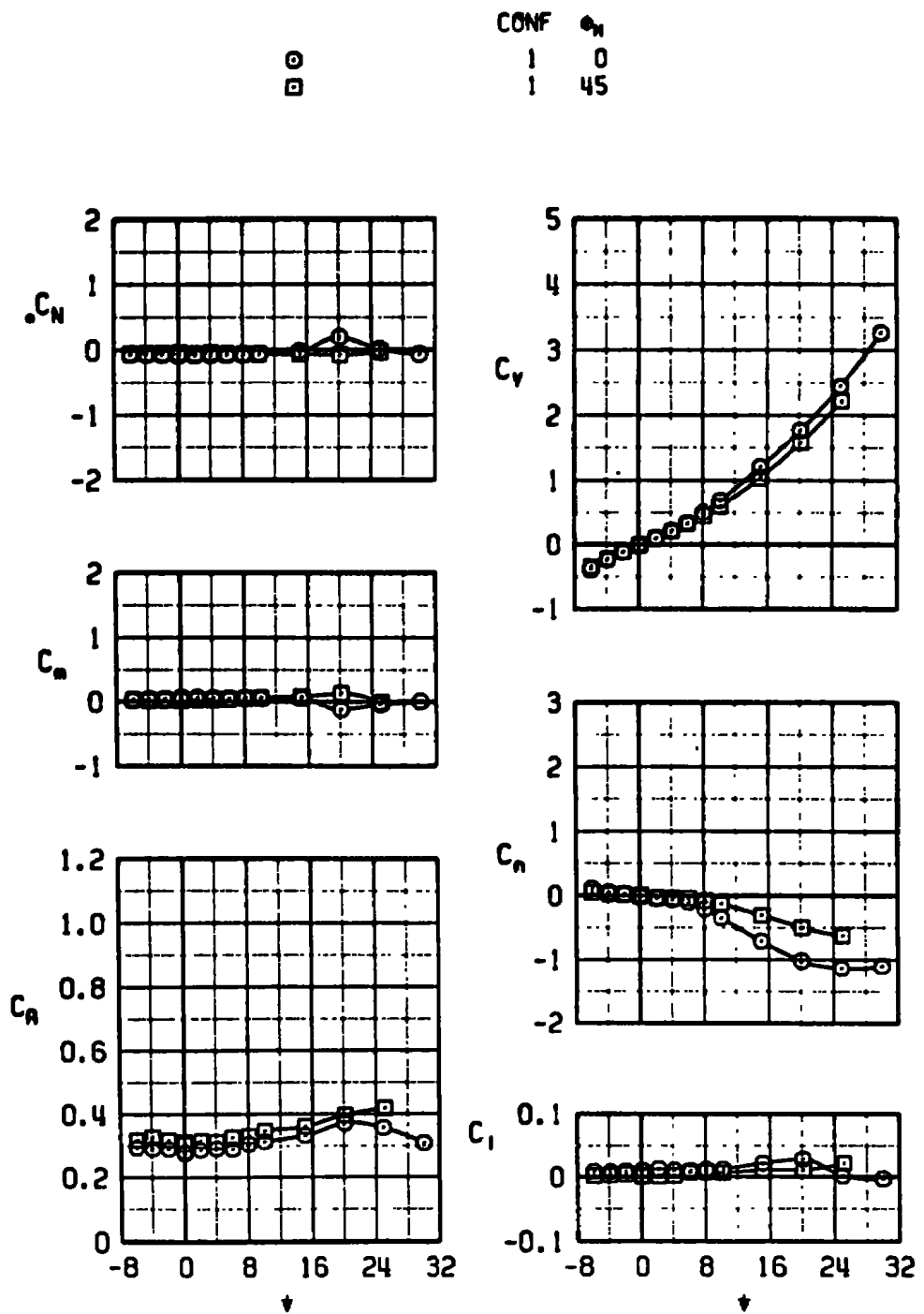
c. $M_\infty = 0.9$
Figure 11. Continued.
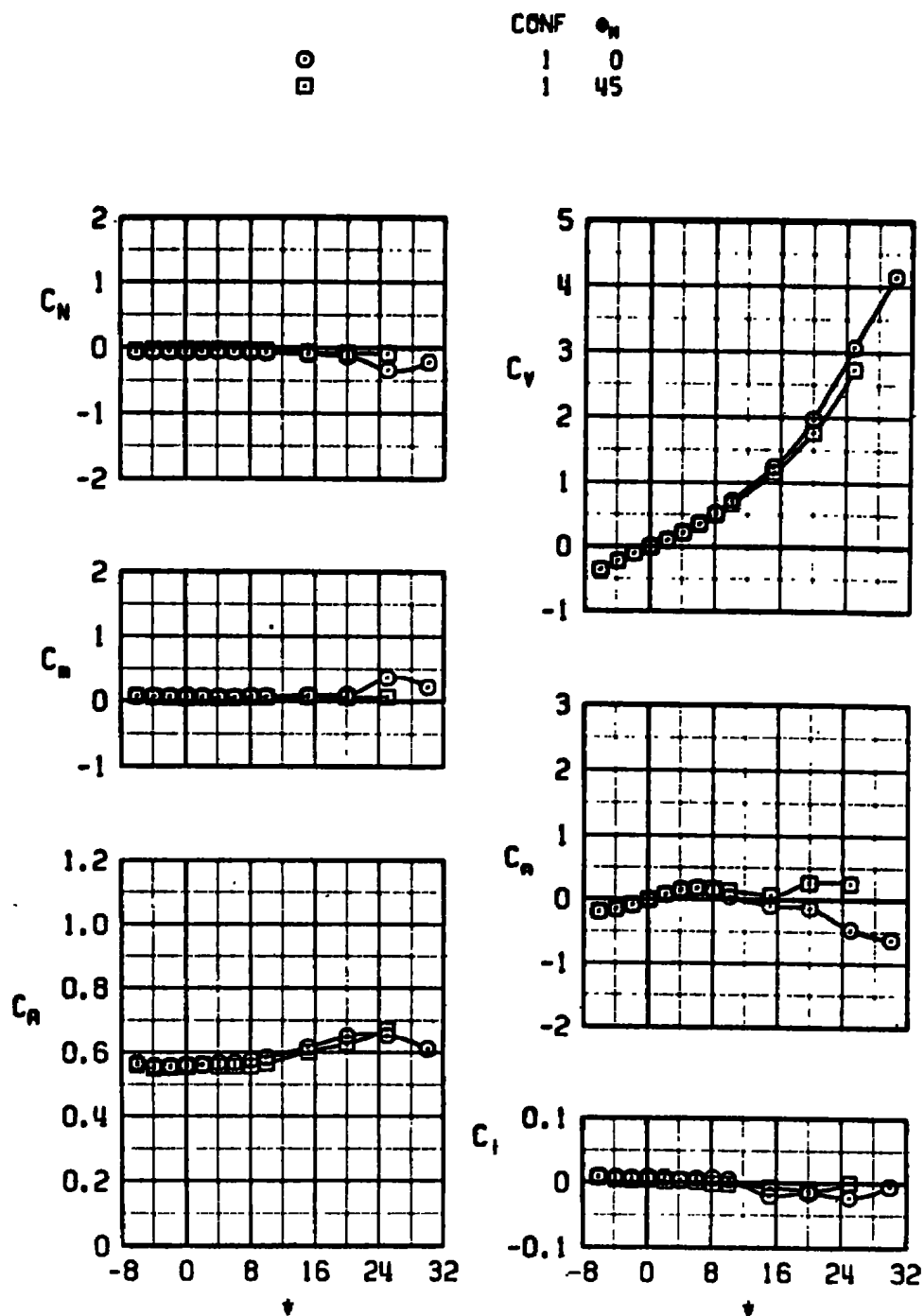
d. $M_\infty = 1.1$
Figure 11. Concluded.
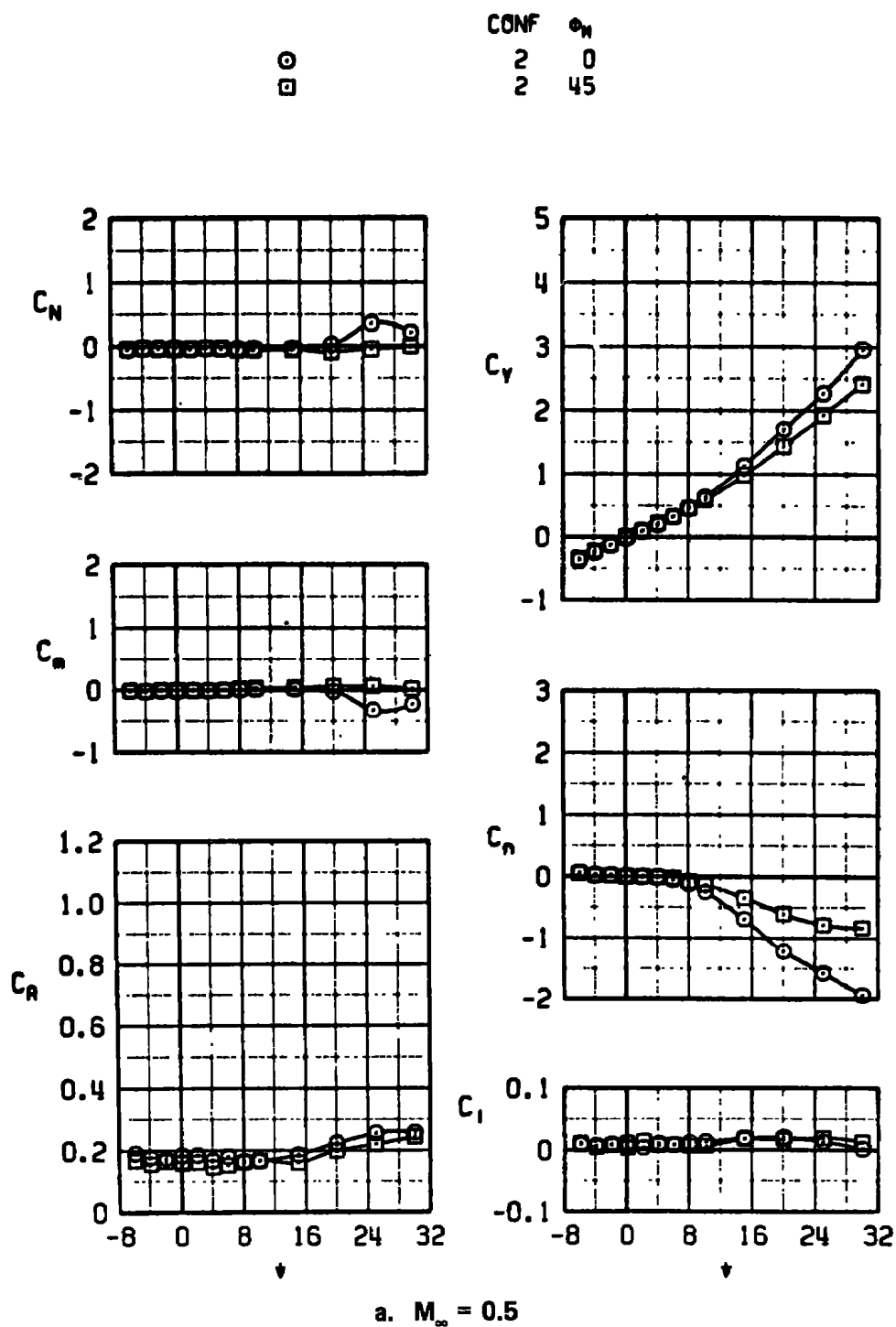
a. $M_\infty = 0.5$

Figure 12. Comparison of free-stream aerodynamic coefficients versus yaw angle
for configuration 2 at $\phi_M = 0$ and 45 deg.
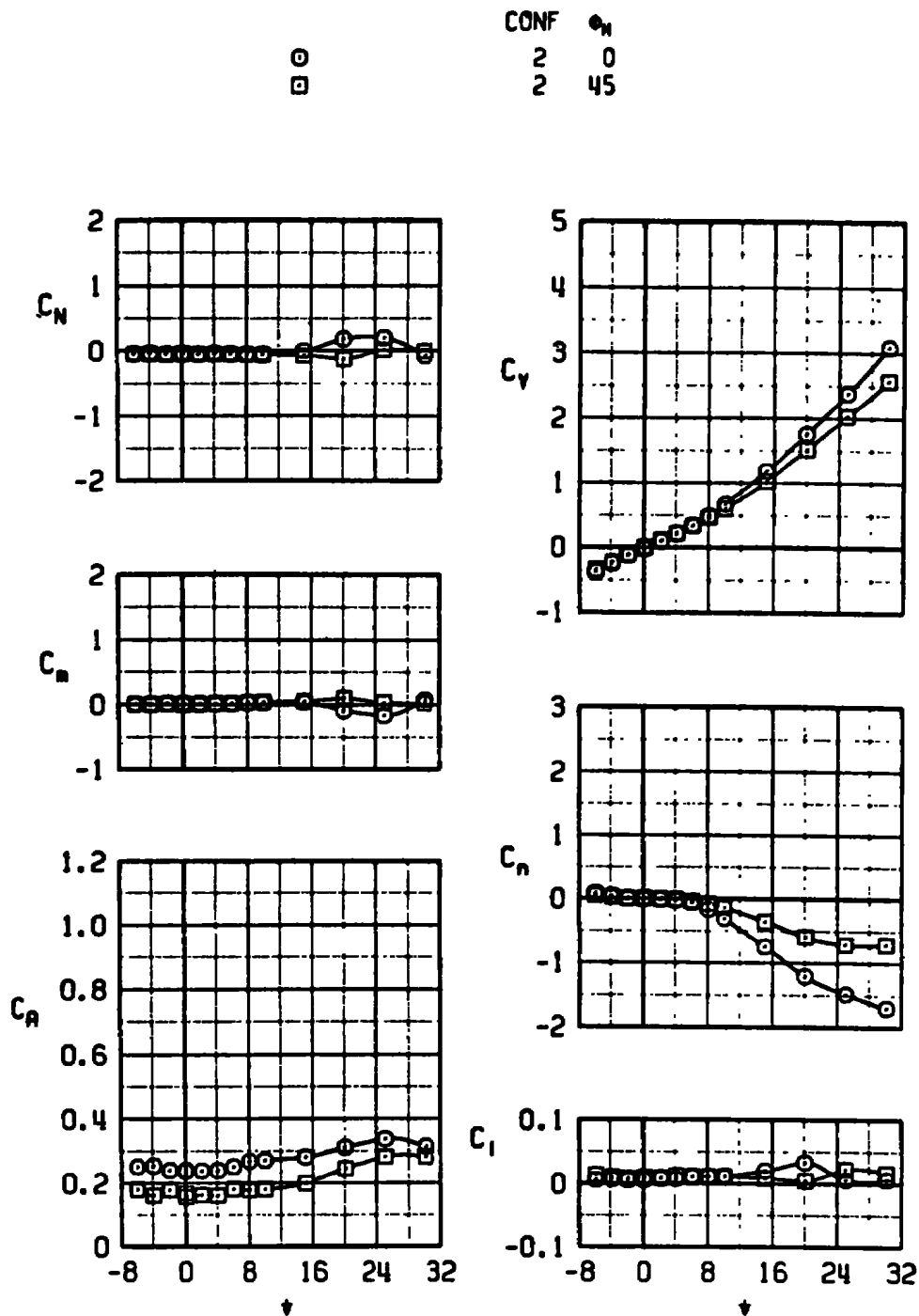
b. $M_\infty = 0.7$
Figure 12. Continued.
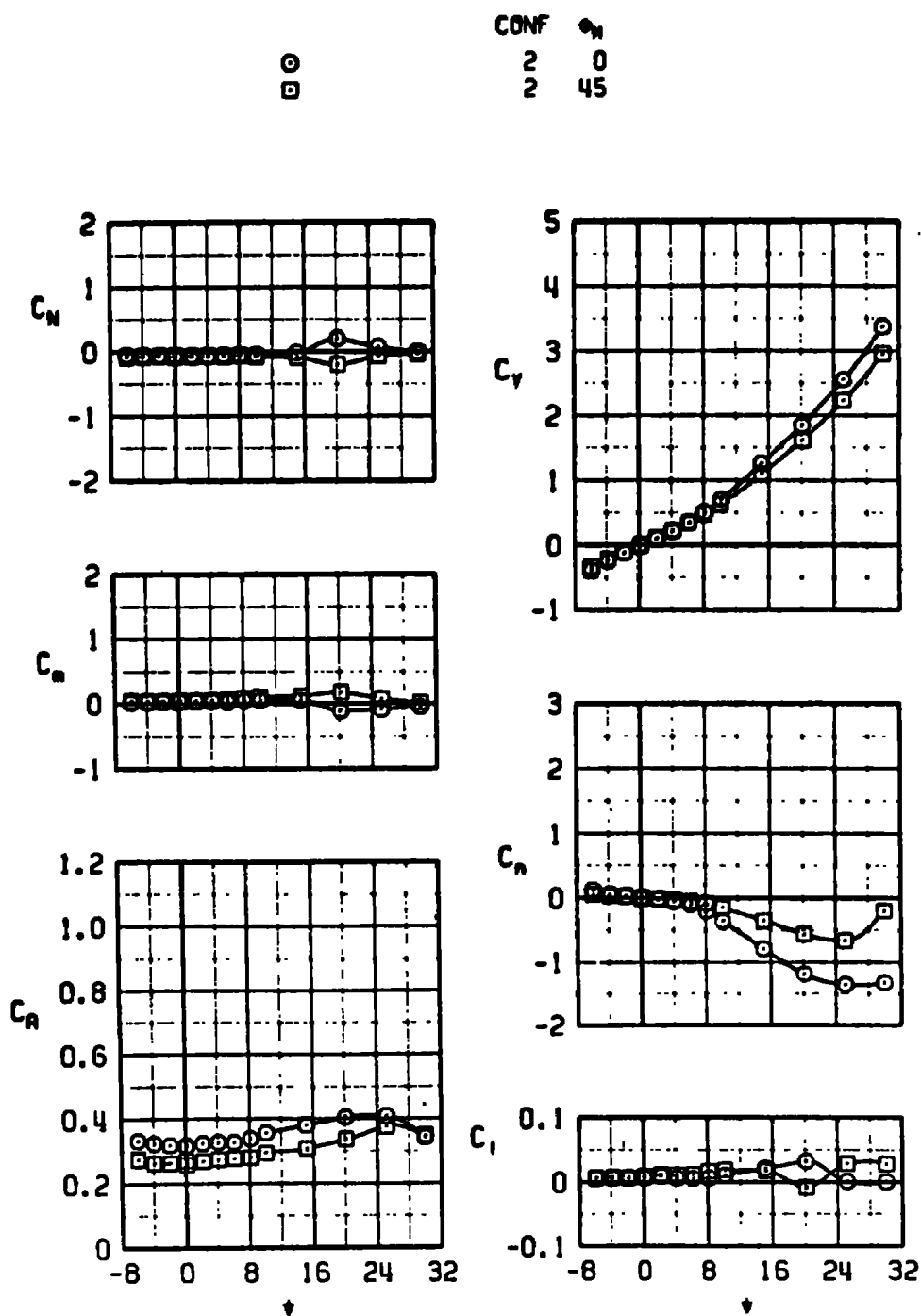
c. $M_\infty = 0.9$

Figure 12. Continued.
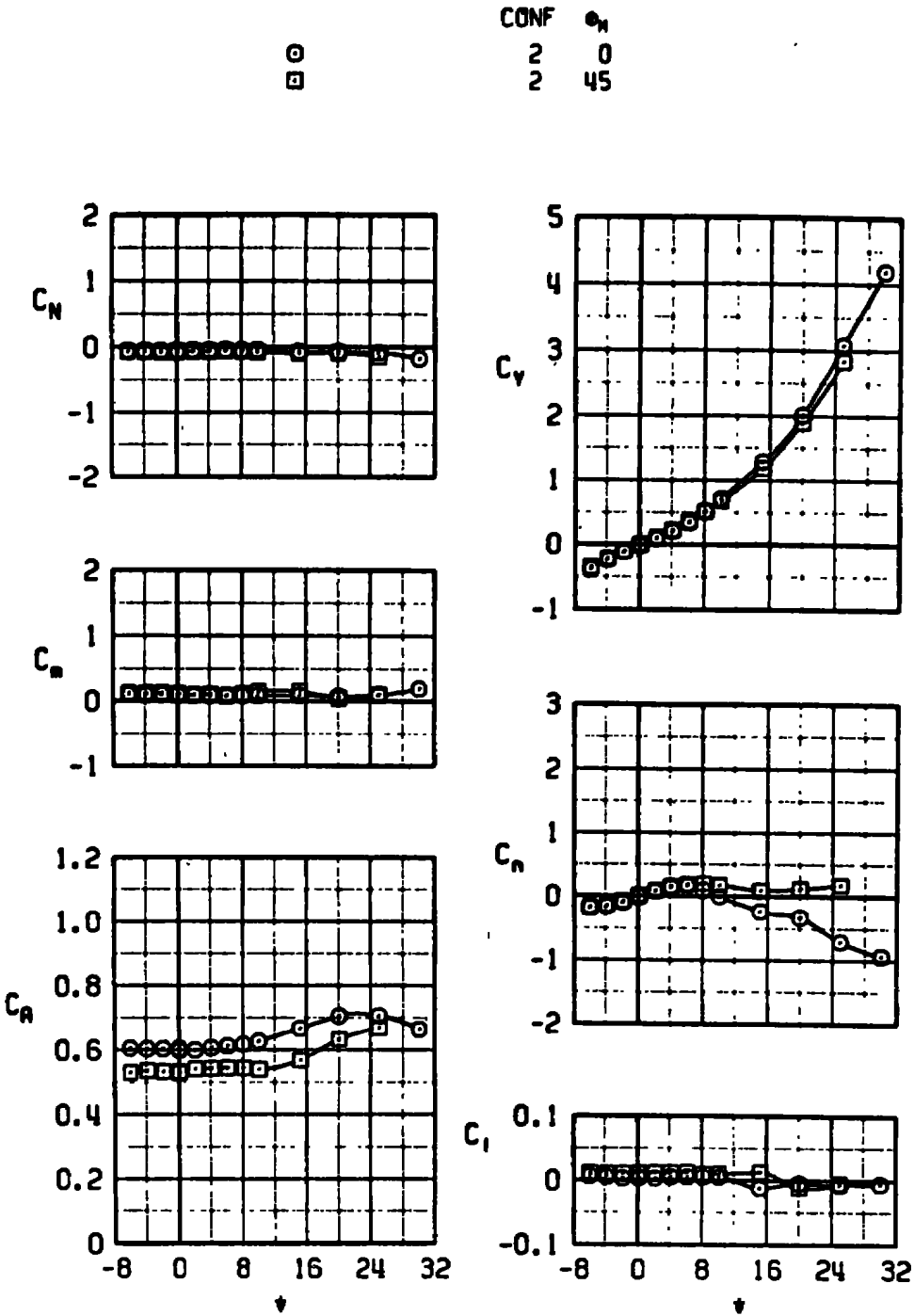
d. $M_\infty = 1.1$

Figure 12. Concluded.
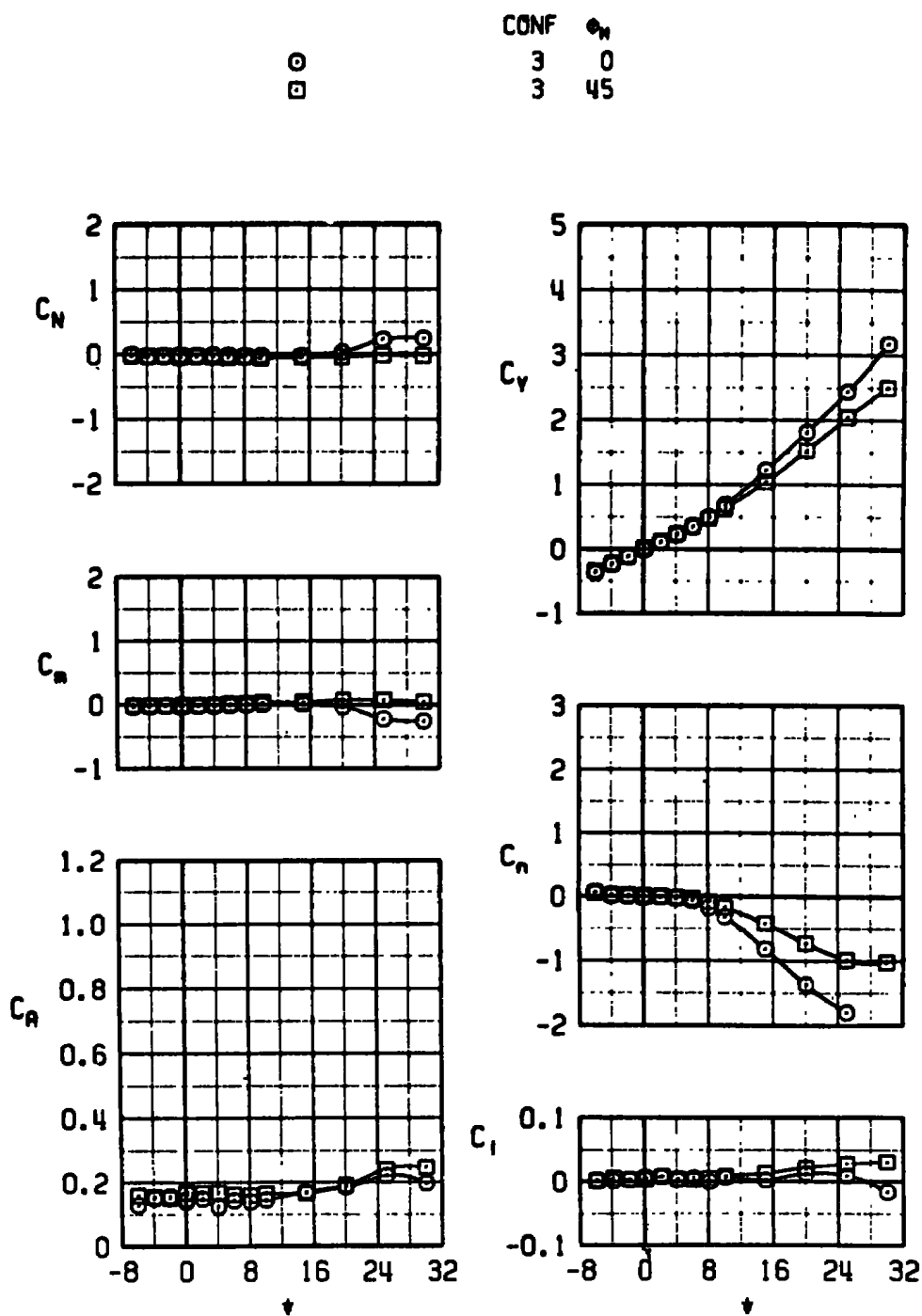
a. $M_\infty = 0.5$

Figure 13. Comparison of free-stream aerodynamic coefficients versus yaw angle for configuration 3 at $\phi_M = 0$ and 45 deg.
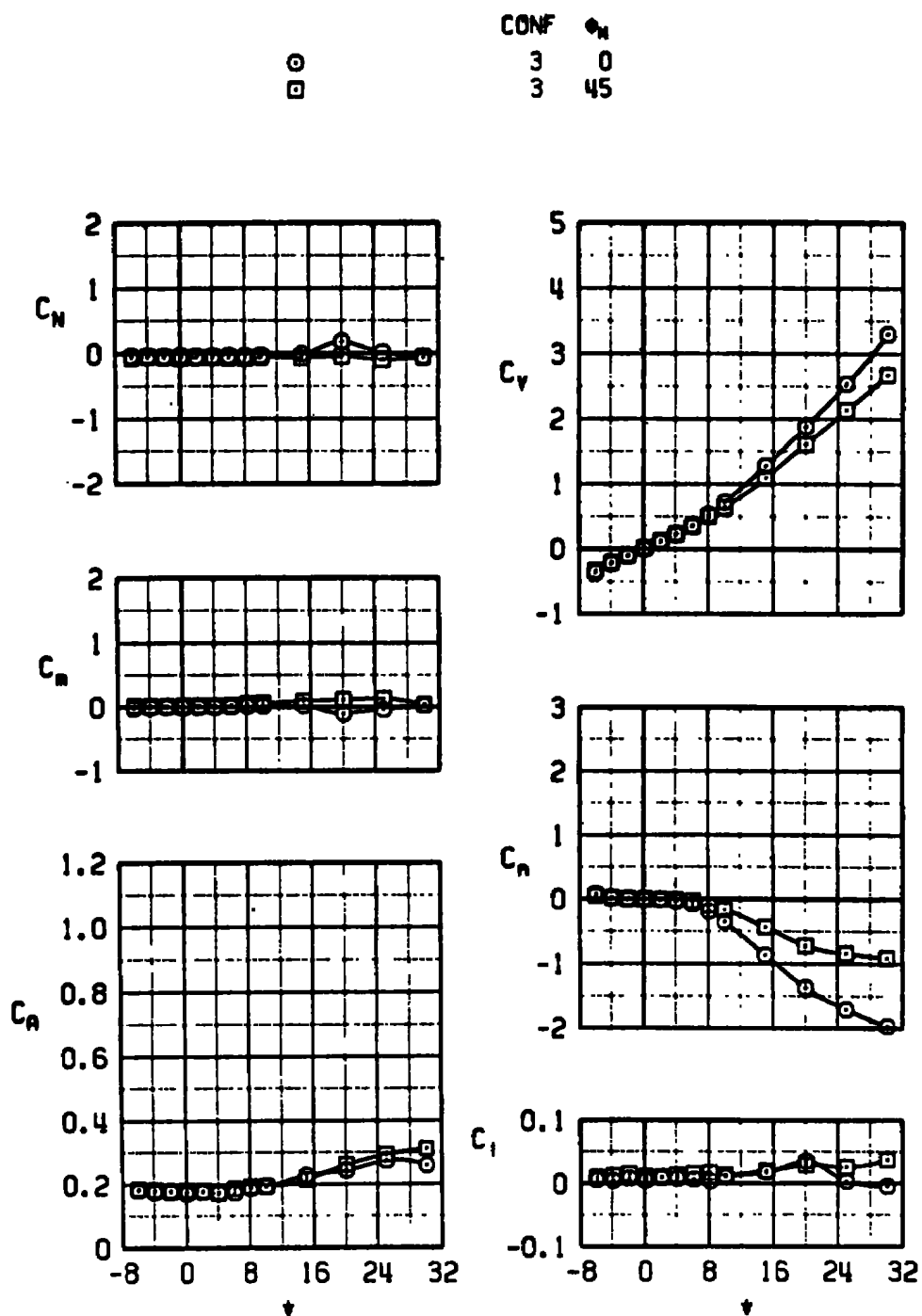
b. $M_\infty = 0.7$
Figure 13. Continued.
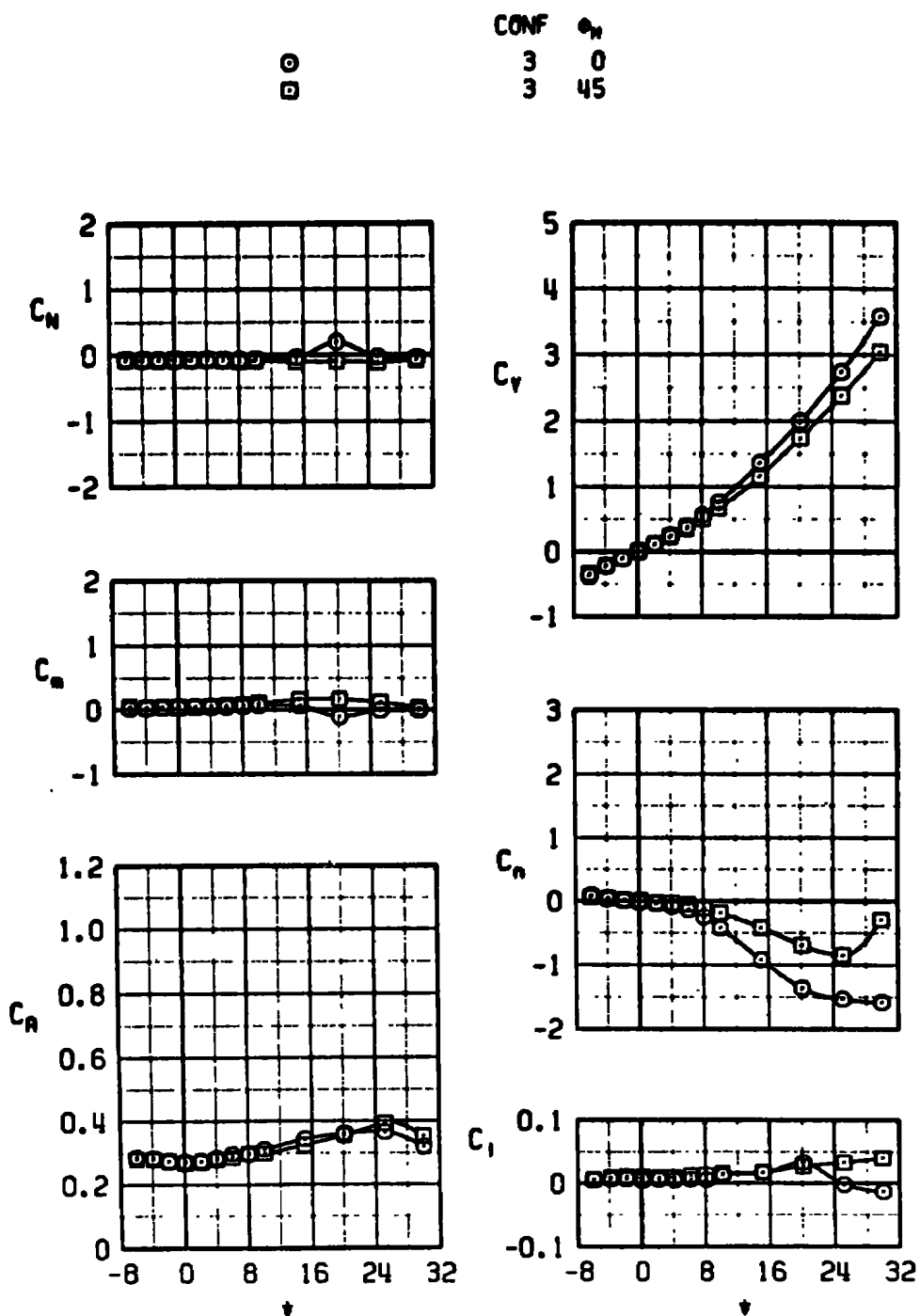
c. $M_\infty = 0.9$
Figure 13. Continued.

31
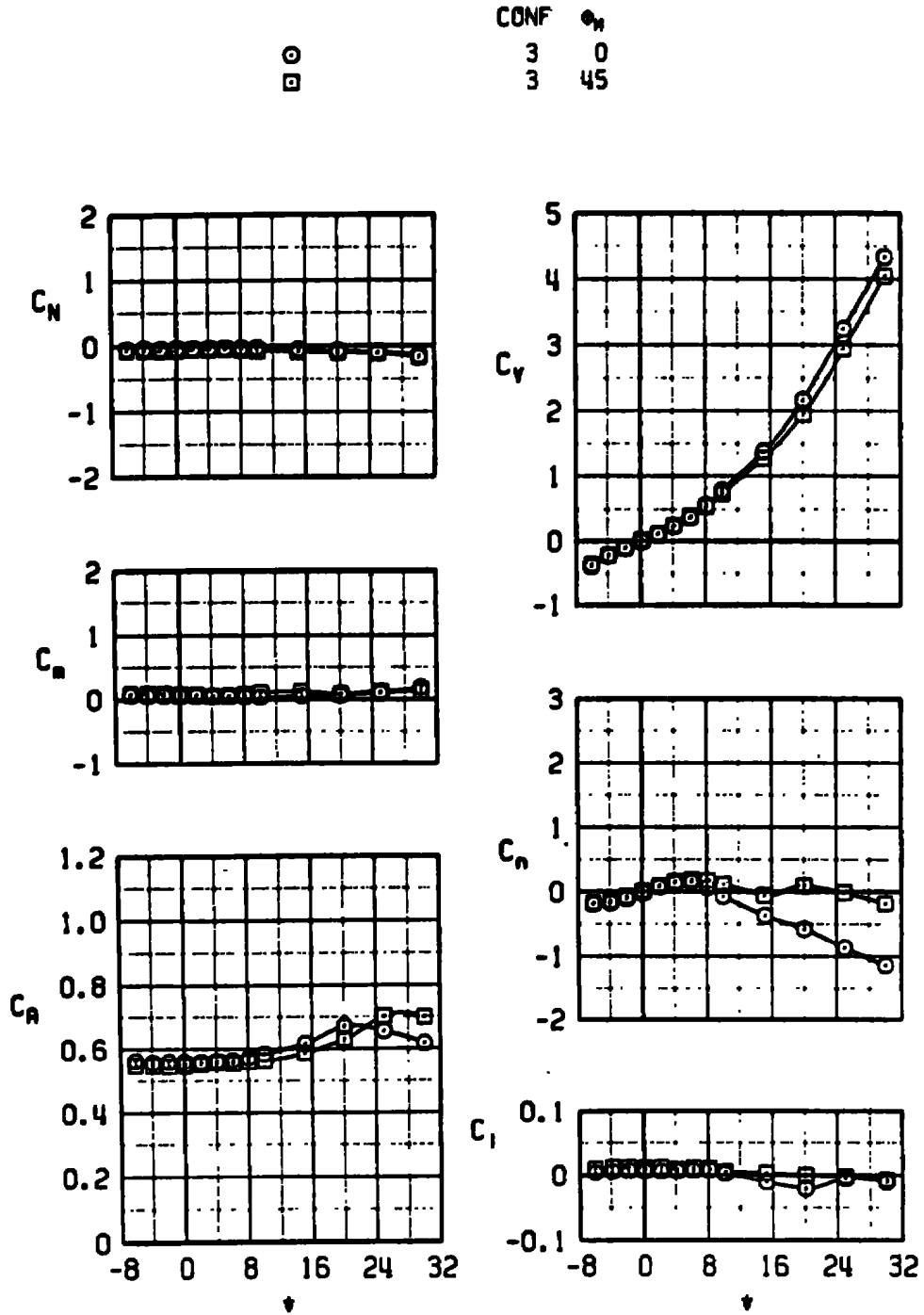
d. $M_\infty = 1.1$
Figure 13. Concluded.
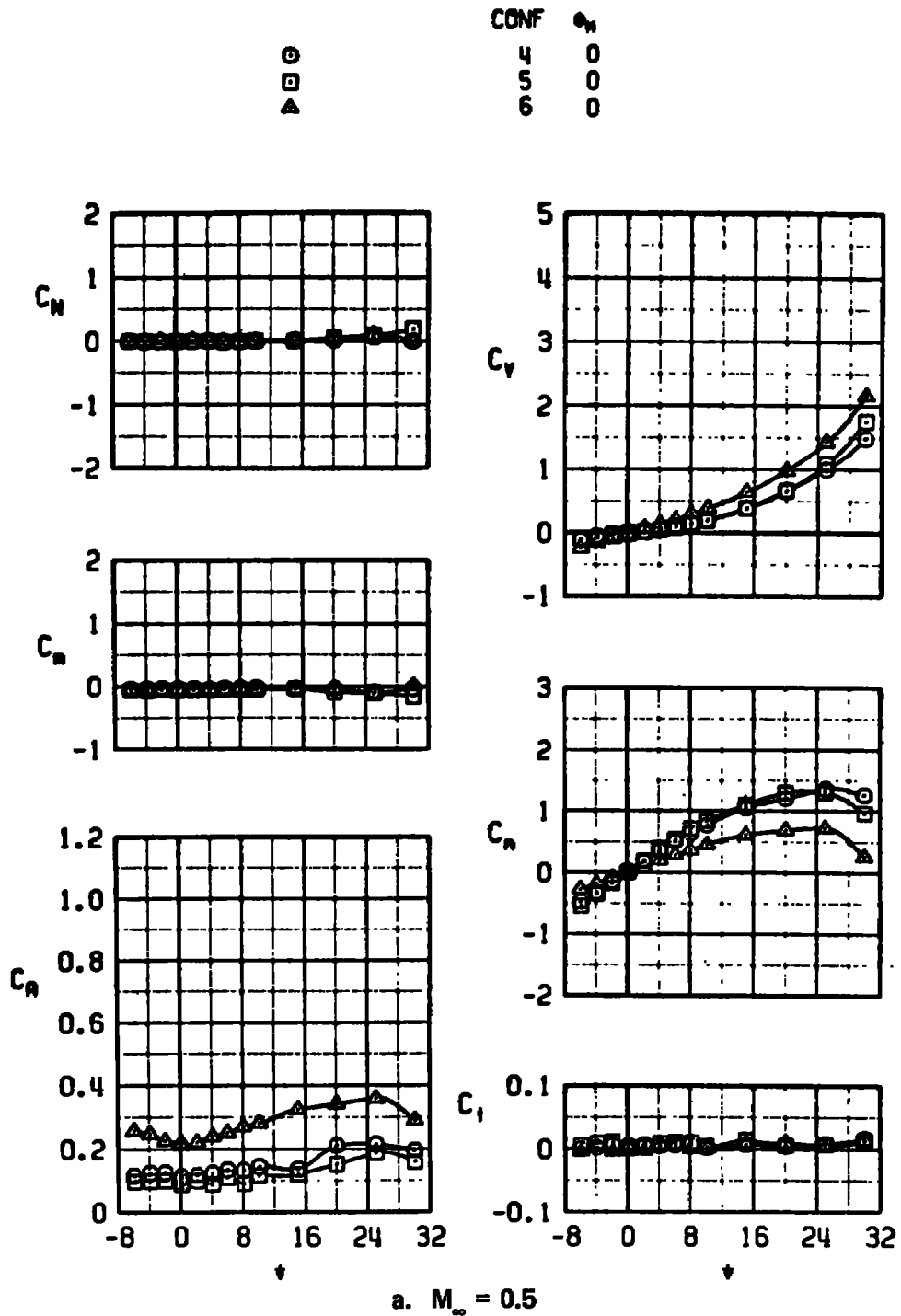
a. $M_\infty = 0.5$

Figure 14. Comparison of free-stream aerodynamic coefficients versus yaw angle
for configurations 4, 5, and 6.
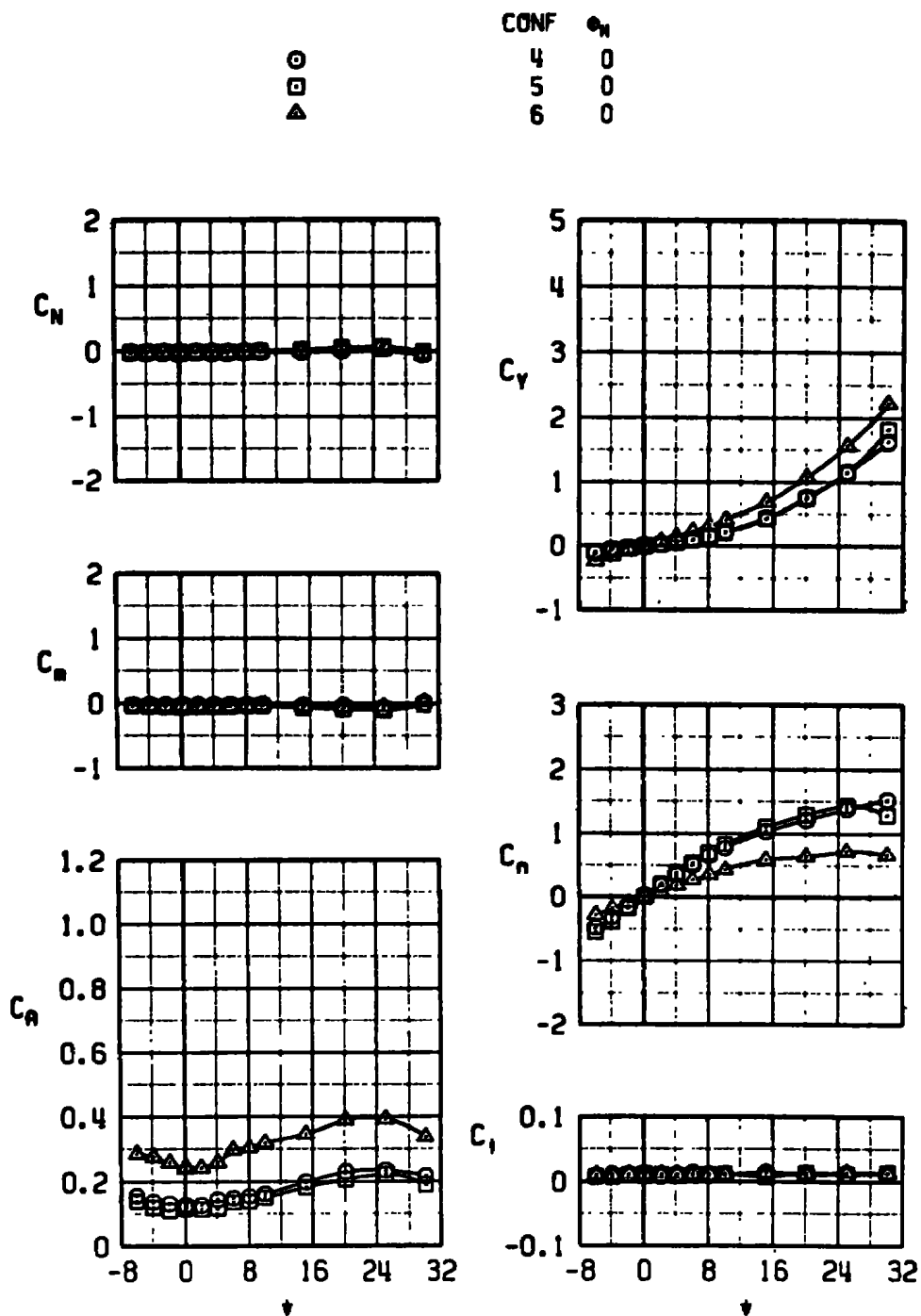
b. $M_\infty = 0.7$
Figure 14. Continued.
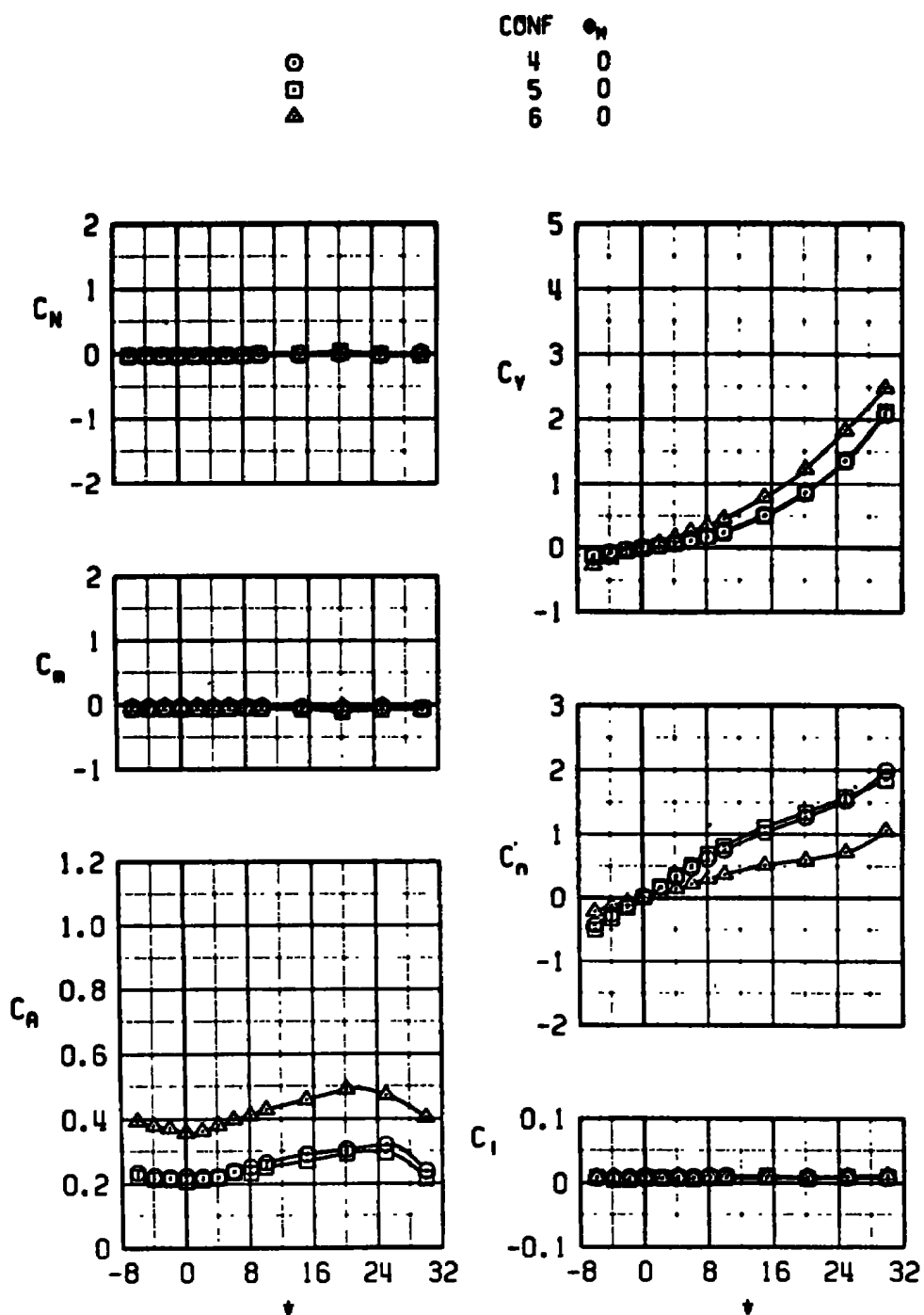
c. $M_\infty = 0.9$
Figure 14. Continued.
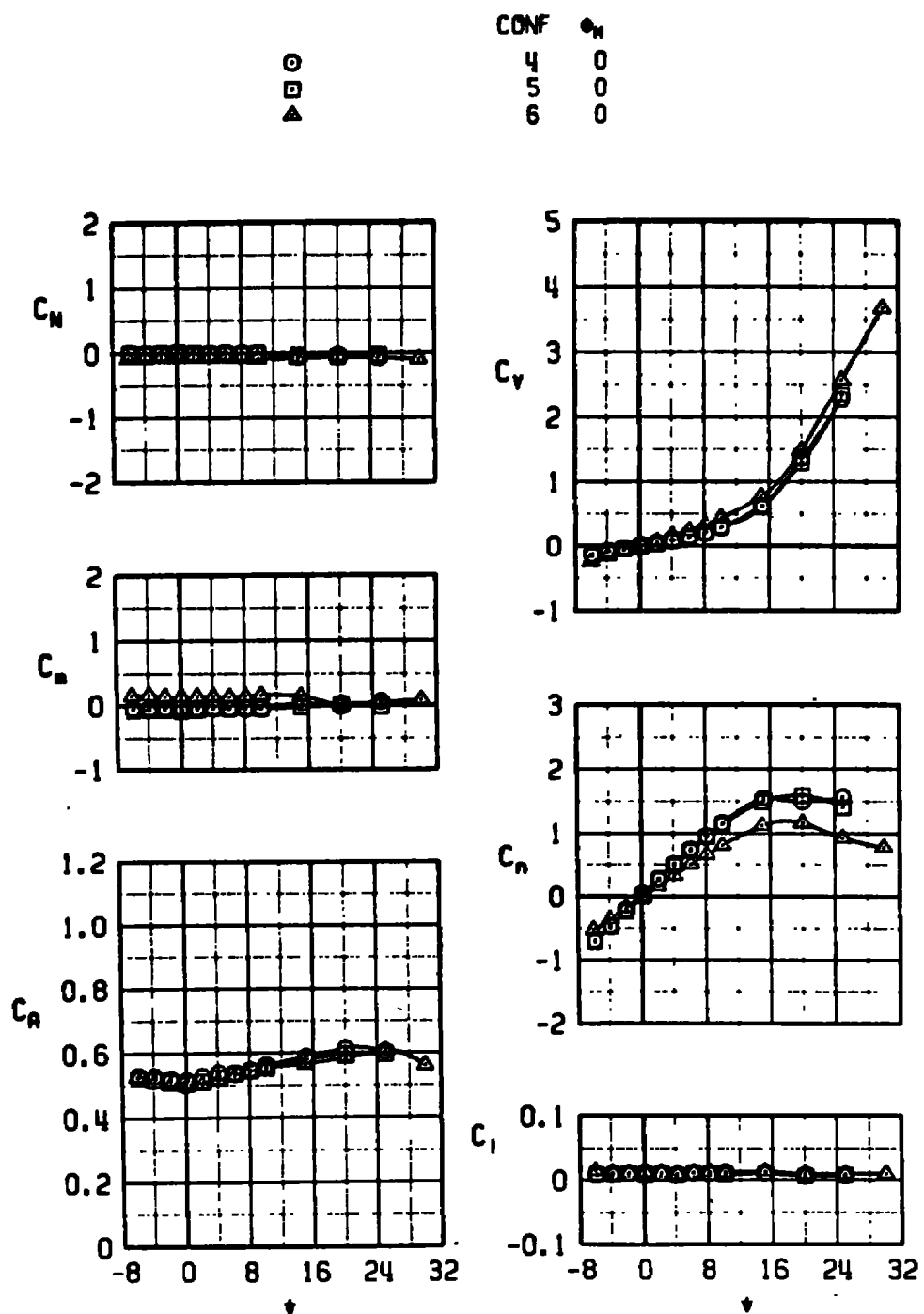
d. $M_\infty = 1.1$
Figure 14. Concluded.

CONF	ϕ_M	α	X
⊙	1	0	1	0
▣	1	0	4	0
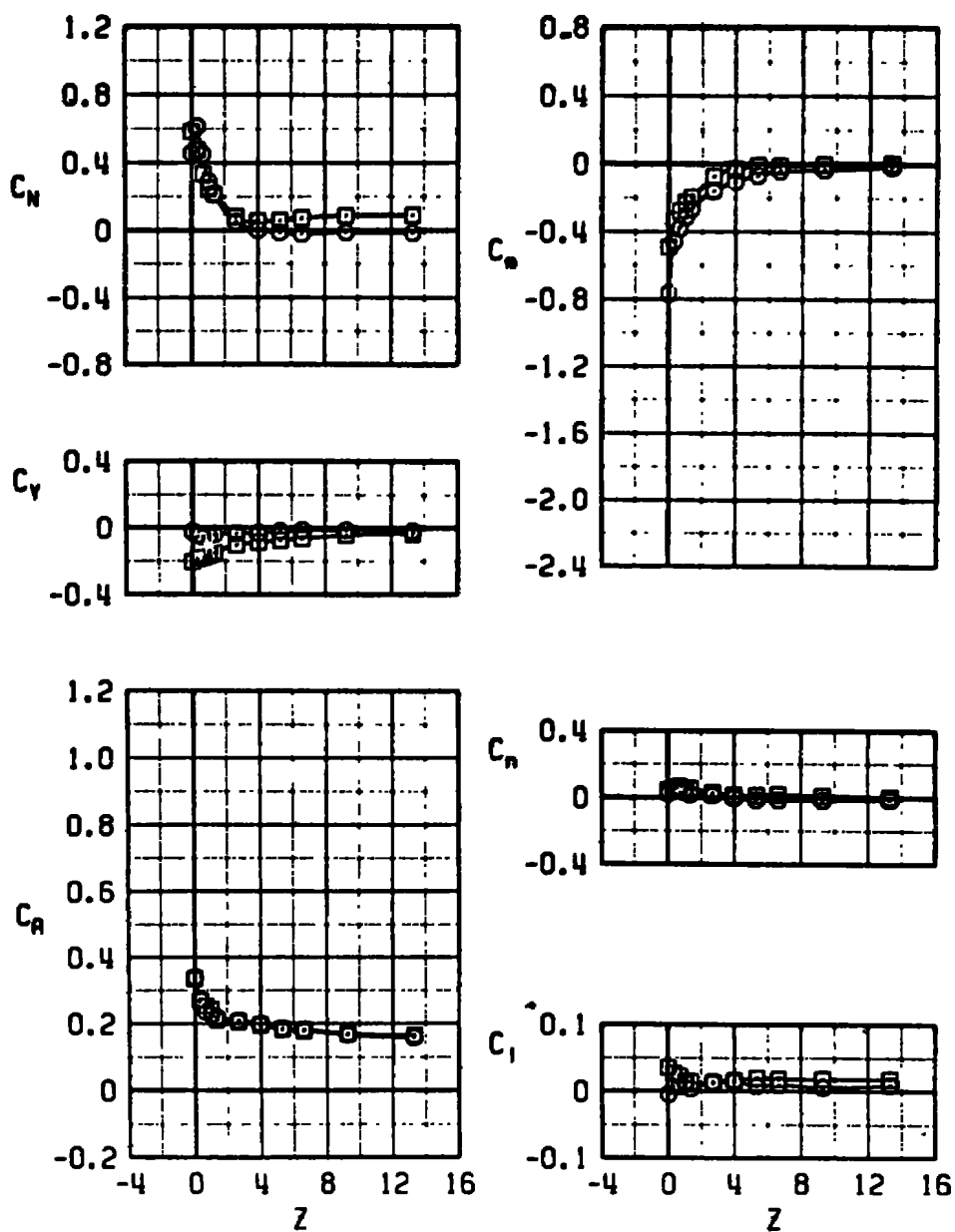
a. $M_\infty = 0.5$

Figure 15. Flow-field aerodynamic coefficients versus Z for configuration 1 at $\phi_M = 0$.
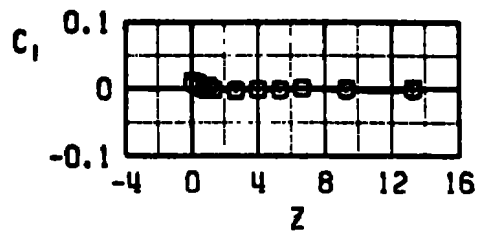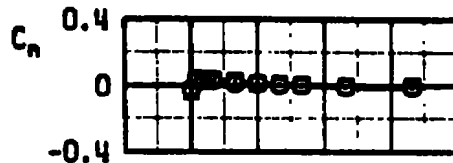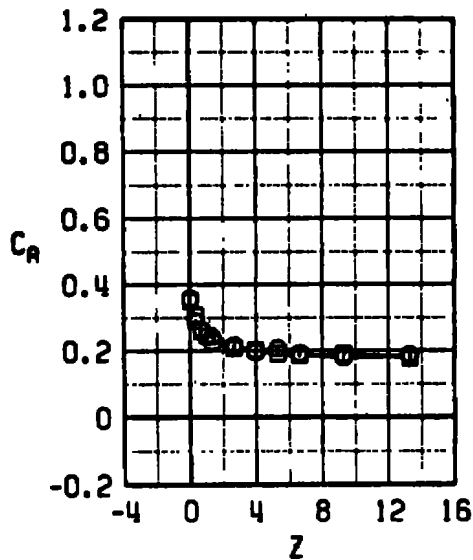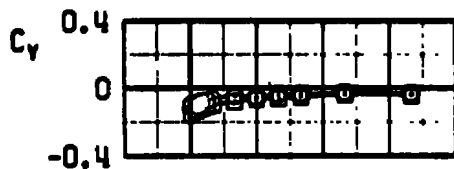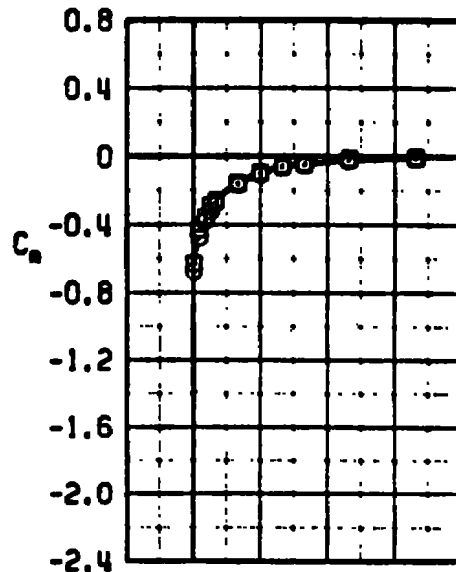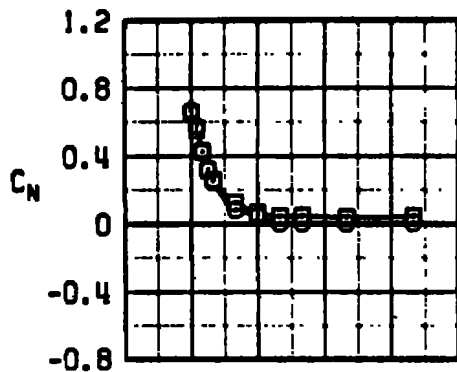
b. $M_\infty = 0.7$
Figure 15. Continued.
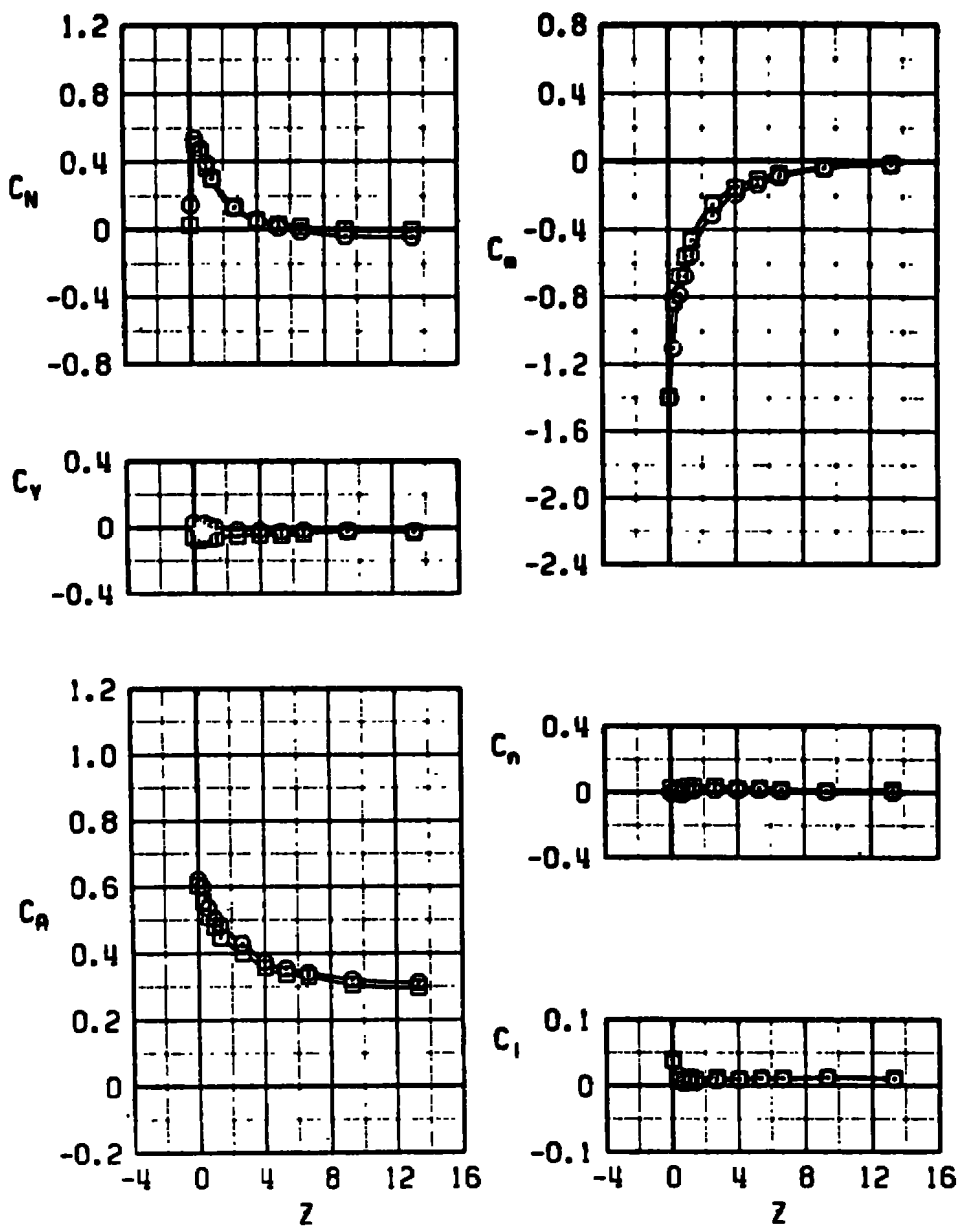
c. $M_\infty = 0.9$
Figure 15. Continued.
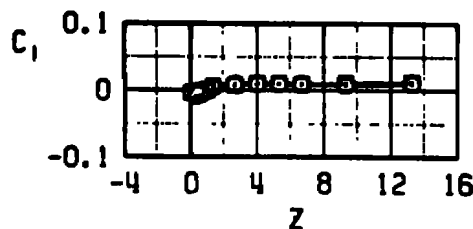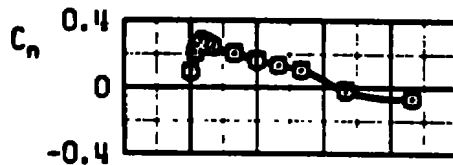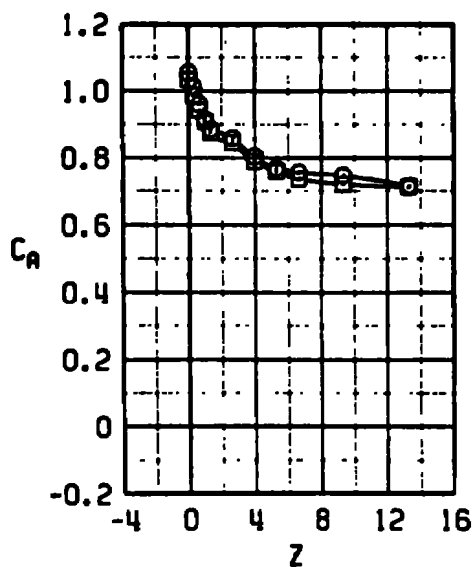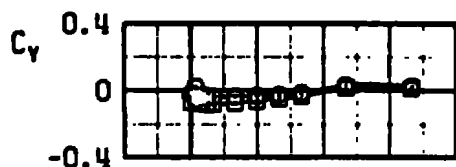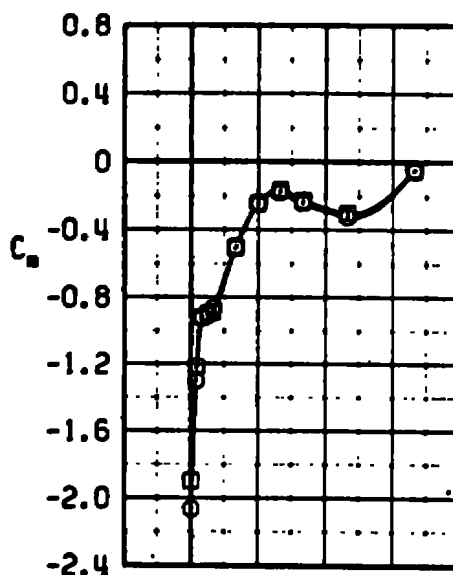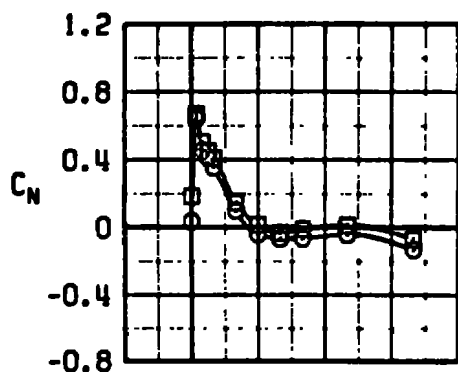
d. $M_\infty = 1.1$

Figure 15. Concluded.
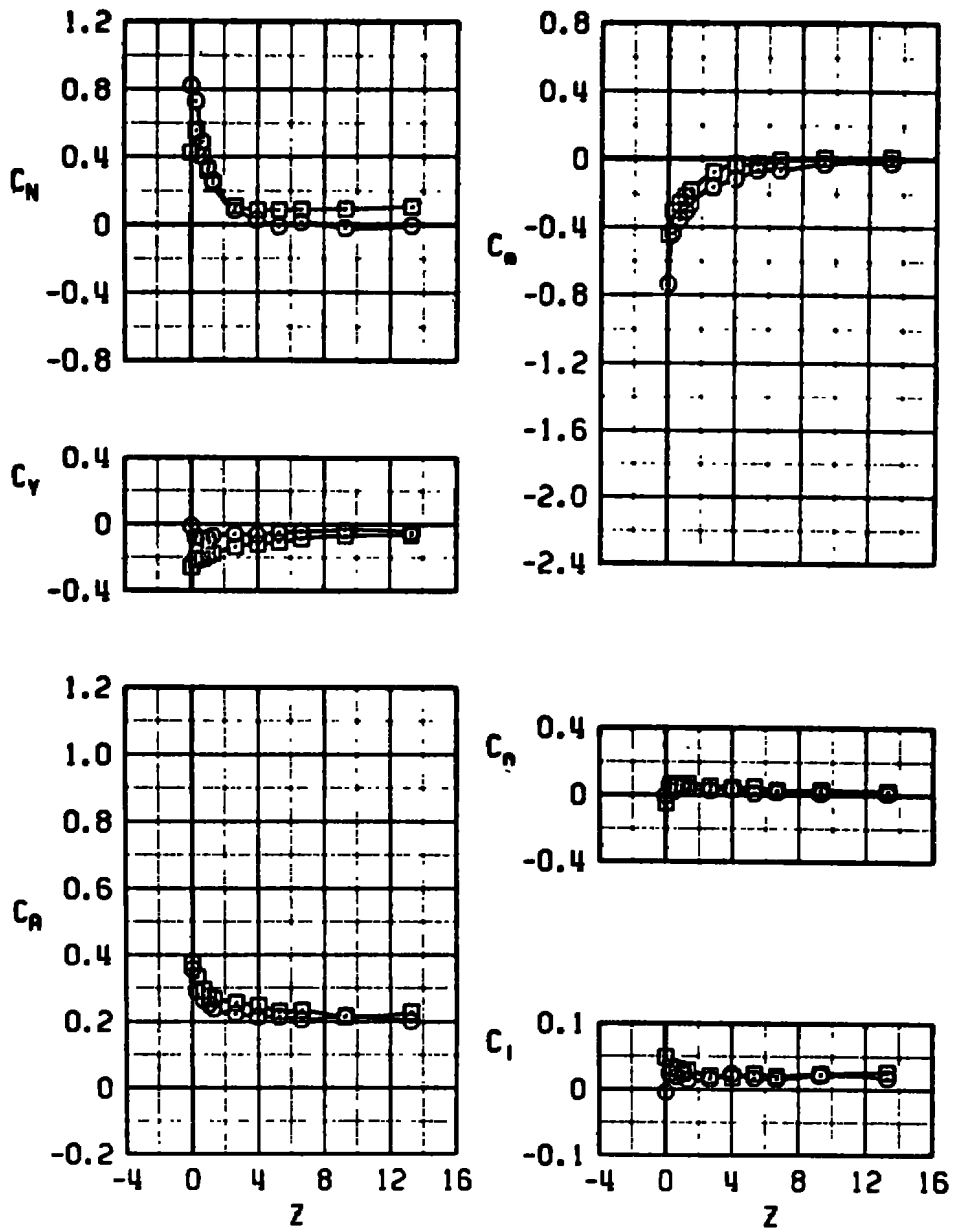
a. $M_\infty = 0.5$

Figure 16. Flow-field aerodynamic coefficients versus Z for
configuration 2 at $\phi_M = 0$.
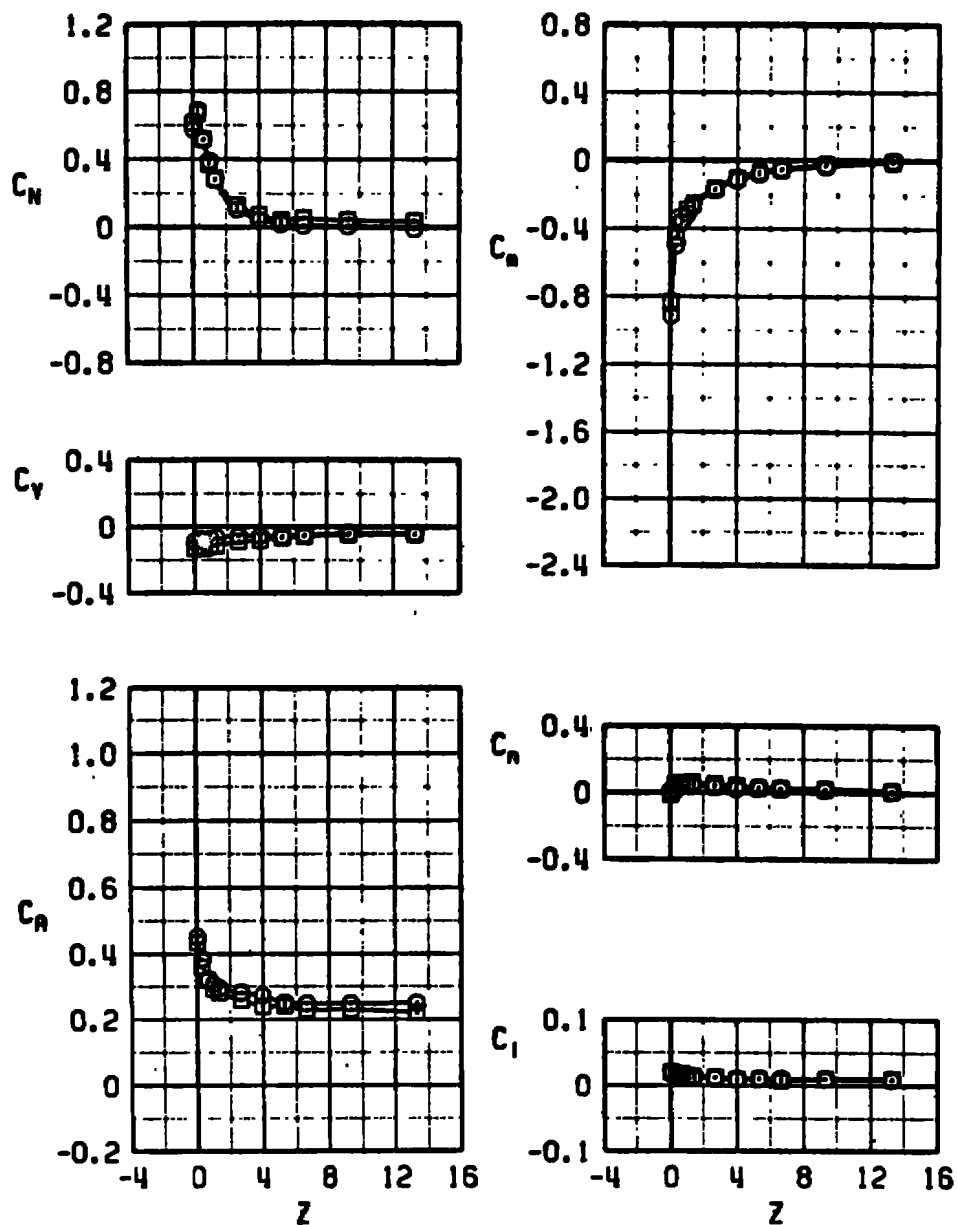
b. $M_\infty = 0.7$

Figure 16. Continued.

c. $M_\infty = 0.9$

Figure 16. Continued.

CONF	ϕ_M	α	X
⊙	2	0 0	0
⊡	2	0 1	0
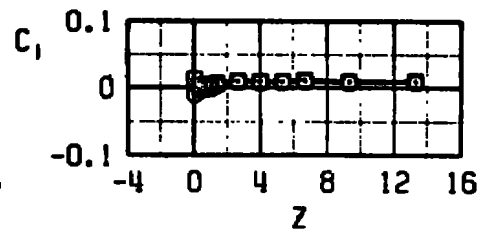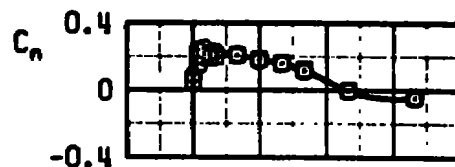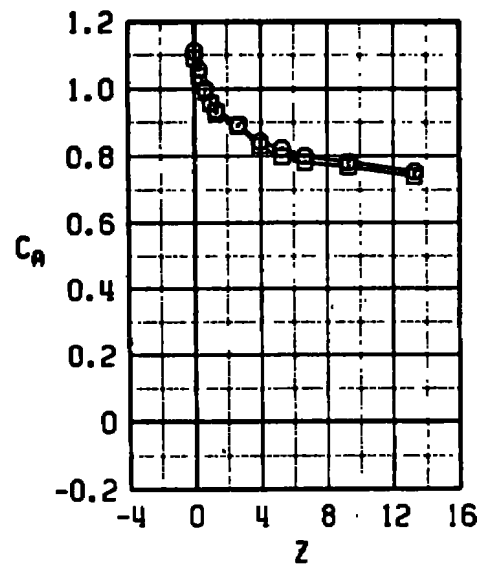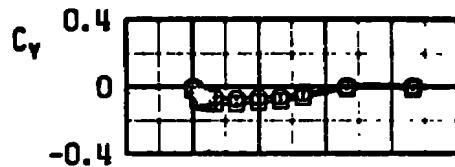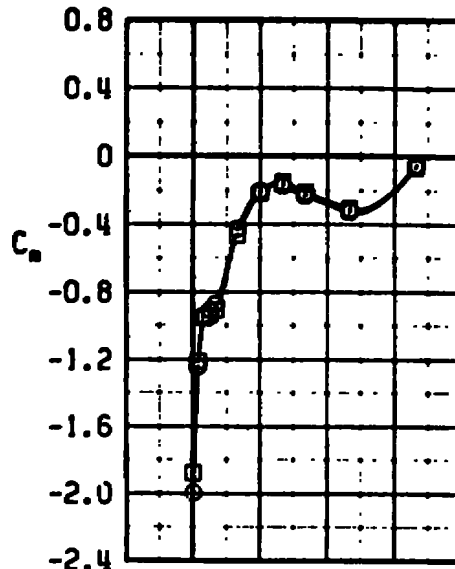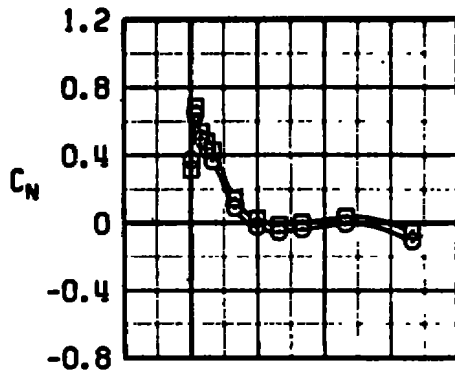
d. $M_\infty = 1.1$

Figure 16. Concluded.
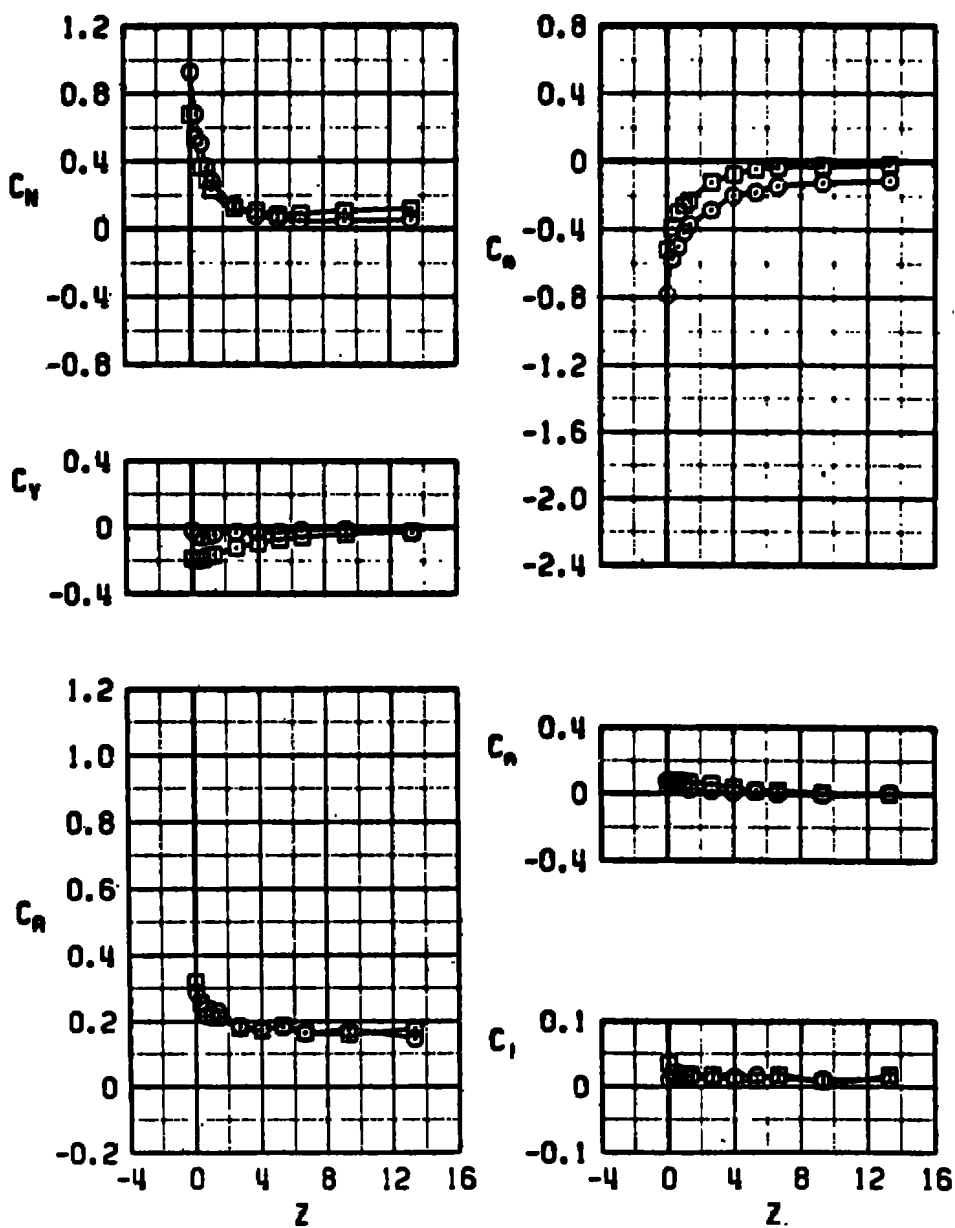
a. $M_\infty = 0.5$

Figure 17. Flow-field aerodynamic coefficients versus Z for
configuration 3 at $\phi_M = 0$.
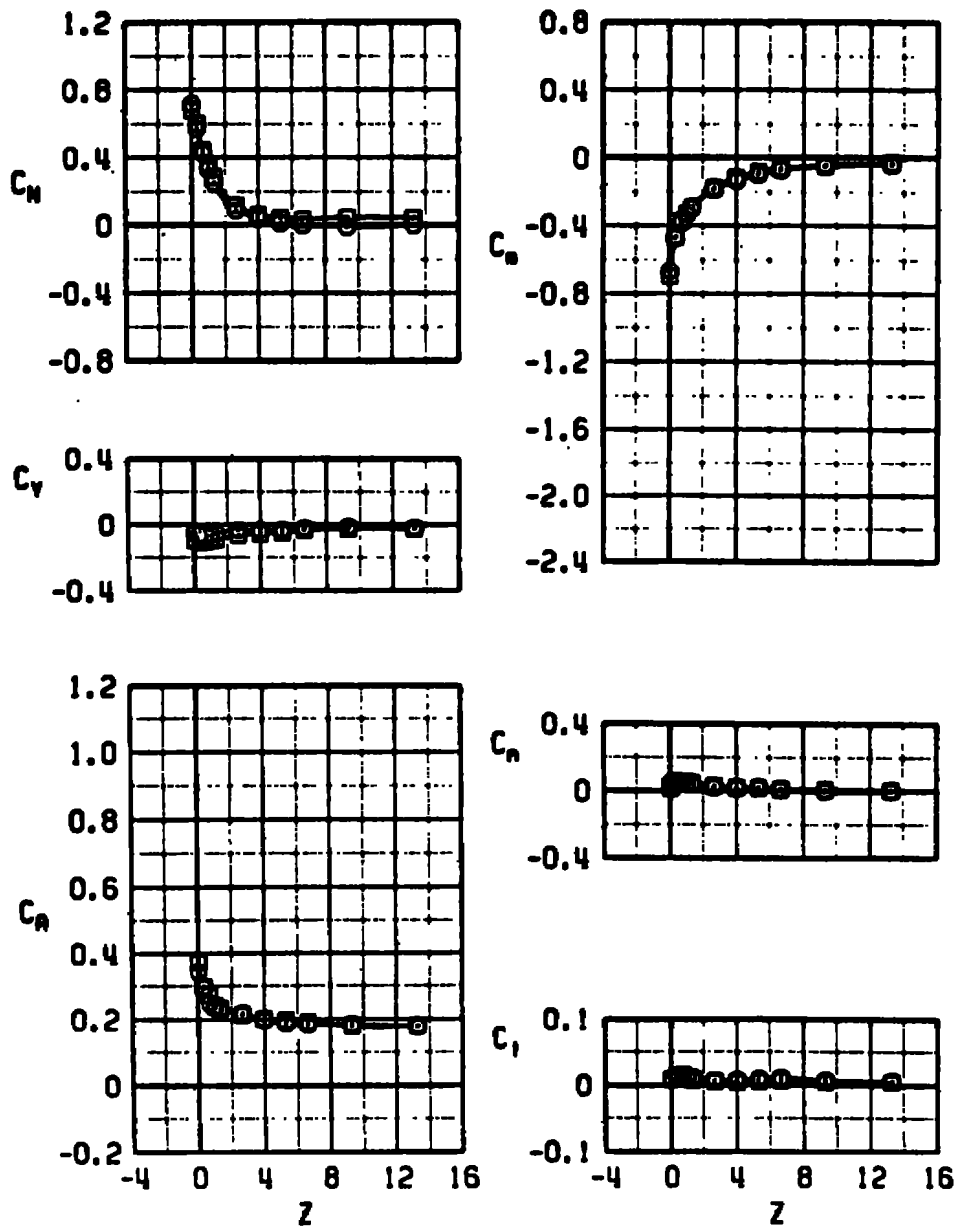
b. $M_\infty = 0.7$
Figure 17. Continued.

	CONF	ϕ_M	α	X
⊙	3	0	0	0
◻	3	0	1	0
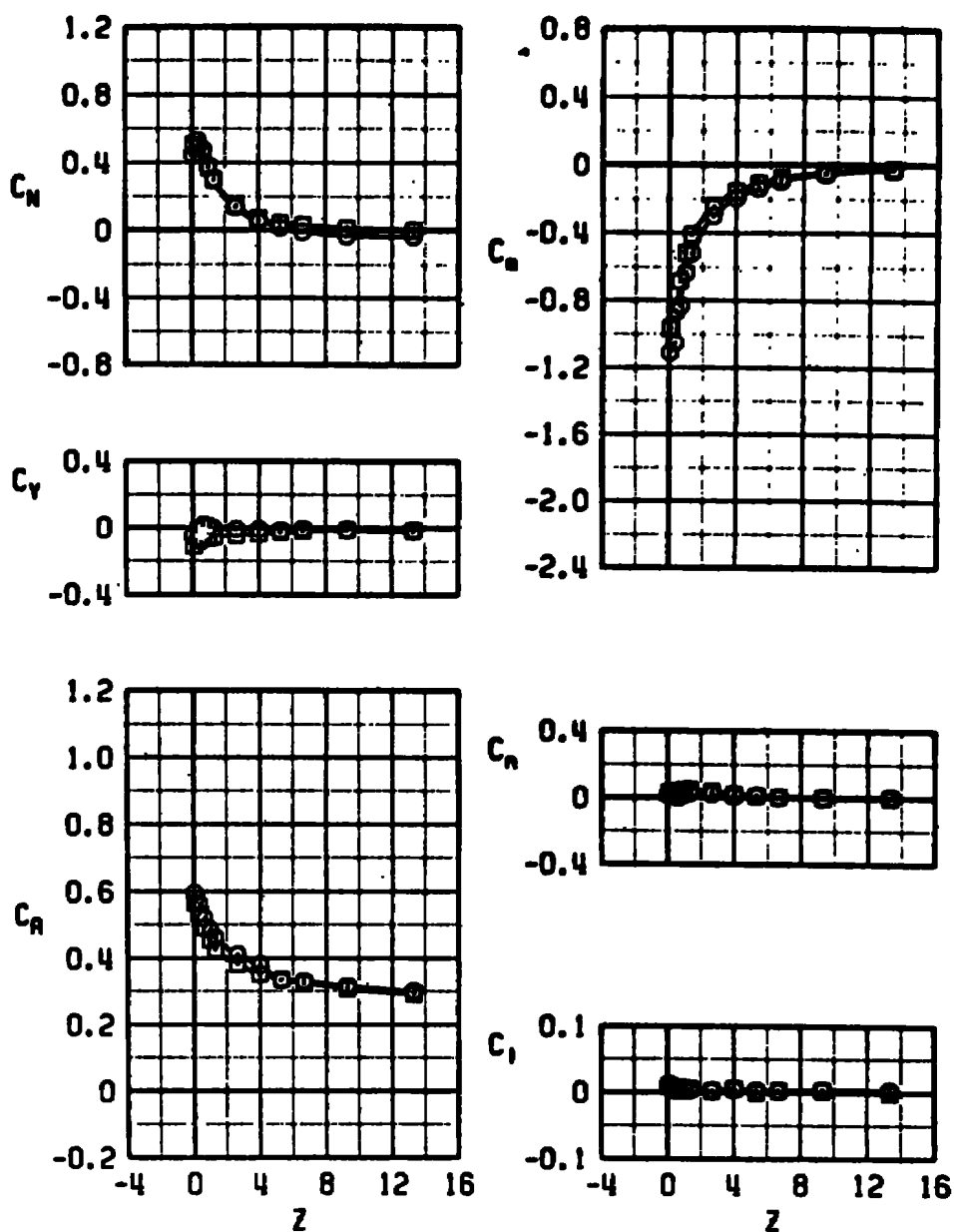
c. $M_\infty = 0.9$

Figure 17. Continued.

47
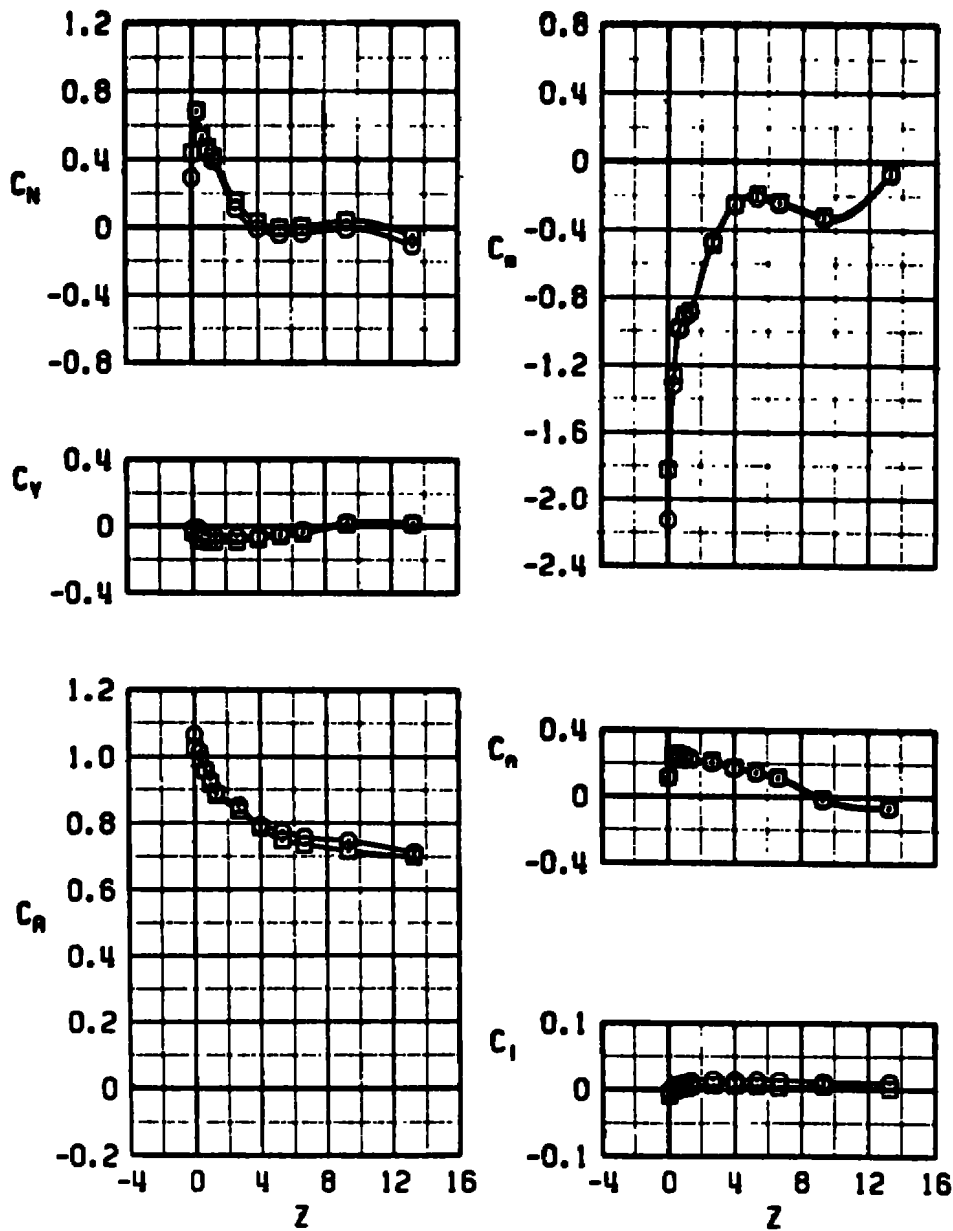
d. $M_\infty = 1.1$

Figure 17. Concluded.
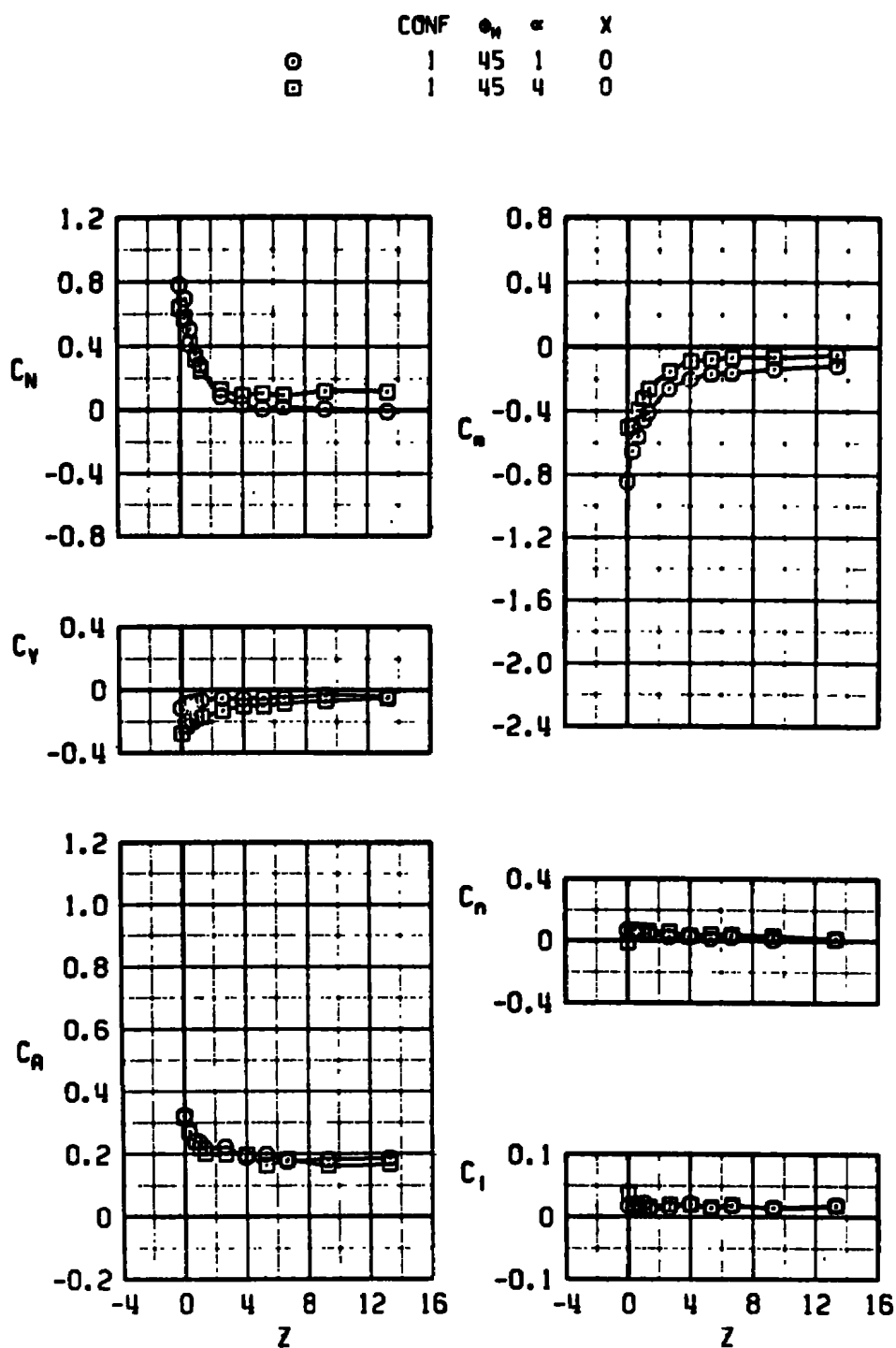
a. $M_\infty = 0.5$

Figure 18. Flow-field aerodynamic coefficients versus Z for configuration 1 at ϕ_M = 45 deg.
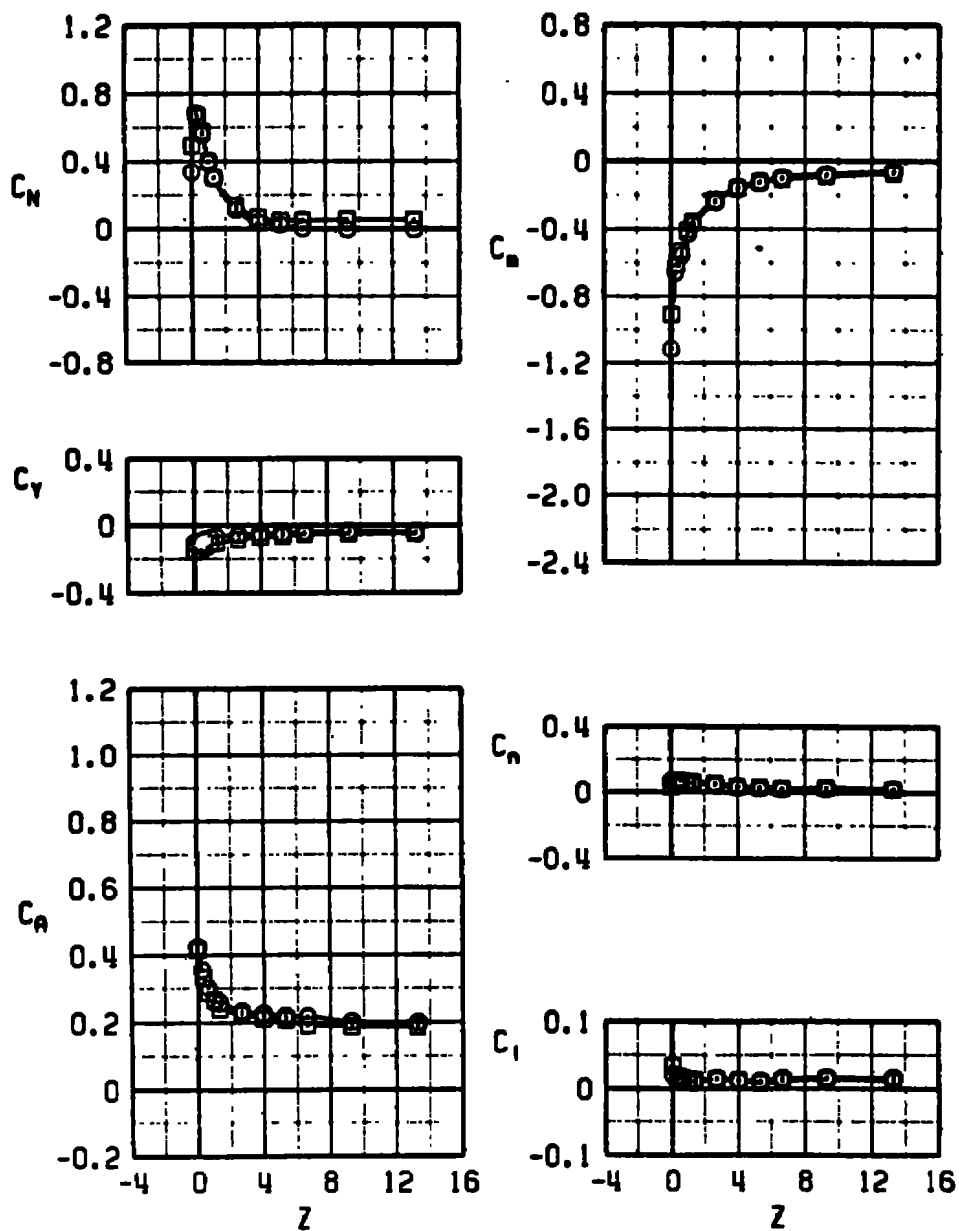
b. $M_\infty = 0.7$
Figure 18. Continued.
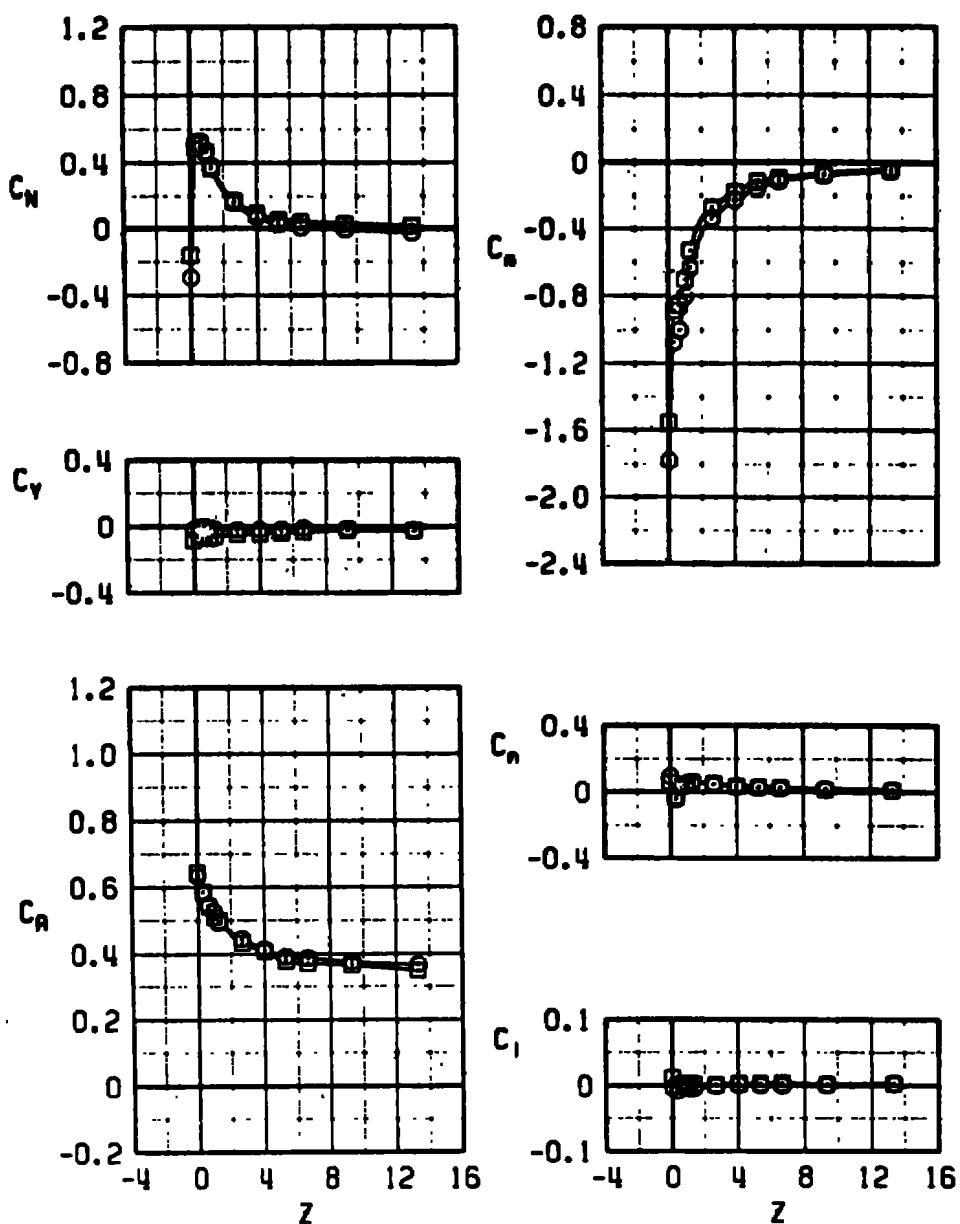
c. $M_\infty = 0.9$
Figure 18. Continued.
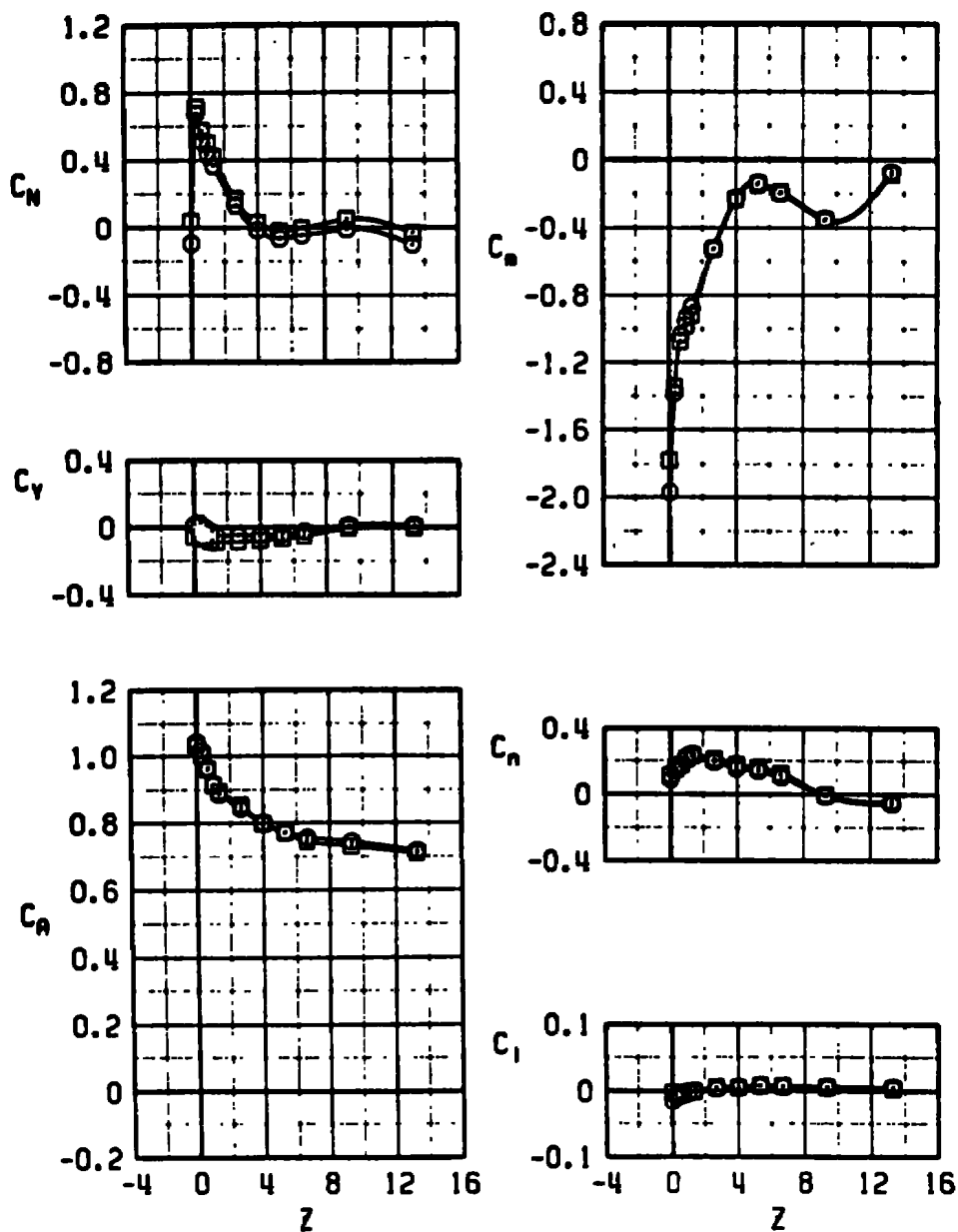
d. $M_\infty = 1.1$
Figure 18. Concluded.
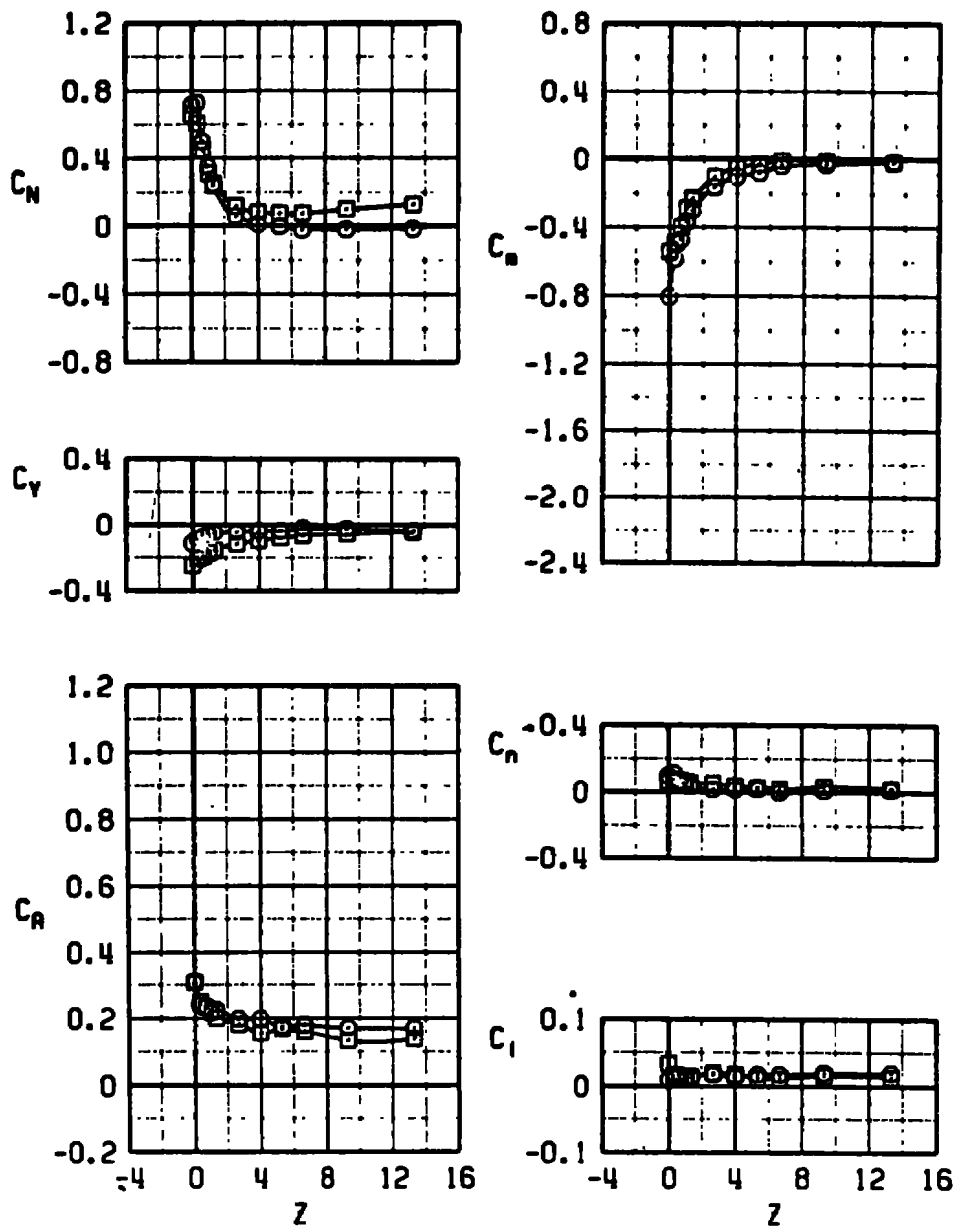
a. $M_\infty = 0.5$

Figure 19. Flow-field aerodynamic coefficients versus Z for configuration 2 at $\phi_M = 45$ deg.
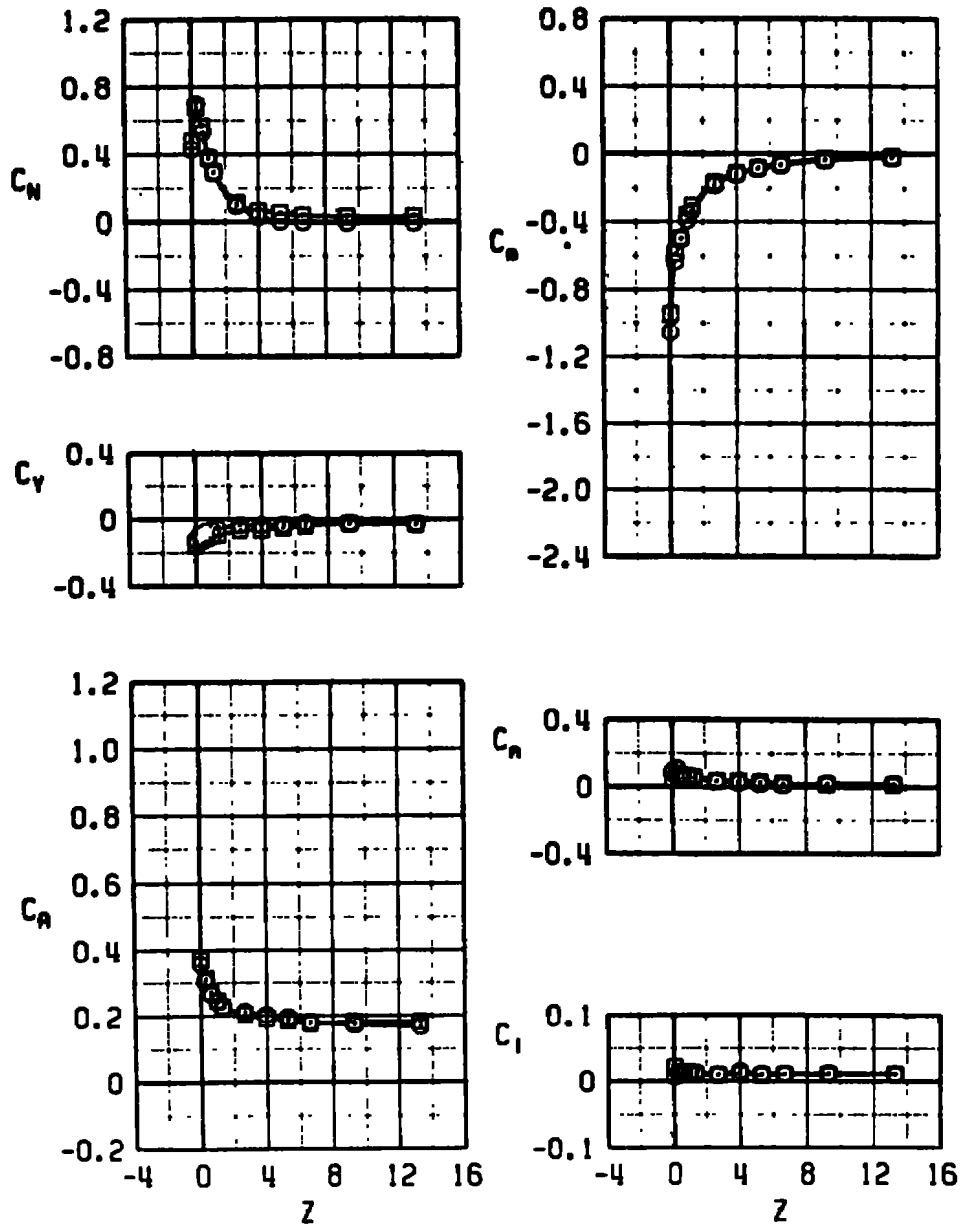
b. $M_\infty = 0.7$
Figure 19. Continued.
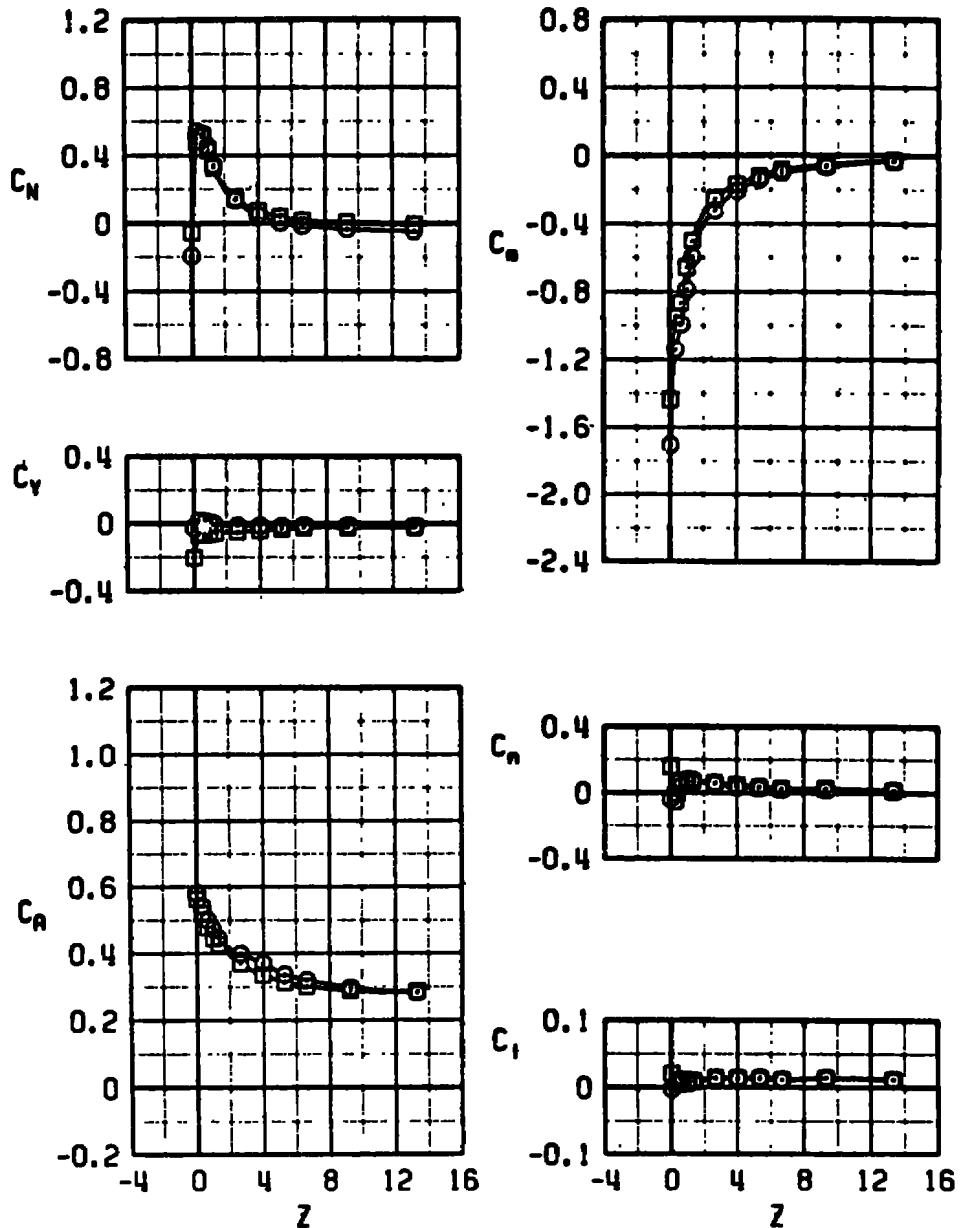
c. $M_\infty = 0.9$
Figure 19. Continued.
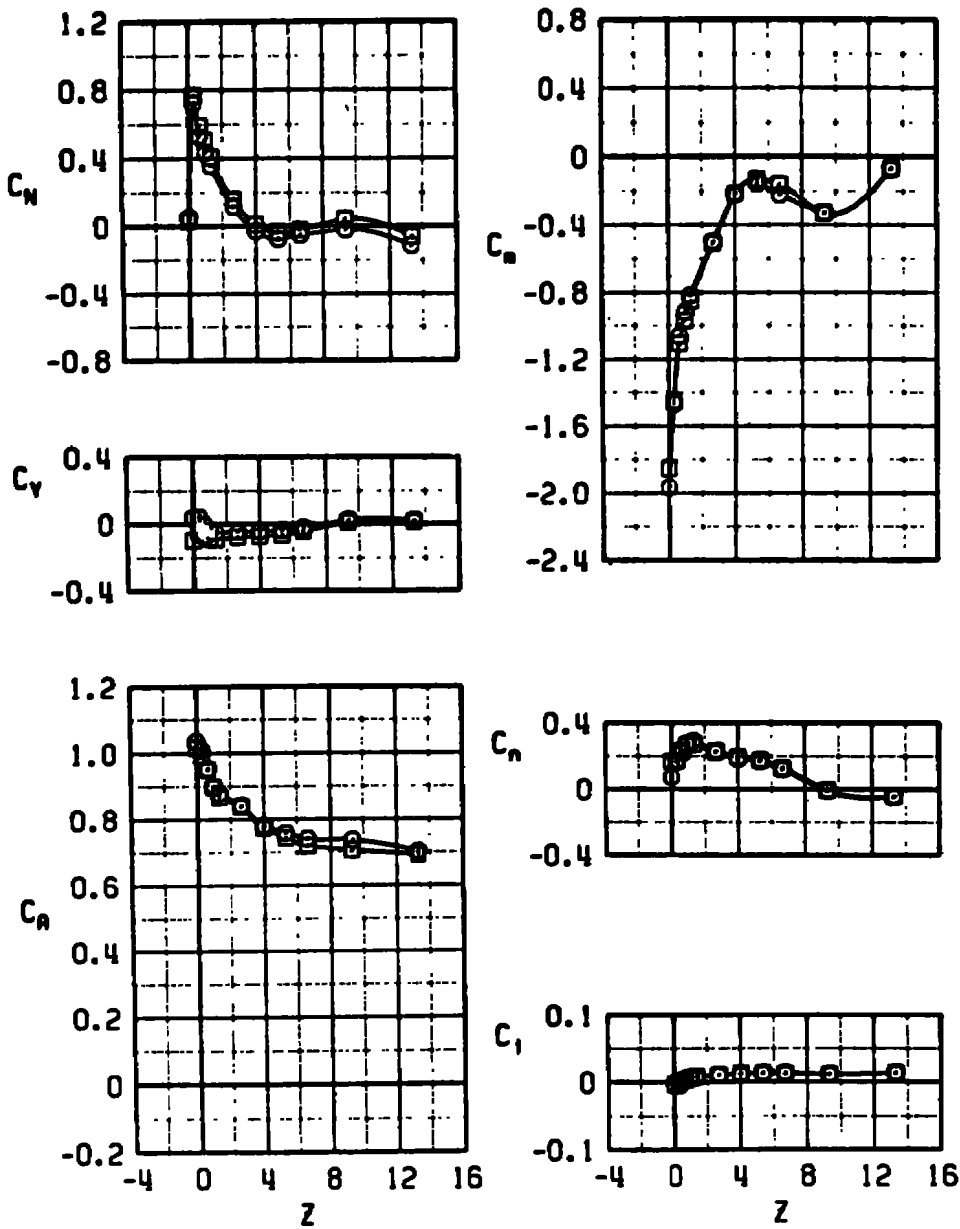
d. $M_\infty = 1.1$
Figure 19. Concluded.
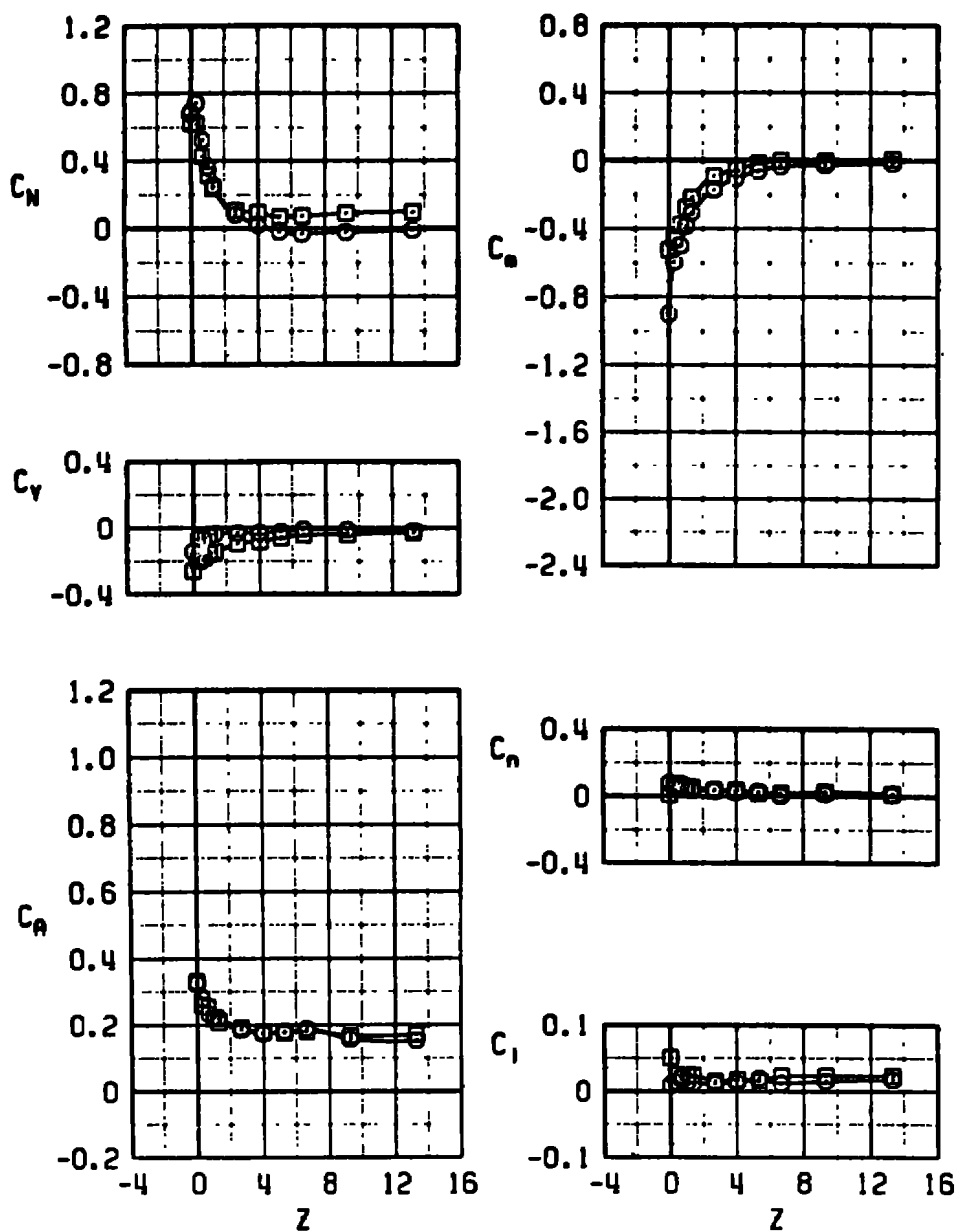
a. $M_\infty = 0.5$

Figure 20. Flow-field aerodynamic coefficients versus Z for configuration 3 at $\phi_M = 45$ deg.
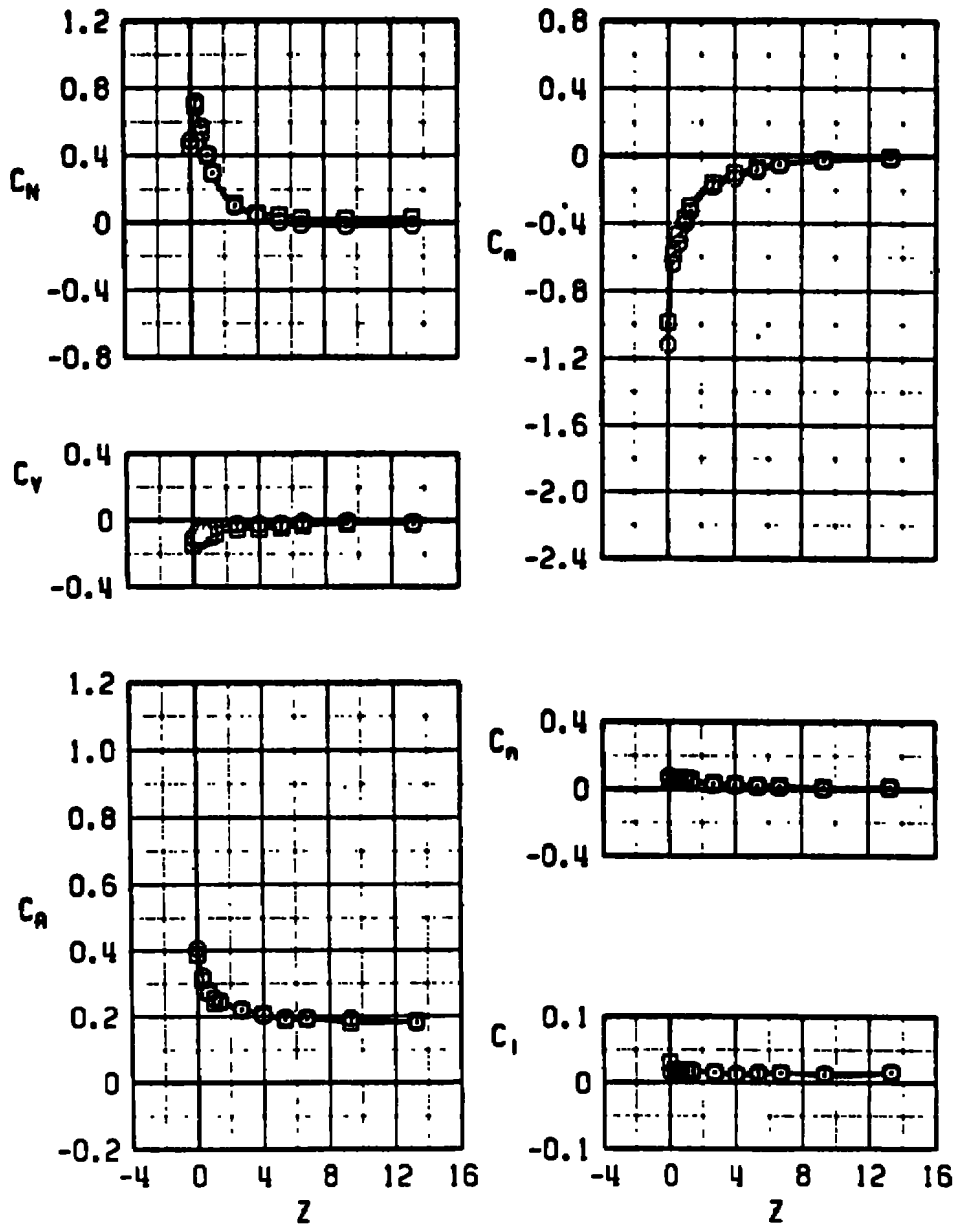
b. $M_\infty = 0.7$
Figure 20. Continued.

CONF	ϕ_M	α	X
⊙	3	45	0	0
⊡	3	45	1	0
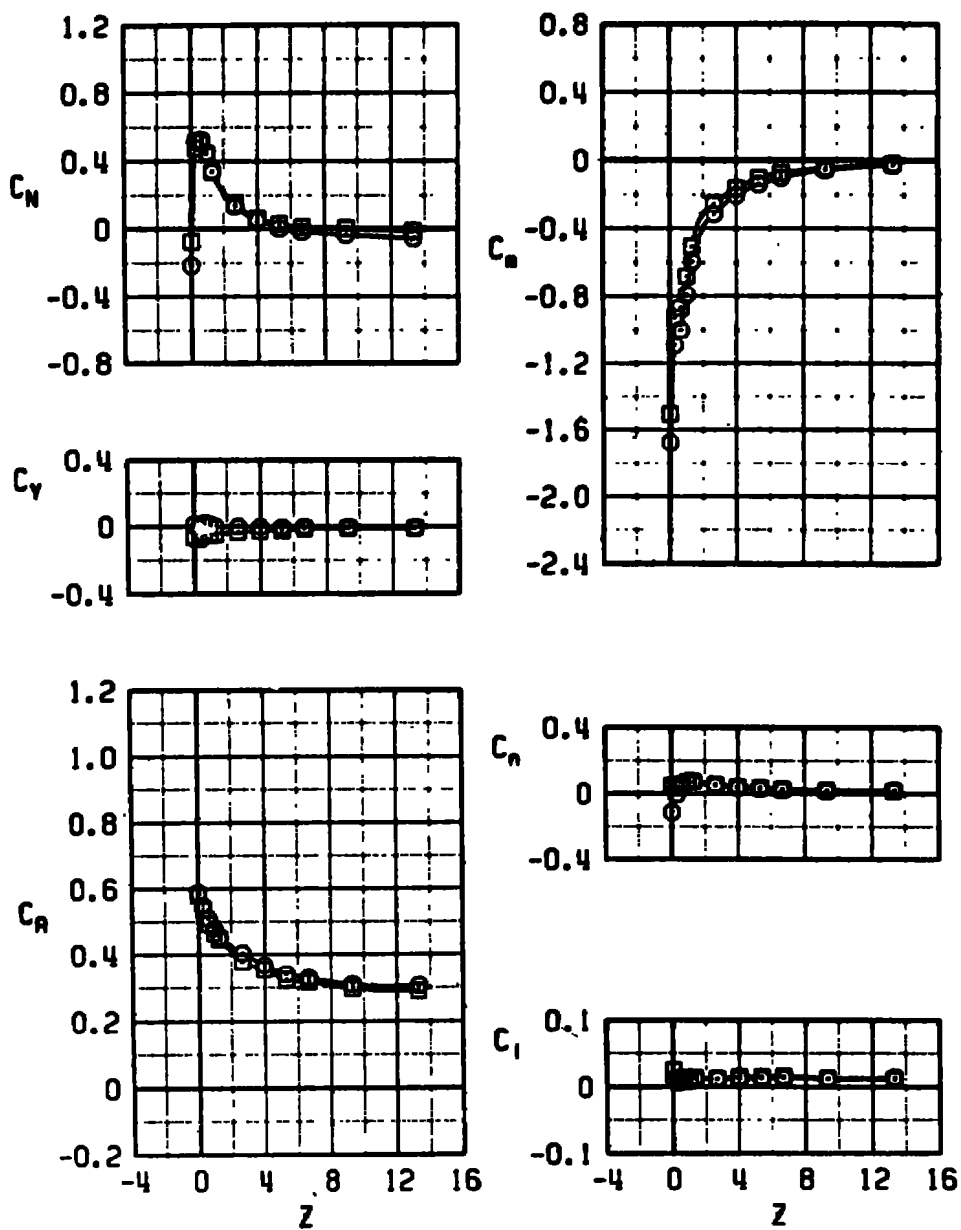
c. $M_\infty = 0.9$
Figure 20. Continued.
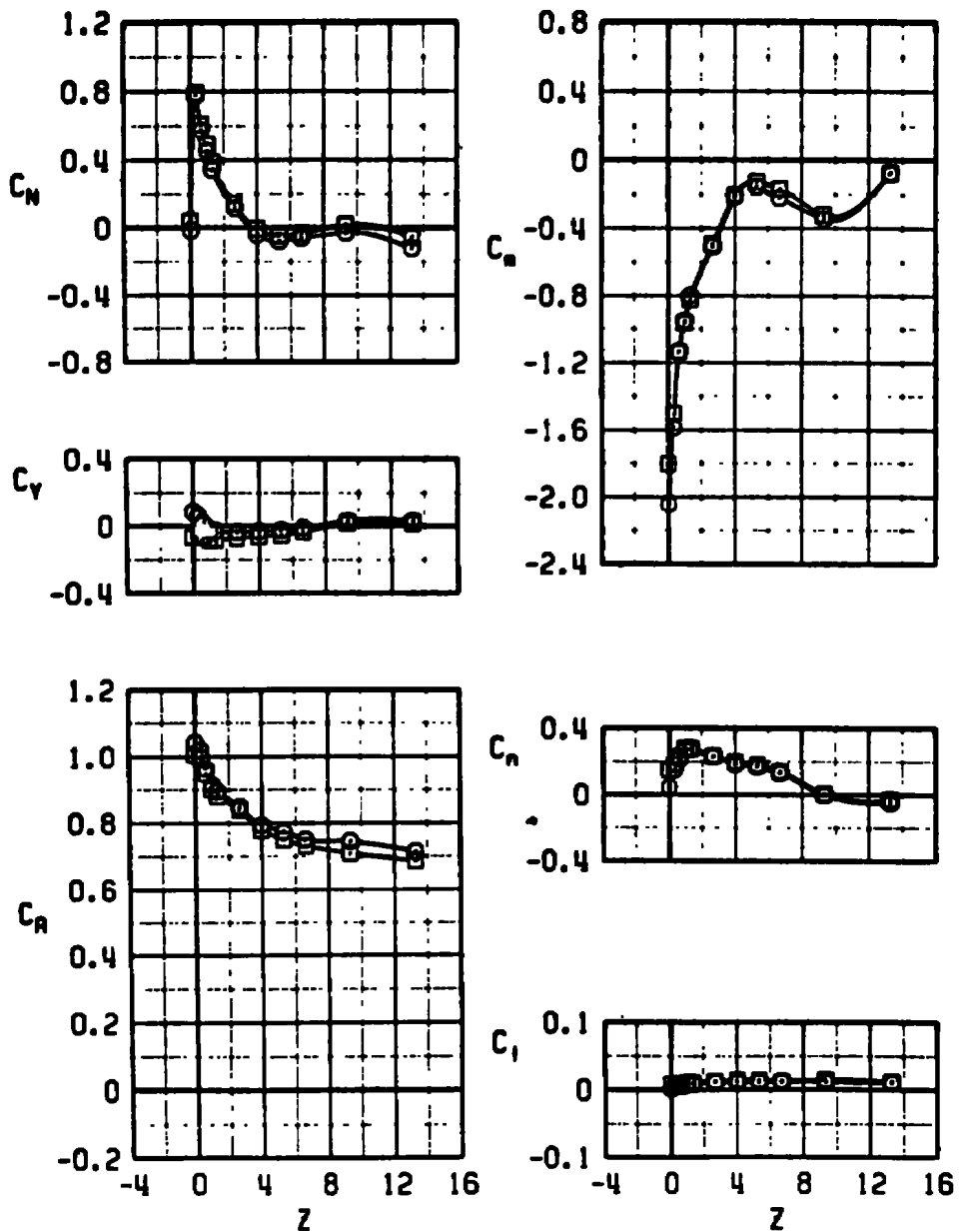
d. $M_\infty = 1.1$
Figure 20. Concluded.
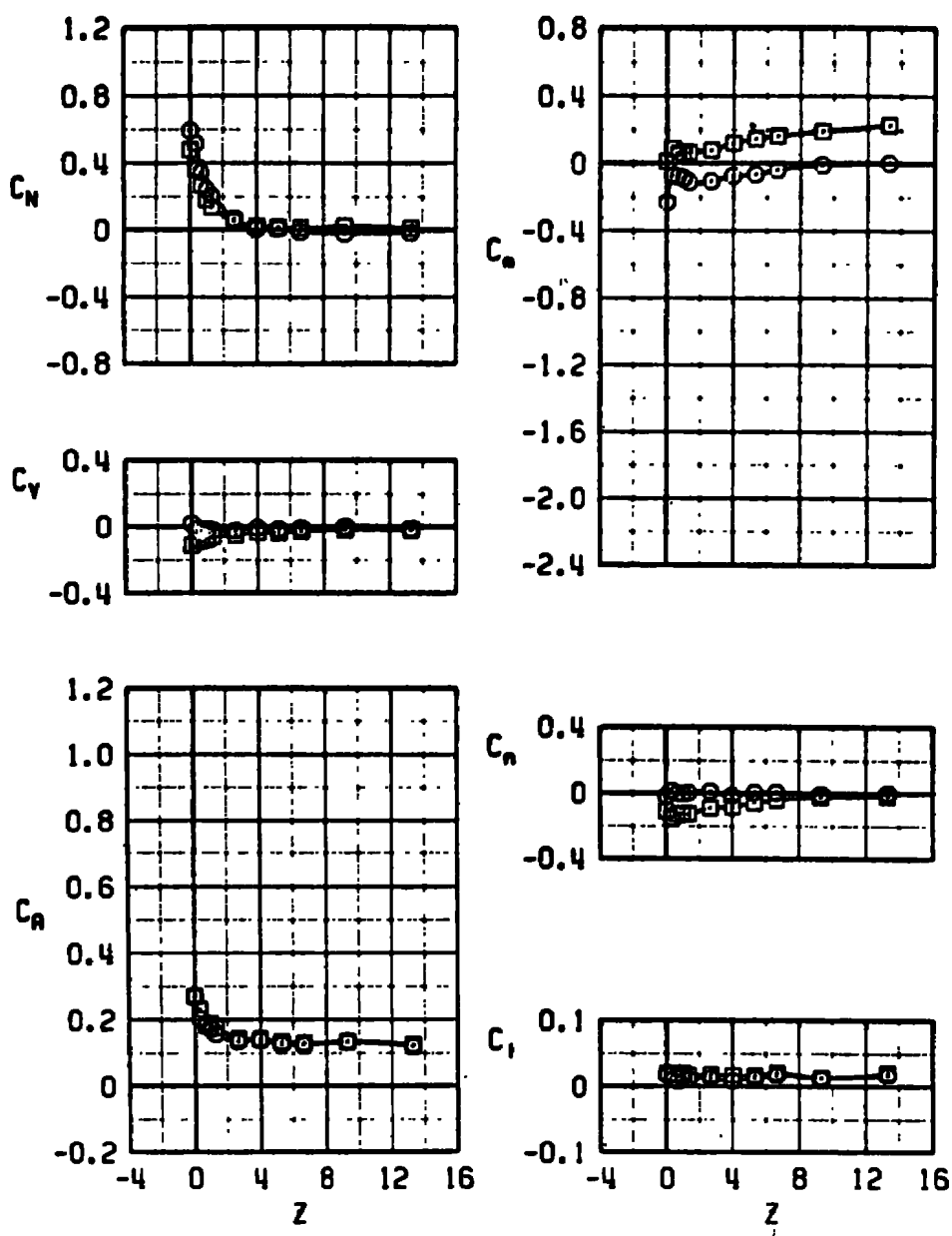
a. $M_\infty = 0.5$

Figure 21. Flow-field aerodynamic coefficients versus Z for configuration 4.
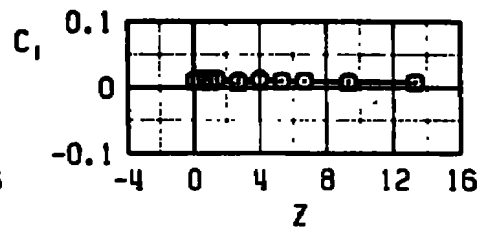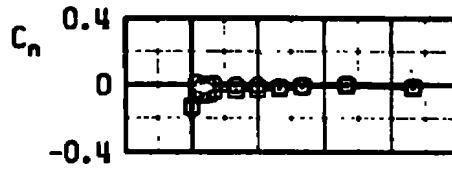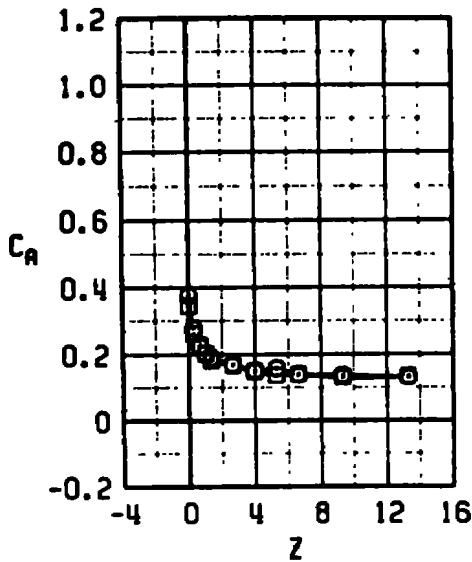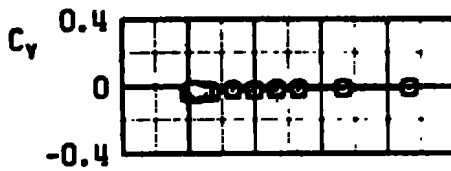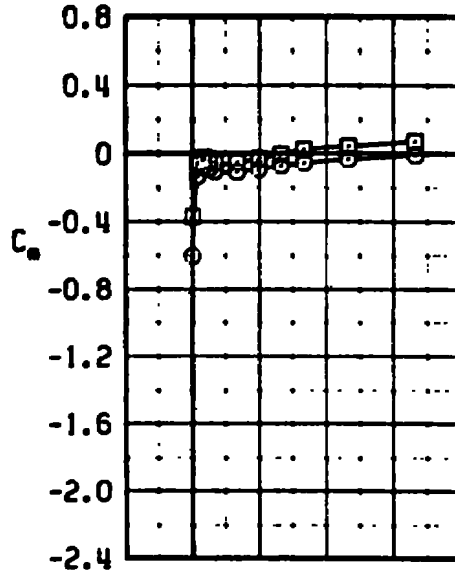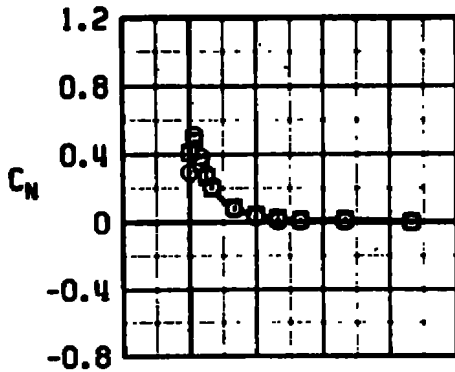
b. $M_\infty = 0.7$
Figure 21. Continued.
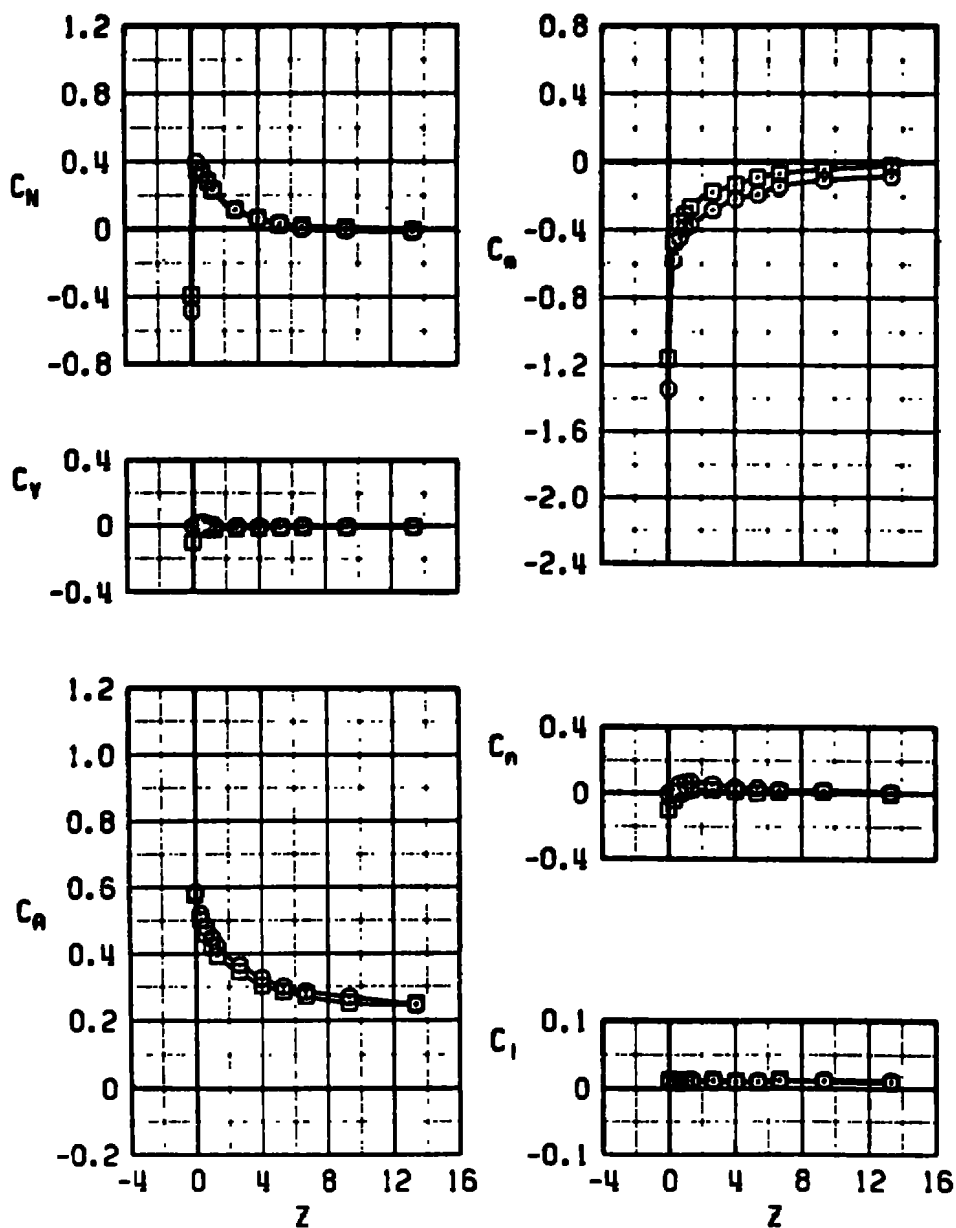
c. $M_\infty = 0.9$
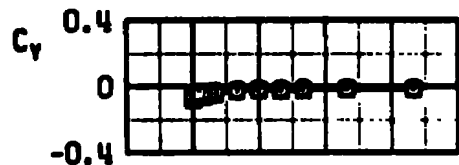
Figure 21. Continued.
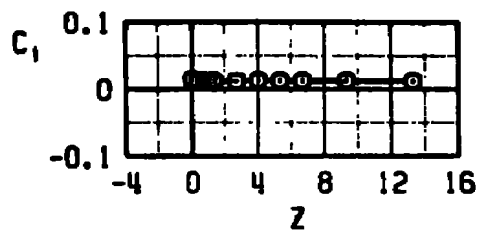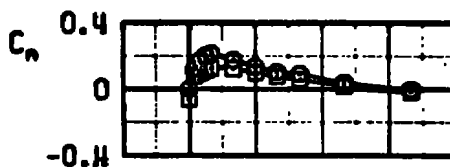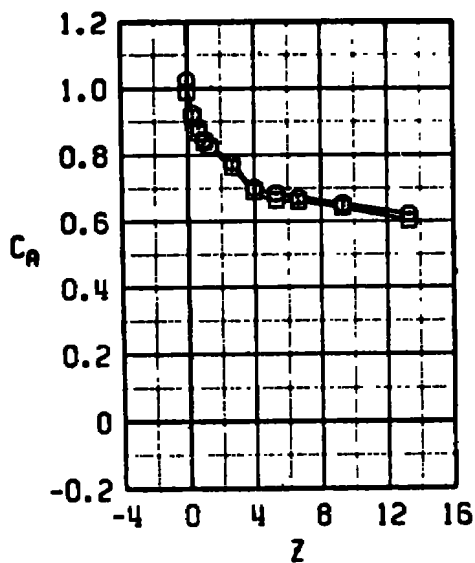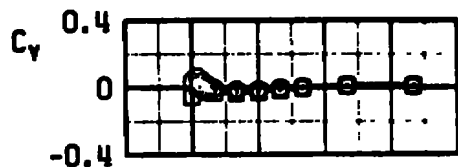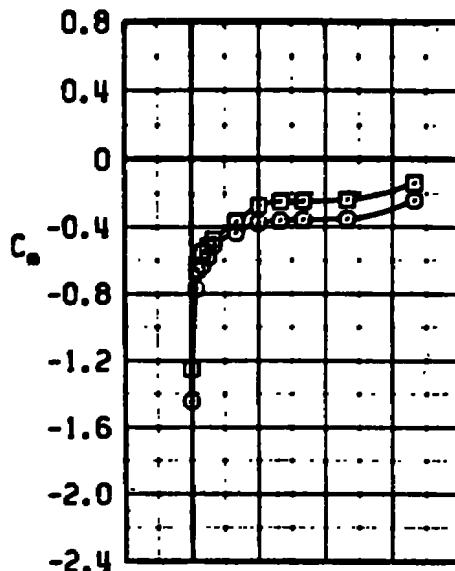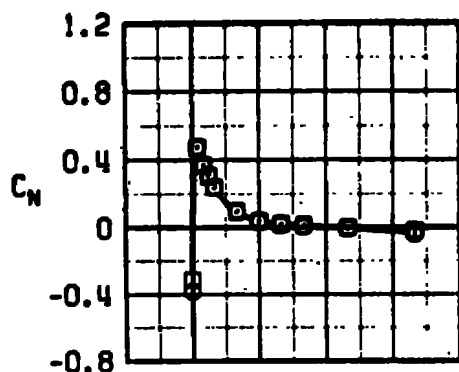
d. $M_\infty = 1.1$

Figure 21. Concluded.
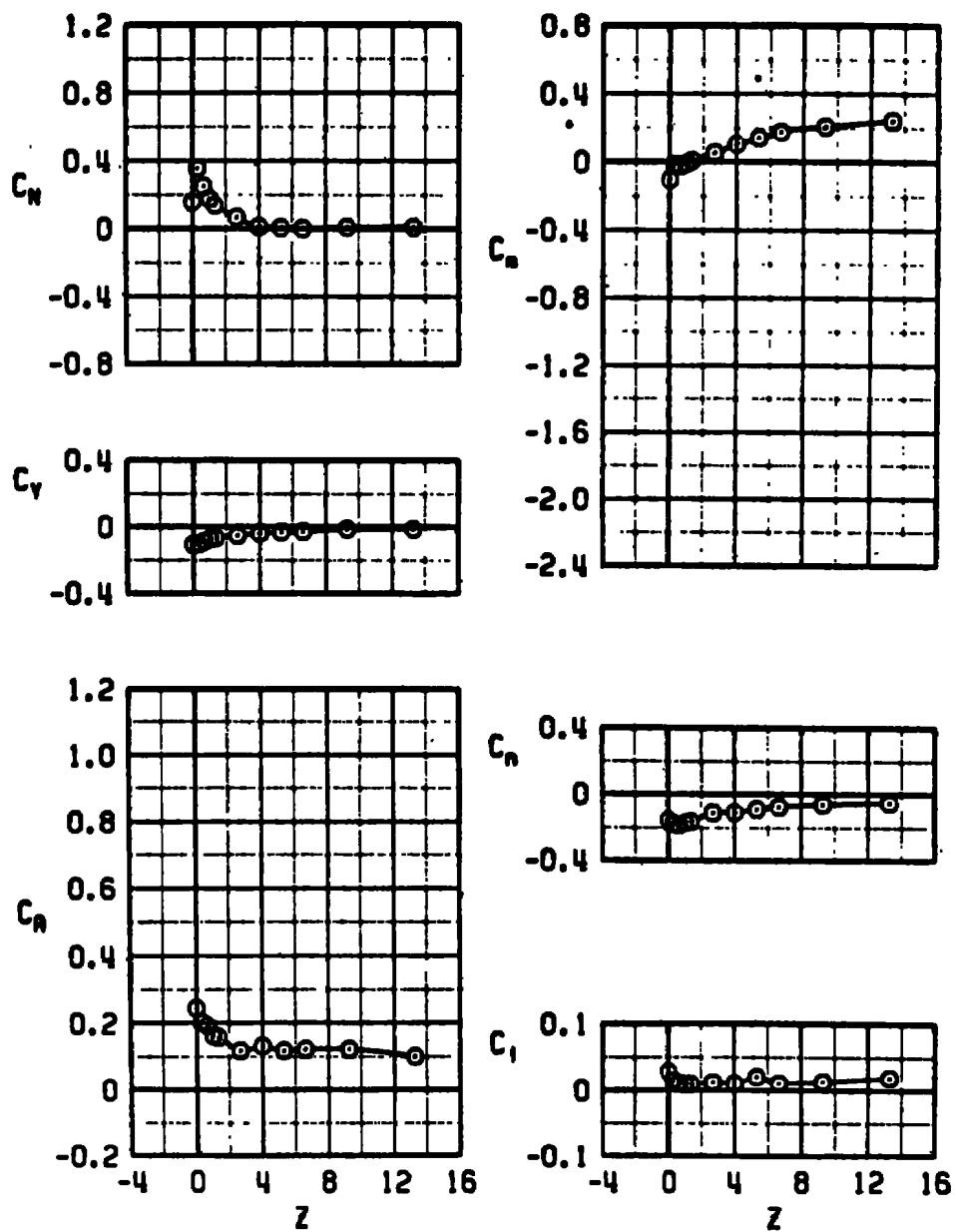
a. $M_\infty = 0.5$

Figure 22. Flow-field aerodynamic coefficients versus Z for
configuration 5.
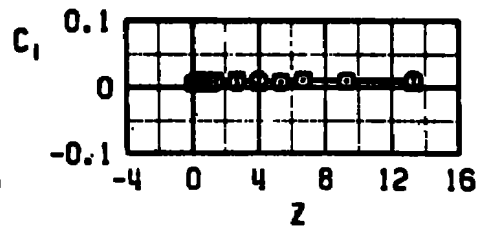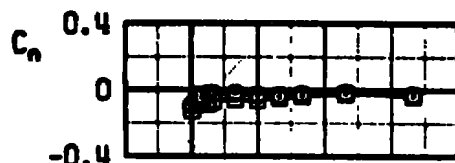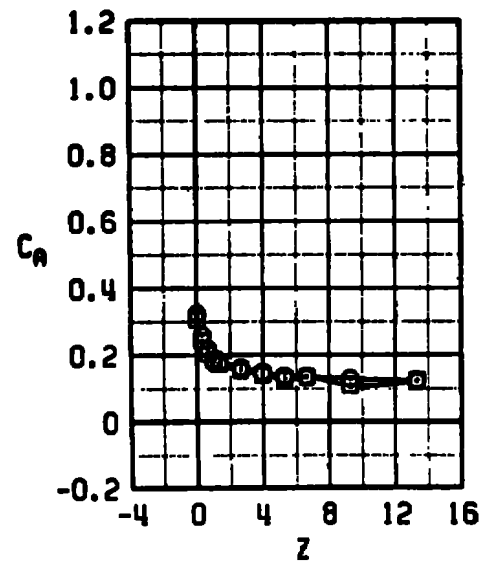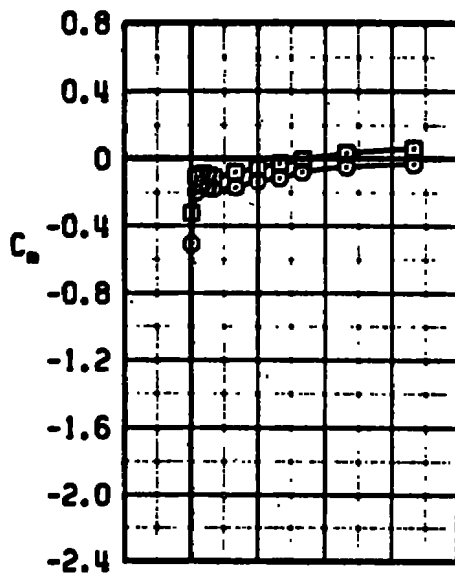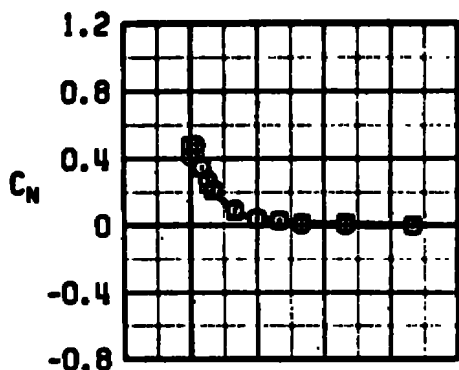
b. $M_\infty = 0.7$
Figure 22. Continued.

	CONF	q_N	α	X
⊙	5	0	0	0
▣	5	0	1	0
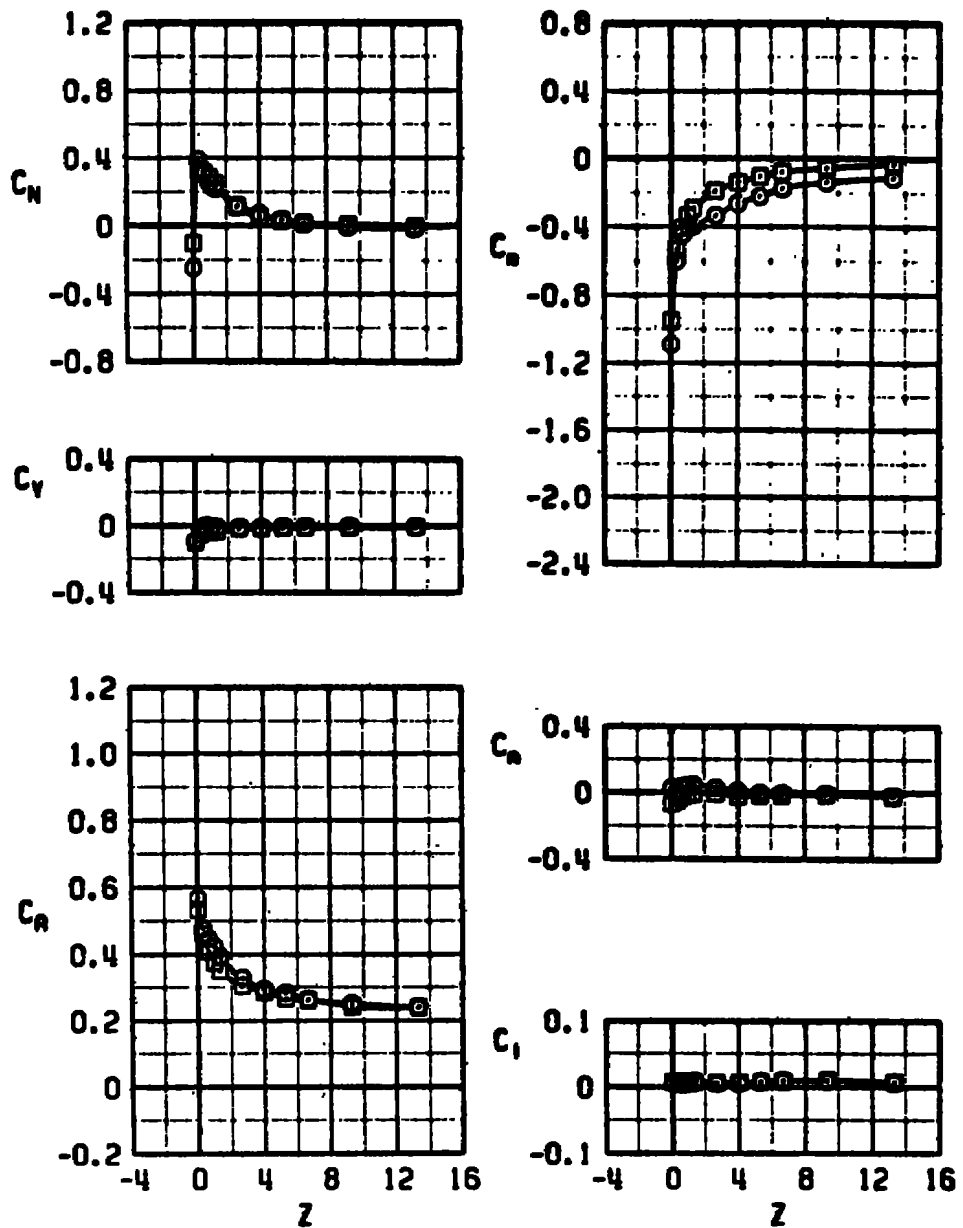
c. $M_\infty = 0.9$

Figure 22. Continued.
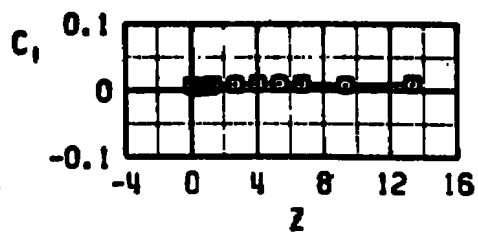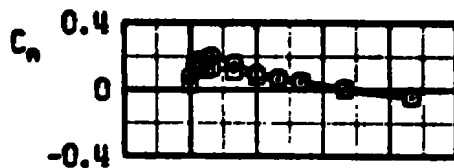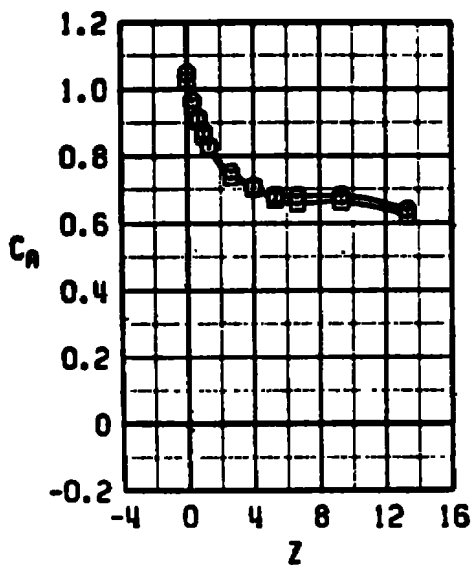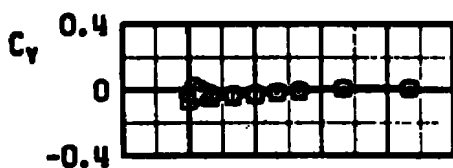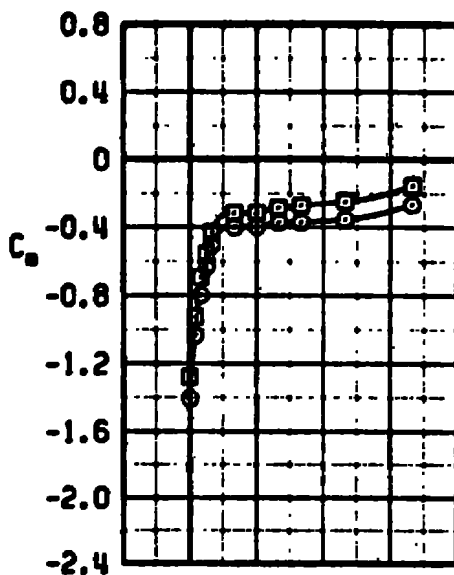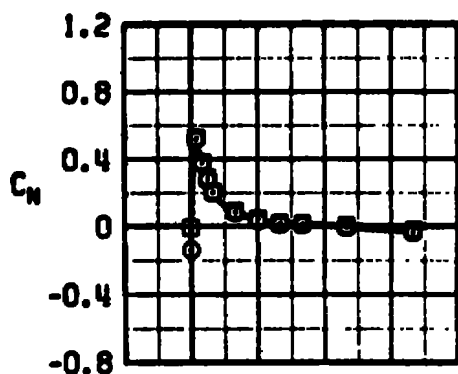
d. $M_\infty = 1.1$
Figure 22. Concluded.
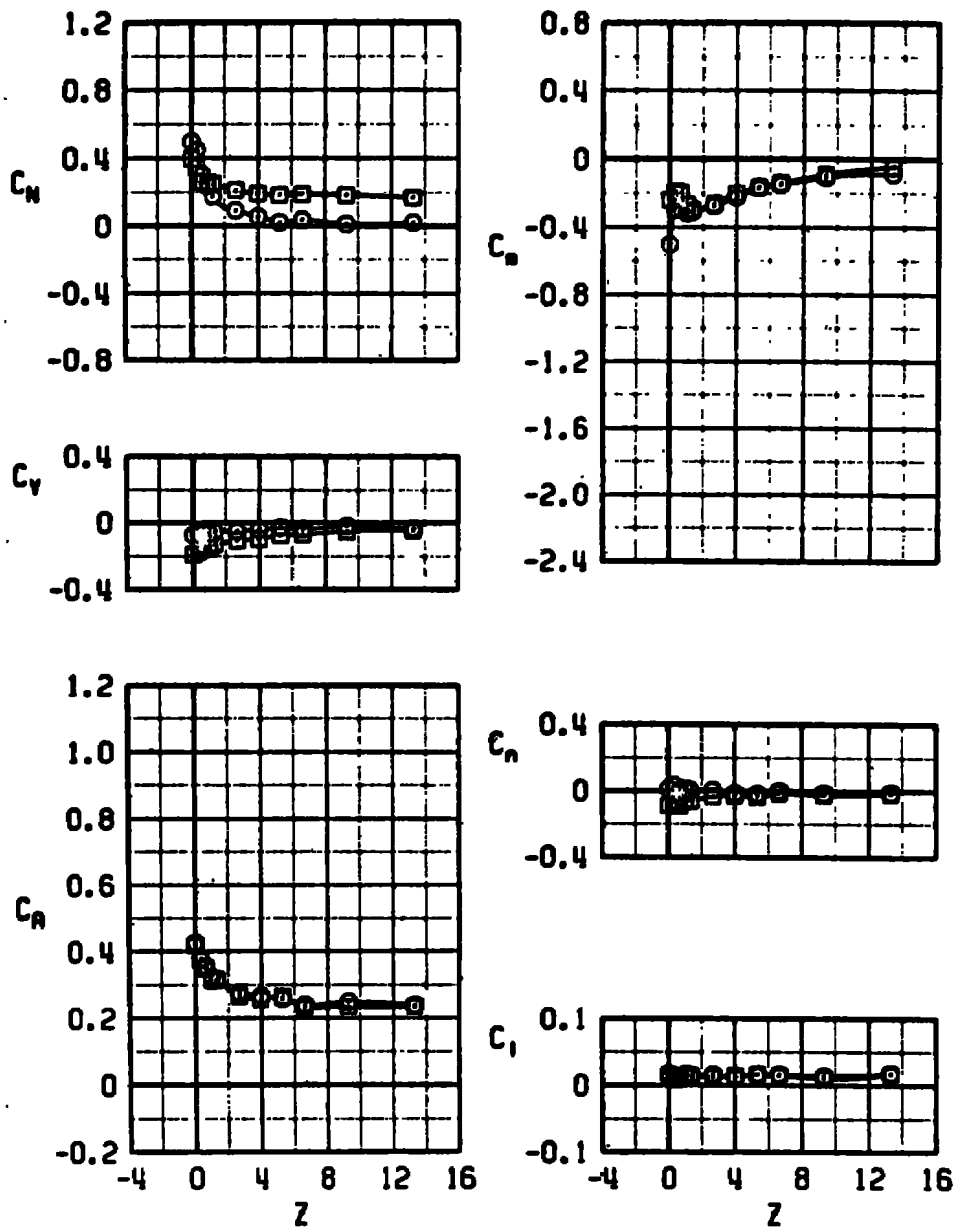
a. $M_\infty = 0.5$

Figure 23. Flow-field aerodynamic coefficients versus Z for configuration 6.
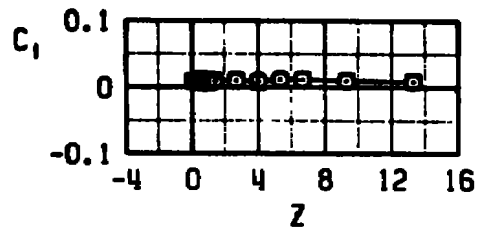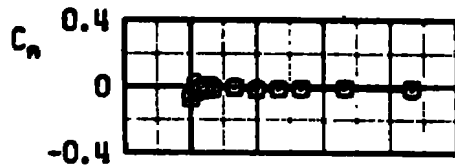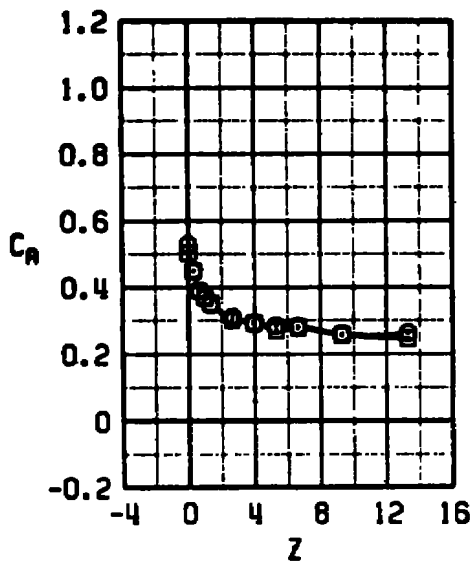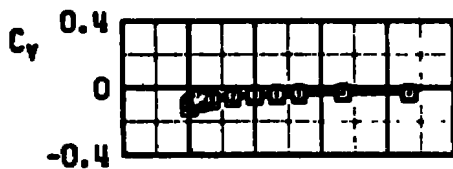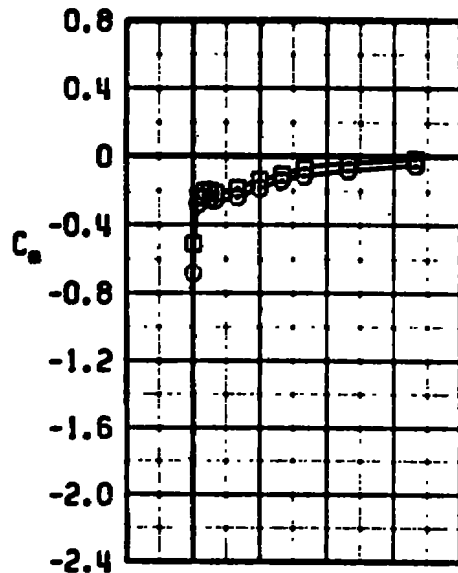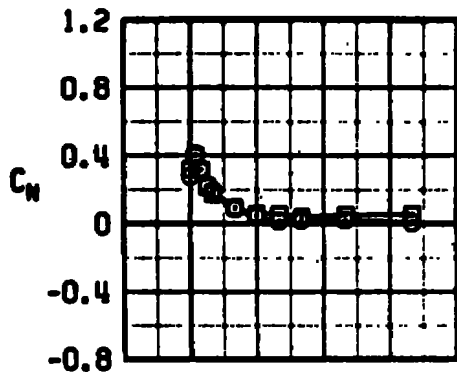
b. M∞ = 0.7
Figure 23. Continued.
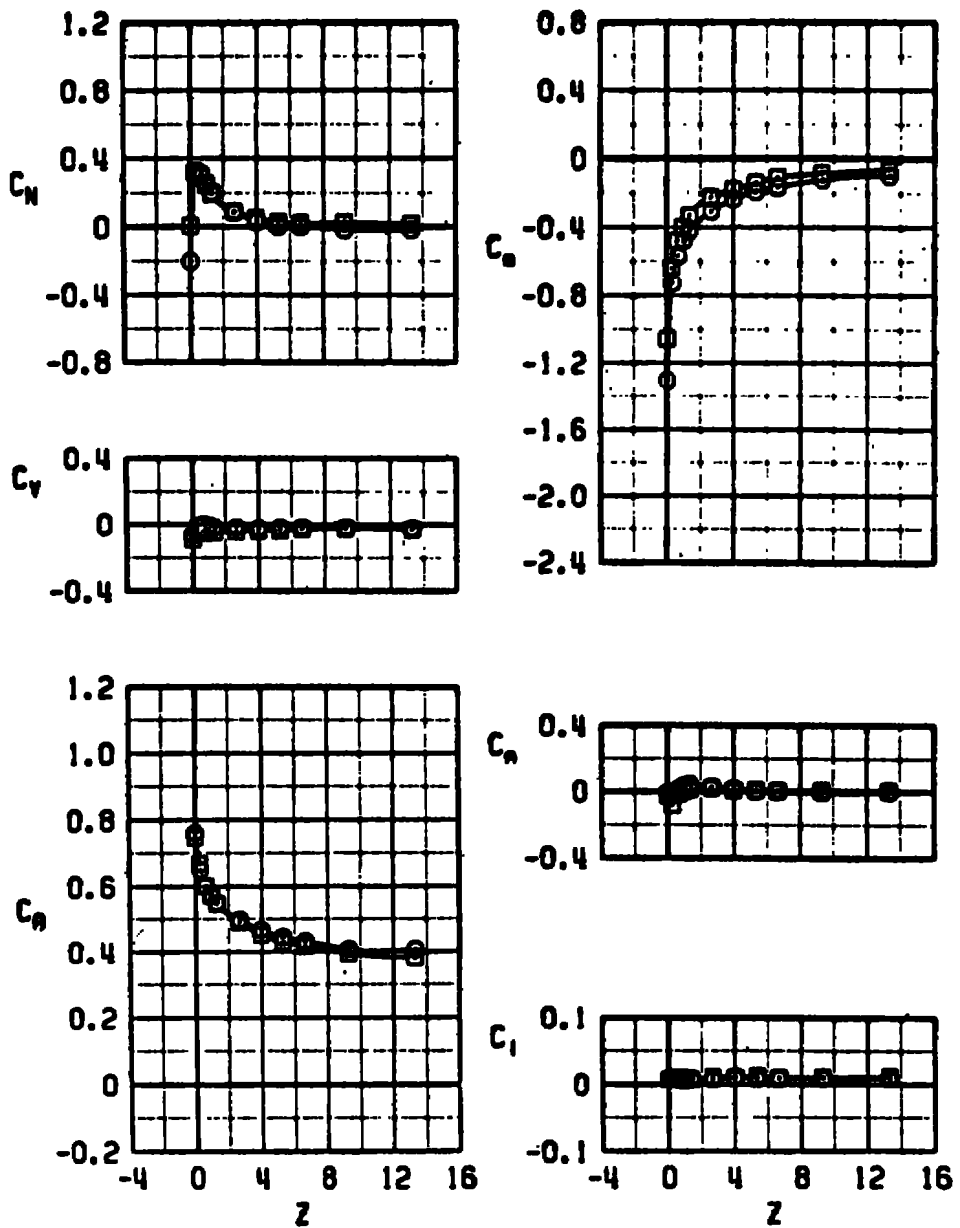
c. $M_\infty = 0.9$
Figure 23. Continued.
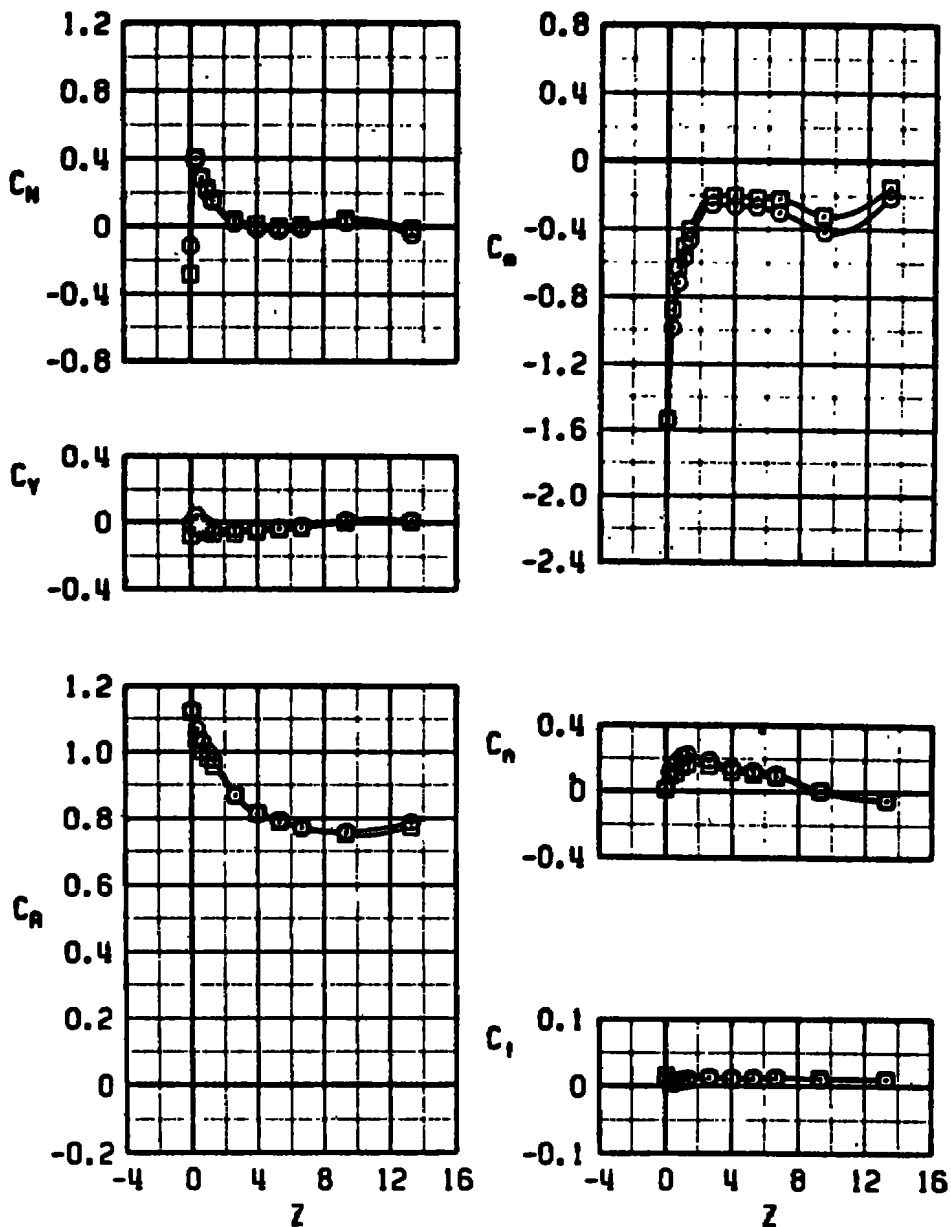
d. $M_\infty = 1.1$

Figure 23. Concluded.

Table 1. Data Uncertainties

TUNNEL CONDITIONS AND COEFFICIENTS	$M_\infty = 0.5$	$M_\infty = 0.7$	$M_\infty = 0.9$	$M_\infty = 1.1$
M_∞	± 0.0021	± 0.0021	± 0.0028	± 0.0061
q_∞	± 1.3	± 1.3	± 1.3	± 1.7
C_N	± 0.0656	± 0.0393	± 0.0294	± 0.0249
C_m	± 0.0779	± 0.0468	± 0.0353	± 0.0304
C_Y	± 0.0691	± 0.0416	± 0.0316	± 0.0292
C_n	± 0.0926	± 0.0556	± 0.0417	± 0.0352
C_A	± 0.0749	± 0.0449	± 0.0338	± 0.0286
C_ℓ	± 0.0477	± 0.0286	± 0.0215	± 0.0181

NOMENCLATURE

A	Store fin tip chord, in.
BL	Aircraft buttock line from plane of symmetry, in., model scale
C_A	Store measured axial-force coefficient, axial force/$q_\infty S$
C_ℓ	Store rolling-moment coefficient, rolling moment/$q_\infty Sd$
C_m	Store pitching-moment coefficient, pitching moment/$q_\infty Sd$ (see Fig. 7 for moment reference point)
C_N	Store normal-force coefficient, normal force/$q_\infty S$
C_n	Store yawing-moment coefficient, yawing moment/$q_\infty Sd$
C_Y	Store side-force coefficient, side force/$q_\infty S$
d	Store reference diameter, 0.800 in., model scale
FS	Aircraft fuselage station, in., model scale
M_∞	Free-stream Mach number
q_∞	Free-stream dynamic pressure, psf
Re	Free-stream Reynolds number based on store length
S	Store reference area, 0.00349 ft^2, model scale
WL	Aircraft waterline from reference horizontal plane, in., model scale
a	Parent-aircraft model angle of attack relative to the free stream, deg
ϕ_M	Store model roll angle, deg
ψ	Angle between the projection of the store longitudinal axis in the X_T-Y_T plane and the X_T axis, deg

TUNNEL AXIS SYSTEM COORDINATES

X_T	Parallel to the tunnel centerline, positive direction is forward
Y_T	Perpendicular to the X_T axis and the vertical plane of symmetry of the tunnel, positive direction is to the left looking upstream

Z_T Perpendicular to both the X_T and Y_T axes, positive direction is toward the tunnel top wall

PYLON AXIS SYSTEM COORDINATES

X   Parallel to the store longitudinal axis in the carriage position, positive direction is forward as seen by the pilot

Y   Perpendicular to the X axis and parallel to the tunnel axis X_T-Y_T plane, positive direction is to the right as seen by the pilot

Z   Perpendicular to both the X and Y axes, positive direction is downward as seen by the pilot

The pylon axis system origin is coincident with the store cg in the carriage position (1 deg nose down relative to angle of attack). The axes are rotated with respect to the tunnel axis by the carriage position pitch angle of the store.